EXPLORING THE IMPORTANCE OF MOSQUITO HEMOCOELIC AND SALIVARY GLAND COMPONENTS DURING HOST-PATHOGEN INTERACTIONS

By

Jonas King

Dissertation

Submitted to the Faculty of the

Graduate School of Vanderbilt University

in partial fulfillment of the requirements

for the degree of

DOCTOR OF PHILOSOPHY

in

Biological Sciences

December, 2012

Nashville, Tennessee

Approved:

Professor Julian F Hillyer

Professor Laurence J. Zwiebel Professor

Professor Patrick Abbot

Professor Seth Bordenstein

Professor Chuck Sanders

For my family.

ACKNOWLEDGEMENTS

I would first like to thank Dr. Julián Hillyer for his support and guidance. By being in his lab, I think I learned much more about the true essence of being a scientist than I would have if I had chosen to join another lab. Julián is a perfectionist, a devoted teacher, and understands that philosophical achievements are best attained through a healthy debate.

I thank my committee members, Drs. Larry Zwiebel, Chuck Sanders, Seth Bordenstein and Patrick Abbot. Throughout this process I have received constructive comments and criticisms from everyone on my committee. On certain occasions I have also received important career guidance and suggestions on how to live a better life.

I thank my collaborators: Dr. Courtney Murdock, Dr. John Gibbons, Dr. Ken Vernick, Dr. Paul Lago, David Rinker, and excellent undergraduate students Justin Glenn, Jon Andereck and Sarah Coggins. I learned a lot about new areas of biology from you and I thank you for your enthusiasm and willingness to tolerate my colorful personality.

There is much to be learned from casual philosophizing, and there are far too many names for me to list here. In recollecting the last five years, the names that stand out most in my mind are: Leonidas Salichos, Sarah Lawson, Dr. Jason Pitts, Dr. Wan-Hsin Lin, Dr. Josh Broussard, Garrett League and Dr. Rhoel Dinglasan. I thank you for your insightfulness.

I would like to thank my family, especially the three I was closest to during my PhD work: my brother Spencer Murray, father Bob King, and wonderful wife Lydia King.

They are the reason I do what I do and I thank them for their love and support. Lastly, I would like to thank all the freethinkers throughout history, especially those who elected to be exiled, crucified, burned at the stake, or drawn and quartered, rather than submit to the designs of despots and madmen.

TABLE OF CONTENTS

LIST OF TABLES BY CHAPTER

Table Page

CHAPTER V

LIST OF FIGURES BY CHAPTER

Figure Page

CHAPTER II

CHAPTER III

CHAPTER IV

CHAPTER V

PREFACE

Traversal of the hemocoel, avoiding or surviving interactions with the insect's innate immune system, invasion of the female mosquito's salivary glands, and injection into the vertebrate host, are key host-parasite interactions that are normally necessary for disease transmission by mosquitoes. These processes represent complex and perilous steps in the life-cycle of mosquito-vectored pathogens, which could possibly be targeted in disease control strategies [1-4]. General knowledge of mosquito circulatory physiology, immunology, and salivation are also important because the mosquito's phylogenetic position and well-defined interactions with diverse pathogens make it a good system for comparative immunology and evolutionary analyses [5-7]. Despite the importance of these processes, the physiological and molecular mechanisms underpinning them remain largely unknown. In the introductory chapter, I will outline certain aspects of mosquito biology that come into play during their role as disease vectors and relate them to the research I have carried out during my time as a PhD student. In the subsequent chapters, I will present the work that I have conducted over the past five years and explain how our results have helped advance knowledge of these important aspects of mosquito biology.

CHAPTER I

INTRODUCTION: INSECT VECTORS OF HUMAN DISEASE AND THE ROLE OF INSECT HEMOCOEL COMPONENTS DURING PARASITE LIFE CYCLES

Hematophagy

Hematophagy (blood-feeding) has independently evolved at least 20 times within the arthropods, and 11 times in the dipterans [5]. It is believed that two evolutionary scenarios can explain how hematophagy originated in these insect lineages [8]. First, predatory insects that possess piercing mouthparts seem predisposed to evolve into blood feeders. Second, living in close association with a potential vertebrate host also appears to have led to hematophagy on occasion. For example, the transition from insects feeding on sloughed keratin, to chewing lice, and finally to biting lice. As insects lose essential biochemical pathways that are redundant once blood feeding is a normal part of their existence, many become dependent on blood meals either as a means of survival, or to optimize fecundity. Once blood-feeding is fully espoused and becomes a routine part of a species' livelihood, individual insects often begin feeding multiple times in their lifetime. Because the world outside the host's body is a hostile place for most microscopic parasites, the ability for them to exploit the mobility of an arthropod that feeds repeatedly on suitable vertebrates becomes a choice evolutionary strategy. Consequently, opportunistic microbes have relentlessly evolved to optimize their use of arthropods as a means of reaching a new vertebrate body to parasitize [9].

For tens of millions of years [10], the females of many mosquito species have sought a blood meal prior to the production of eggs and have become efficient vectors

for a great diversity of vertebrate pathogens. Humans are a relatively new species in most parts of the world [11]. However, we often live in extremely high densities near fresh water, and we are large, hairless, and normally inactive during the night. For these simple reasons, along with many more complex factors, I believe that very few people have ever lived who have not experienced the bite of a mosquito. Since the development of agriculture and the spread of Neolithic societies we have represented a major niche for mosquitoes and an assortment of the diseases they transmit [12]. This is probably best evidenced by the evolution of mosquito species that specialize in feeding on us [13]. Even in the modern world, mosquitoes are responsible for vectoring diseases that cause much misery and death [9].

Vector-borne diseases and their life cycles

Mosquito-borne diseases remain a grim problem for mankind. For example, more than 40 percent of the world's population lives in areas with endemic malaria [14]. *Plasmodium falciparum*, the protozoan that causes malignant human malaria, infects many tens of millions of people each year. It frequently kills more than one million of these people, the vast majority of which are young children [15]. Long-term cognitive effects have also been documented in patients who were infected with malaria as a child [16]. In addition to physical distress, pervasive malaria infection is believed to be partially responsible for limiting the economic health of endemic countries. Some researchers speculate that malaria has lowered the GDP by more than 50 percent in several countries [17]. Besides malaria, mosquitoes are also vectors for the dengue virus, filarial nematodes and a variety of other neglected tropical diseases. Together these diseases cause millions of infections and tens of thousands of deaths each year. The filarial

worms, while responsible for relatively few deaths, perennially infect more than 100 million people and lead to great physical suffering, social stigma, and economic strife [18].

Resistance to drugs and insecticides, deteriorating infrastructure and global warming are promoting the reappearance of malaria in areas from which it had been eliminated [19]. While crucial advancements have been made towards understanding mosquito host seeking behavior [20] and attempts are being made towards effective vaccines against several insect vectored diseases [21], future efforts to control the mosquito vector and disease transmission could be facilitated by novel strategies [19]. By further characterizing the mechanics of mosquito-microbe and mosquito-vertebrate interactions, we hope to uncover possible targets for the development of novel control strategies. A better understanding of these interfaces will also increase our knowledge of host-parasite evolution.

There is a wide phylogenetic divergence seen in the parasites that mosquitoes vector, from viruses to metazoans. However, some deviation of a general pattern is often followed during the parasites' time spent inside a mosquito (the extrinsic incubation period). First, a mosquito takes a blood meal from a host that is infected with a species of microbial pathogen capable of developing within that type of mosquito. The pathogen then undergoes a series of tissue invasions and developmental and/or amplification steps before migrating through the mosquito body cavity (hemocoel), encountering the mosquito immune system, and invading the salivary glands (protozoan and viruses) or proboscis (nematodes;[9]). Once here, the pathogens lie in wait to be introduced into a new vertebrate host when the mosquito blood feeds. In the next three sections, I will detail the latter steps in this process, using *Plasmodium* as an example and focusing on how each step relates to my research at Vanderbilt.

Midgut egression and migration through the hemocoel

Once inside the lumen of the mosquito's midgut, many species of pathogen invade the gut epithelium. They then either stay in the gut, or migrate into another tissue, where they undergo transformative or amplifying steps [9]. In the case of *Plasmodium*, gametocytes fuse to form a zygote that quickly develops into a motile ookinete, which uses gliding motility and the secretion of degradative enzymes to invade the gut cells [22]. *Plasmodium* then develops into thick-walled oocysts which develop over the course of 10-15 days [1], depending on the species, into cysts containing hundreds of sporozoites. These sporozoites then egress from the midgut and must quickly migrate through the hemocoel and enter the salivary glands. If they do not, they are killed in the hemolymph [1]. Sporozoites are motile, and it remains unknown if they actively navigate the hemocoel or rely primarily on passive movement, i.e. hemolymph flow. It is therefore important that along with investigating *Plasmodium* motility [23], we also investigate the structures and activities of the mosquito circulatory system.

The circulatory system shares some similarities across all insect taxa [24, 25]. All organs are located in an open hemocoel and are bathed in hemolymph which is propelled through the body by a dorsal vessel. The vessel can be divided into the actively pumping abdominal heart and the thoracic aorta which passively conducts hemolymph to the head. The segmental chambers of the abdominal heart contain valves termed "ostia" which allow hemolymph entry into the heart in holometabolous insects [26]. Insects have also evolved various accessory pulsatile organs which help maintain hemolymph flow through the extremities [27]. It is within these smaller pulsatile organs, various ostia types, and the presence of different types of circulating immune cells that insect circulatory systems often show variance [26, 28]. This is expected given the scale of insect evolutionary history [8]. While there is some available data on the general

structures of the insect circulatory system, little work has been done characterizing the rates, or modes of hemolymph flow.

At the start of my PhD research, most available data on the mosquito circulatory system came from two papers written in the mid-twentieth century, one of which had usually been overlooked by subsequent researchers [29, 30]. The more recognized report relied solely upon basic light microscopy to cursorily describe the anatomy of the circulatory system [28, 31]. Comparative inferences of mosquito circulation were also not possible, because in the last 50 years little data has been generated from flies from the suborder Nematocera, which contains the mosquitoes and other vectors such as black flies and sand flies. We characterized the circulatory system and flow dynamics of hemolymph (insect blood) in *Anopheles gambiae* to gain insight into the mode of parasite migration through the hemocoel. Our work showed that the circulatory system of this important vector is more dynamic than previously believed and may be responsible for a majority of pathogen dispersal throughout the body (Chapter II;[32, 33]).

Interactions with the insect immune system

The insect immune system exists in intimate association with the circulatory system and likely has for most of its evolutionary history [34]. The immune response relies entirely upon innate, germline-encoded reactions to microbial challenge and injury and involves both cellular and humoral components [25, 35, 36]. The cellular immune response is defined by phagocytosis and encapsulation by hemocytes [36, 37], while the humoral response involves the activation of signaling cascades culminating in the production of antimicrobial molecules [35, 38, 39]. It has been shown that *Plasmodium* numbers are greatly reduced during migration through the hemocoel by the destruction

of sporozoites [1], and it seems likely that this destruction involves hemocyte activity [40, 41]. While most modern studies have focused on systemic transcriptional changes in response to infection and analyses of cellular signaling pathways involved in immunity, there remains a dearth in our knowledge of the basic physiology and cell biology of the insect immune response.

In mosquitoes, bacteria and microspheres injected into the hemocoel were known to rapidly accumulate in foci near each pair of abdominal ostia [1]. We hypothesized that either of two previously unreported cellular immune responses is involved in formation of uptake foci near the ostia. First, it is known from other insects that hemocytes will aggregate in response to certain stimuli [42, 43], suggesting that hemocytes could be responding similarly near the ostia. Second, large pinocytic cells known as pericardial cells occur in the vicinity of the ostia and have been implicated in immune activity along with their defined role as nephrocytes [1, 41, 44, 45]. We focused on the role of these two cell types in the phagocytosis of innate materials and pathogens in the periostial regions flanking the heart. We found that large aggregates of periostial hemocytes were responsible for the phagocytic foci and characterized their formation and role in pathogen clearance (Chapter III). We hypothesize that this interaction between the circulatory and immune systems helps maintain homeostasis following infection. We also discuss analogous responses in vertebrates which share some striking parallels to our observations in mosquitoes.

Assumptions about the total number and types of hemocytes present in a mosquito have been of key importance during several modern studies, although the numbers and relative prevalence of various hemocyte types reported sometimes differ by orders of magnitude [46-50]. These discrepancies represent a major problem in mosquito biology, and we developed novel staining methods to gain a better

understanding of hemocyte populations. We were especially interested in the prevalence and roles of sessile hemocytes, which are only vaguely understood in any insect and were virtually unknown in mosquitoes. Our novel methods yielded an accurate count of total hemocytes, including both sessile and circulating cells, and we qualitatively assessed their activities during an immune response (Chapter IV).

Another key question in insect immunity concerns the means by which circulating hemocytes increase in number following immune stimulus [25, 46, 51]. At the onset of this study, there was little hard evidence for any of the three plausible sources: (1) the activation of hemocyte release from a discrete hematopoietic organ, (2) the release of sessile hemocytes into circulation, or (3) the autonomous division of circulating hemocytes. To this end, we used total body hemocyte counts to show that both sessile and circulating numbers increase following infection. We then used treatments with a variety of spindle poisons and tubulin staining to directly assay the possibility of autonomous proliferation of circulating hemocytes. Mitotic indices in perfused cells, following infection, showed that some level of autonomous mitosis occurs in the hemocoel.

Invasion of the salivary glands and injection into the vertebrate host: More than just flying syringes

Once the hemocoel has been traversed and immune response has been endured, pathogens invade the salivary glands. At this point the mosquito is capable of disease transmission during blood-feeding. In the case of malaria, recent research suggests that this process involves a series of complex interactions between the mosquito, *Plasmodium,* and the vertebrate skin [52-54]. Work done to characterize salivary gland invasion suggests that this process is mediated by multiple protein-protein

interactions and involves several stages of membrane traversal [55, 56]. Once inside the glands, additional signals initiate transcriptional changes and prepare the sporozoites for invasion of the vertebrate liver [57]. One exciting prospect for research into salivary gland biology is the use of transgenesis to render mosquitoes incapable of disease transmission [2, 4, 58]. Ito et al. [59] was the first to show that a transgene, in this case an oligopeptide, was capable of lowering the numbers of *Plasmodium* sporozoites in the salivary glands of infected mosquitoes. The action of this oligopeptide has now been shown to involve the disruption of a specific interaction between a *Plasmodium* surface protein named TRAP, and the *Anopheles* salivary gland protein SAGLIN [60].

Another exciting reason to study mosquito salivary glands is the possible development of vaccines which block disease transmission, or the use of salivary components as markers in epidemiologic studies [3, 61]. It has even been proposed that saliva components could represent an untapped source of pharmacological compounds [5]. Hematophagous arthropods have been evolving to maximize the efficiency of blood feeding for tens of millions of years. During this time, they have placed a heavy selective pressure on their vertebrate hosts to counteract disease transmission. This coevolutionary interaction is evidenced by the complex cocktail of immunomodulatory salivary components seen in hematophagous arthropods and by the often exaggerated response of vertebrate mast cells to stimulation by insect bites [62]. Due to its strong immunomodulatory actions, which are often tailored to affect specific host species, it has been shown that arthropod saliva can amplify the transmission of pathogens [63, 64]. Consequently, it has been proposed that a vaccine which neutralizes salivary factors might offer protection from such pathogens [3]. Among the specific components of saliva, immunomodulatory proteins have been shown to be effective vaccine targets [3, 65, 66]. Along with immunomodulation by the saliva, many salivary proteins are highly

immunogenic and produce a strong antibody response. It has also been shown that such immunogenic components can serve as a means of assessing individual exposure to mosquito bites [61, 67].

In *Aedes aegypti,* a salivary gland specific protein (aaSGS1) was shown to be important during the invasion of salivary glands by *Plasmodium gallinaceum* sporozoites [68]. Specifically, the injection of anti-aaSGS1 antibodies during sporozoite migration reduced salivary gland invasion by approximately 65 percent. This protein shares little homology with any protein of known function and was predicted to occur on the basal surface of the salivary gland in *Aedes*. We worked to characterize this gene family in the malaria mosquito, *Anopheles gambiae*. Surprisingly, data from our work on SGSs showed that they are a major component and immunogen of the mosquito saliva and are likely immunomodulatory (Chapter V).

Preview of subsequent chapters

In the subsequent chapters we have used microscopy and molecular techniques to answer some of the questions described above. In Chapter II we explored the circulatory dynamics of the mosquito hemolymph and found that hemolymph moves much more rapidly than previously thought. This indicates that parasites migrating through the hemocoel are likely utilizing passive motility. In Chapters III-IV we characterized the mosquito cellular immune response and describe several exciting discoveries. Namely, we explored the nature of sessile hemocytes and discovered major sessile phagocytic foci formed by hemocytes in response to infection. We also found that hemocytes proliferate in response to infection, with results suggesting that this is by autonomous mitosis in the hemocoel. In Chapter V we investigated the role of mosquito

SGS proteins during sporozoite invasion of salivary glands and during salivary interactions with the vertebrate host. Finally, in Chapter VI I relate my work to a broad view of mankind's fight against infectious disease, and to our longing to understand the evolutionary processes that led to our existence and continue to affect our lives. I also include some suggestions for future researchers studying hemocytes and briefly describe my own future pursuits.

CHAPTER II

STRUCTURAL MECHANICS OF THE MOSQUITO HEART AND ITS FUNCTION IN BIDIRECTIONAL HEMOLYMPH TRANSPORT

Preface:

This chapter presents part of the work we conducted focusing on the structures and dynamics of the mosquito circulatory system. This work gave me the opportunity to help direct two very talented undergraduates that I worked with extensively. The chapter, as presented, was published in the *Journal of Experimental Biology* in early 2010 [33]. Justin Glenn and I worked together for most of this study and we share co-first authorship of the manuscript. I was responsible for much of the technique development, imaging, and analyses of flow dynamics, along with assistance in manuscript preparation and answering reviewer comments. The second undergraduate I worked with, Jon Andereck, focused on the role of abdominal contractions in creating hemolymph flow. For this project I was responsible for the development of techniques and conceptual support during manuscript preparation. Due to my more hands-off role, this second project was not included in my dissertation. He was first author, and I was second, on a paper published in *PLoS ONE* in late 2010 [32].

Abstract:

The insect circulatory system transports nutrients, signaling molecules, wastes, and immune factors to all areas of the body. The primary organ driving circulation is the dorsal vessel, which consists of an abdominal heart and a thoracic aorta. Here, we present qualitative and quantitative data characterizing the heart of the mosquito, *Anopheles gambiae*. Visual observation showed that the heart of resting mosquitoes contracts at a rate of 1.37 Hz (82 beats per minute) and switches contraction direction, with 72% of contractions occurring in the anterograde direction (toward the head) and 28% of contractions occurring in the retrograde direction (toward the tip of the abdomen). The heart is tethered to the midline of the abdominal tergum by six complete and three incomplete pairs of alary muscles, and propels hemolymph at an average velocity of 8 mm/sec by sequentially contracting muscle fibers oriented in a helical twist with respect to the lumen of the vessel. Hemolymph enters the heart through 6 pairs of incurrent abdominal ostia and one pair of ostia located at the thoraco-abdominal junction that receive hemolymph from the abdominal hemocoel and thoracic venous channels, respectively. The vessel expels hemolymph through distal excurrent openings located at the anterior end of the aorta and the posterior end of the heart. In conclusion, this study presents a comprehensive revision and expansion of our knowledge of the mosquito heart and for the first time quantifies hemolymph flow in an insect while observing dorsal vessel contractions.

Introduction:

Insects employ an open circulatory system for the transport of nutrients, wastes, and signaling molecules [69, 70]. In addition, the insect circulatory system functions in thermoregulation, promoting ventilation through the tracheal system, and the circulation of humoral immune molecules and immune blood cells (hemocytes) that survey tissues for foreign invaders. The general anatomy of the insect circulatory system consists of a dorsal vessel that extends the length of the insect, an open body cavity (hemocoel), and numerous accessory pulsatile organs [69, 70]. The dorsal vessel is a tube that is divided into a thoracic aorta and an abdominal heart that contains valves called ostia, which allow hemolymph to enter the lumen. Hemolymph inside the dorsal vessel is pumped toward the head or the tip of the abdomen where it empties into the hemocoel and moves until it reenters the heart. Because of the passive nature of hemolymph flow in the hemocoel, insects also use a series of autonomous accessory pulsatile organs to pump hemolymph to the appendages and other regions that would otherwise experience low flow rates [27]. However, insects have evolved over 400 million years so it is not surprising that there are numerous variations to this general plan, especially given the broad range of insect sizes and behaviors. Variations include the presence or absence of segmental blood vessels originating from the heart [26], various forms of ostia [6], a closed versus open posterior heart [70, 71], differing populations of circulating hemocytes [28], and differing ratios of forward versus backward hemolymph flow [72]. Based on recent observations in *Drosophila* and other insects [73-75], it has become clear that the circulatory system of insects is far more complex than originally thought.

Within the order Diptera, considerable research efforts have aimed to characterize the structure and development of the *Drosophila* (suborder: Brachycera) heart [75, 76]. However, the hearts of dipterans from the suborder Nematocera have

gone largely ignored, a surprising fact given the ecological and public health significance of an insect group that includes the mosquitoes, sand flies, black flies, and biting midges. Among these, mosquitoes (Culicidae) are the most epidemiologically significant pests and disease vectors, as they transmit deadly human and animal pathogens such as the causative agents of malaria, lymphatic filariasis, and dengue hemorrhagic fever. During their natural life cycle, these pathogens are ingested with infective blood meals, cross the midgut epithelium, and enter the hemocoel, where they migrate to the salivary glands or mouthparts [1, 54, 77]. Understanding the physiological basis of hemolymph flow may increase our knowledge on how these parasites undergo this obligate migration.

Most of what is known about the anatomy of the mosquito circulatory system comes from experiments performed over 30 years ago [78], with the majority of the data originating from two publications that analyzed the circulatory systems of *Anopheles quadrimaculatus* and *Anopheles maculipennis* [29, 79]. The anatomical descriptions in those studies are greatly informative but were limited by the methodologies available at the time, and include observations that are in conflict with one another or have since been proven incorrect. For example, there are conflicting reports regarding the number of alary muscle pairs present in the mosquito abdomen [72], and contrary to what was previously reported [72], several groups have identified and characterized circulating hemocytes in mosquitoes of the genus *Aedes* [28, 47]. Here, we employ a novel approach toward the study of the insect dorsal vessel and present qualitative and quantitative data characterizing the structural mechanics of the mosquito heart.

Materials and methods:

Mosquito rearing and maintenance.

Mosquitoes were reared and maintained in an environmental chamber at 27°C, 75% relative humidity, with a 12 hr light/12 hr dark photoperiod and a 30 min crepuscular period at the beginning and end of each light cycle. *Anopheles gambiae* (SUA2La hybrid) larva were hatched in distilled water, transferred to plastic pans, and fed a slurry of ground koi fish food and baker's yeast. Following pupation, mosquitoes were transferred to 4.73 L containers with a fine-mesh marquisette top. Upon emergence, 10% sucrose-soaked pads were placed on top of the marquisette and adults allowed to feed *ad libitum*. All experiments were performed on adult female mosquitoes at five days post-emergence.

Observation of live mosquito hearts.

Mosquitoes were anesthetized on ice for less than 1 min and restrained dorsal-side-up on Sylgard 184 silicone plates (Dow Corning Corp, Midland, MI) or agarose slides by placing 0.15 mm diameter pins gently against (not through) the anterior pronotal lobe (Figure 1A). The wings were then teased laterally and an additional pin inserted through a non-vascular area (eg. cell R3) of each wing without creating horizontal or vertical tension. This non-invasive restraint method prevented live mosquitoes from attempting to fly while maintaining them in a natural position that allowed for visual observation of the beating heart.

The heart of mosquitoes maintained at approximately 24° C was imaged through the dorsal cuticle using bright field illumination on a Nikon 90i light microscope (Nikon

Corp., Tokyo, Japan) connected to a Photometrics CoolSNAP HQ2 high sensitivity monochrome CCD camera (Roper Scientific, Ottobrunn, Germany). Digital videos of 1-minute duration were acquired for each mosquito at 30 frames per second using Nikon's Advanced Research NIS-Elements software. Initially, contraction morphologies were compared to the flow of endogenous particles or intrathoracically injected 2 µm diameter red fluorescent (580/605) carboxylate-modified latex microspheres (Invitrogen, Carlsbad, CA; see below) to determine the relationship between contraction mechanics and pulse direction. Then, quantitative analyses were carried out by manually annotating contractions and contraction directionality over the entire 60-second recordings of unmanipulated mosquitoes (mosquitoes that had not been injected or otherwise manipulated except for restraint on Sylgard or agarose plates). Analyses were done using three cohorts of 10 mosquitoes each. Each cohort was reared independently of one another and originated from different egg batches. Contraction rate (frequency) is presented as hertz (Hz; contractions/sec).

Particle tracking and measurement of hemolymph flow velocity.

Individual mosquitoes were restrained on Sylgard plates as described above and a finely pulled glass capillary needle was inserted through the anepisternal cleft, also defined as the membrane located between the paratergite, the postspiracular area and the mesepisternum in the lateral mesothorax. A volume of 40-50 nl of 0.1 M phosphate buffered saline (PBS; pH 7.0) containing a 1:10,000 dilution of 2 µm diameter red fluorescent microspheres was injected into the hemocoel of live mosquitoes and allowed to mix with the hemolymph. Once in circulation, videos of 1-minute duration were acquired by low-level fluorescence imaging through the dorsal cuticle using a Nikon

SMZ1500 stereomicroscope connected to a Photometrics CoolSNAP HQ2 camera. Videos were captured using either fixed frame rates or the 1-frame acquisition mode in NIS-Elements. The manual feature of the NIS-Elements' Object Tracking module was then used to track individual particles or groups of particles as they entered and moved through the mosquito heart. Distance traveled and velocities were calculated both from frame-to-frame and for the entire path tracked. For hemolymph velocity analyses, 100 particles in 10 mosquitoes were independently tracked in each contraction direction and only particles that could be tracked for a distance greater than 500 µm were used in the analyses.

Light and Fluorescence microscopy of aldehyde-fixed mosquito whole mounts.

For fluorescence labeling of muscle, live mosquitoes were intrathoracically injected with 0.25 µl of a solution consisting of 1% Triton X (Thermo Fisher Scientific Inc., Waltham, MA), 0.3 µM phalloidin-Alexa Fluor 488 (Invitrogen), and 8% formaldehyde (Electron Microscopy Sciences, Hatfield, PA) in PBS and allowed to incubate for 15 min. For mosquitoes to be viewed as undissected whole mounts, a small cut was made in the 8^{th} abdominal segment and specimens were rinsed by intrathoracically injecting PBS and allowing the buffer to exit through the tip of the abdomen. Whole abdomens were then visualized from the exterior on glass depression slides. For mosquitoes to be viewed as dissected whole mounts, abdomens were dissected along a coronal plane to obtain the dorsal halves, washed 3 times for 5 min each with 0.1% Tween 20 in PBS, and mounted on glass slides using Aqua-Poly/Mount (Polysciences Inc., Warrington, PA). To counter stain the ostia, some specimens were injected with a 1:20 dilution of India ink in PBS several hours prior to phalloidin-Alexa

Fluor 488 injection. Samples were imaged under bright field and fluorescence illumination using a Nikon 90i microscope connected to a Photometrics CoolSNAP HQ2 camera.

For three-dimensional rendering, Z-stacks were created by using a linear encoded Z-motor to acquire images at 0.7 µm Z-intervals for a total Z-range of 40 µm. Z-stacks were then quantitatively deconvolved using the AQ 3D Blind Deconvolution module of NIS Elements and rendered using the volume view feature. For the rendering of detailed fluorescence images with extended focal depth, Z-stacks of whole mounts were acquired and all images in a stack combined to form a focused image using the Extended Depth of Focus (EDF) module of NIS Elements.

Embedding, sectioning, and visualization of aldehyde-fixed mosquito abdomens.

Mosquitoes were severed in the 1st and 8th abdominal segments. The abdomens were dissected along a coronal plane to obtain the dorsal halves, fixed for approximately 12 hours in 4% formaldehyde in 0.1 M phosphate buffer (pH 7.0), and dehydrated through a graded ethanol series. Specimens were then infiltrated with JB4-Plus resin (Electron Microscopy Sciences), and embedded in polyethylene molding trays anaerobically sealed with block holders and wax. Two and a half micrometer thick sections were cut with a glass knife on a Sorvall JB-4 microtome (Sorvall, Newtown, CT) and placed on glass slides. Sections were stained for 15 min with Gill's hematoxylin, rinsed with water, stained for 5 min with Eosin Y, and rinsed again with water. Slides were then dried, mounted with Poly-Mount (Polysciences Inc.), and imaged using differential interference contrast (DIC) optics on a Nikon 90i microscope connected to a Nikon DS-Fi1 high-definition color CCD camera.

Results:

The mosquito heart pumps hemolymph in both anterograde and retrograde directions.

Light and fluorescence microscopy through the cuticle of gently immobilized live mosquitoes confirmed that the dorsal vessel is the primary hemolymph-pumping organ in mosquitoes (Figure 1A). It extends from the posterior of the abdomen to the head and is divided into two anatomically and functionally distinct regions: the heart and the aorta. The heart is an unbranched tube that runs immediately underneath the dorsal midline of the abdominal tergum and is the focus of this study. The aorta is located in the thorax and serves as a conduit for hemolymph actively propelled by the heart [69, 70]. Because of heavy sclerotization in the dorsal portion of the thorax, the aorta of live mosquitoes was not definitively visualized in this study. Analysis of the contraction dynamics of the heart, along with the concurrent visualization of the flow of endogenous lipid droplets and air bubbles, demonstrated that the heart is a dynamic organ which alternates between pumping hemolymph in anterograde (toward the head) and retrograde (toward the tip of the abdomen) directions. Quantitative assessment of contraction mechanics showed that the dorsal vessels of unmanipulated five-day-old mosquitoes in their resting state contract at a rate of 1.37 Hz (SD = 0.15; 82.4 beats per minute; Fig. 1B). Interestingly, the direction in which the heart contracts reverses 5.3 times per minute (SD = 1.78) but the contraction rate does not change with contraction direction (*t*-test $P = 0.8398$): anterograde contractions occur at a rate 1.38 Hz (SD = 0.12) while retrograde contractions occur at a rate of 1.35 Hz (SD = 0.23). Whereas the frequency in which the heart contracts is the same regardless of pulse direction, the heart spends more time, and hence contracts more, in the anterograde direction (*t*-test $P < 0.0001$). The average number of anterograde contractions in a 60 second recording is 59.1 (SD = 2.46) while the average number of retrograde contractions in a 60 second

A. Mosquito restraint and dorsal vessel visualization:

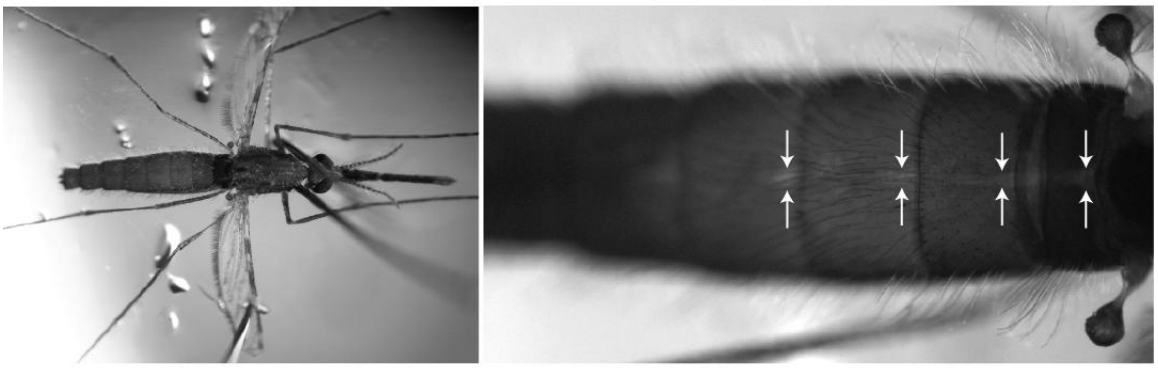

B. Contraction (pulse) rate:

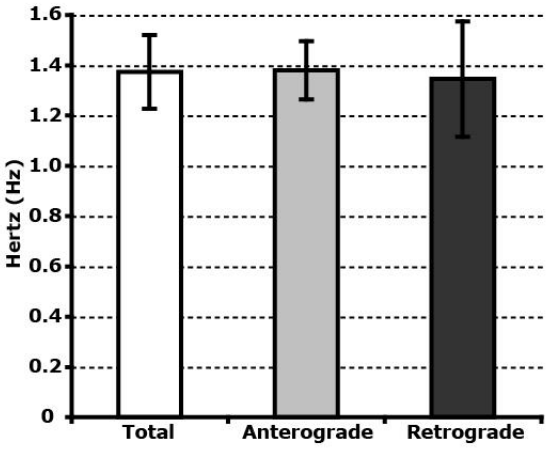

C. Number of contractions in a 60 second recording:

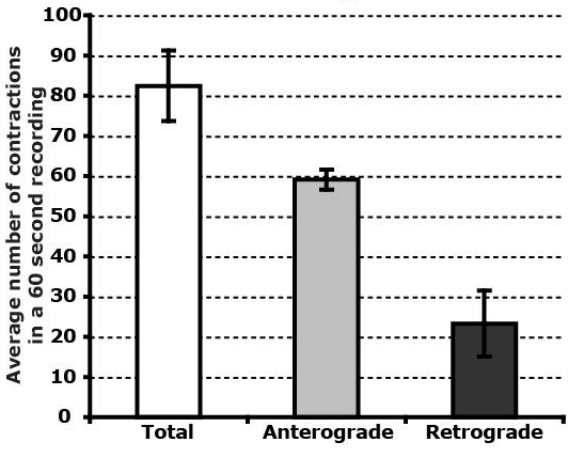

D. Percentage of contractions and time:

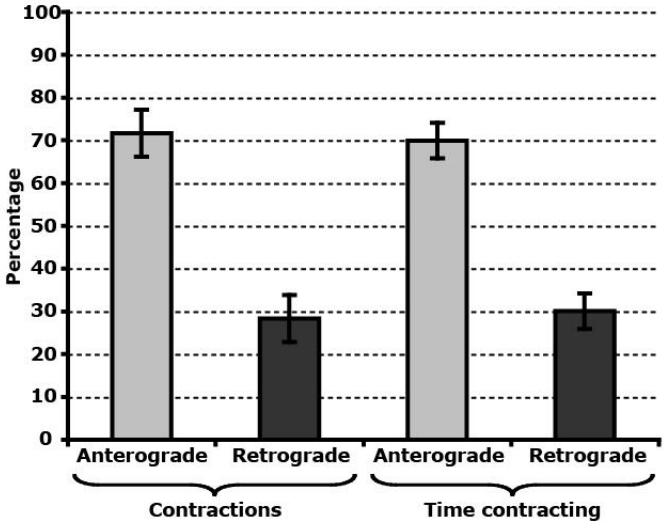

E. Contraction period length:

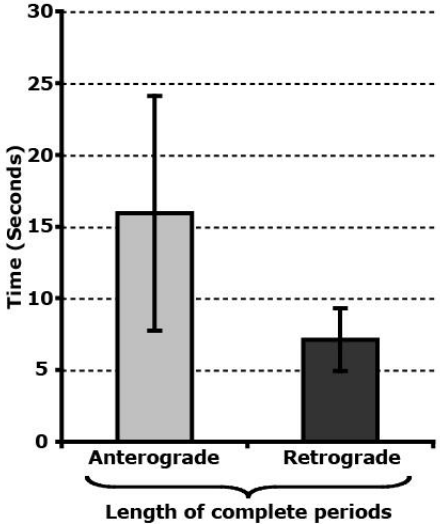

Figure 1. Quantitative analyses of heart contractions. (A) Mosquito restraint system showing pins placed against the anterior pronotal lobe and through non-vascular areas of the wings. Note that no pins are inserted through the body cuticle and that the dorsal vessel and dorsal diaphragm are clearly visible under incandescent light (arrows). (B) The mosquito heart contracts at a rate of 1.37 Hz. Peristaltic contractions can reverse direction, but the contraction rate does not change with contraction direction. (C) In an average 60 second recording, the heart contracts 59 times in the anterograde direction and 23 times in the retrograde direction. (D) Approximately 72% of the contractions occur in the anterograde direction and 28% of the contractions occur in the retrograde direction. In parallel, the heart contracts 70% of the time in the anterograde direction and 30% of the time in the retrograde direction, reaffirming that the contraction rate is the same regardless of direction. (E) The heart of resting mosquitoes switches contraction direction an average of 5.3 times per minute, contracting for 16 consecutive seconds in the anterograde direction before switching and contracting for 8 consecutive seconds in the retrograde direction. (n = 3 independent cohorts of 10 mosquitoes each).

recording is 23.3 (SD = 8.23; Fig. 1C). Hence, 71.7% (SD = 5.5) of contractions are in the anterograde direction, depositing hemolymph in the head, while 28.3% (SD = 5.5) of the contractions occur in the retrograde direction, depositing hemolymph in the last segment of the abdomen (Figure 1D). In concert with these data, mosquitoes spend 70.0% (SD = 4.12) of the time contracting the heart toward the head and 30.0% (SD = 4.12) of the time contracting the heart toward the tip of the abdomen, suggesting that hemolymph flow is primarily directed toward the head (Figure 1D). When we analyzed data from complete periods, the length of each period was highly variable: anterograde periods averaged 15.9 seconds (SD = 7.1) while retrograde periods averaged 8.2 seconds (SD = 2.2; Fig. 1E). Finally, these observations were confirmed by visualizing the trajectory of intrathoracically injected red fluorescent microspheres in a parallel group of mosquitoes.

Peristaltic contractions of the heart drive hemolymph flow but the contraction mechanism changes with propulsion direction.

Detailed high magnification observation of the heart's second abdominal segment as well as the entire abdomen of unmanipulated mosquitoes revealed that, regardless of directionality, hemolymph propulsion is accomplished by wave-like peristaltic contractions that are represented by the transition of systolic (contraction) and diastolic (relaxation) phases in each abdominal segment. The direction of the wave-like sequential contractions of the heart dictates the direction of hemolymph flow. That is, peristaltic contractions originating in the posterior of the heart travel toward the head and propel hemolymph in the anterograde direction. Conversely, peristaltic contractions that begin near the junction between the thorax and the abdomen and progress toward the

tip of the abdomen propel hemolymph in the retrograde direction. While peristalsis drives both anterograde and retrograde contractions, the contraction mechanism changes with propulsion direction. Anterograde contractions involve a smooth peristalsis where systole does not completely close the dorsal vessel. In contrast, retrograde contractions seem more forceful and the systole phase appears to involve a complete constriction of the heart.

Hemolymph flows through the heart at velocities greater than 8 mm/sec.

Tracking of intrathoracically injected red fluorescent microspheres showed that flow through the dorsal vessel is rapid and parallels the high rate of heart contractions. Also, similar to the data on contraction rate, no significant difference was seen between anterograde versus retrograde hemolymph velocity (*t*-test $P = 0.391$; Fig. 2). On average, hemolymph flowed in the anterograde direction at a velocity of 8.03 mm/sec (SD = 2.17) and in the retrograde direction at a velocity of 8.29 mm/sec (SD = 2.01). All microspheres were tracked for a minimum distance of 0.5 mm and the average distances tracked were 1.28 mm (SD = 0.32) in the anterograde direction and 1.43 mm (SD = 0.30) in the retrograde direction. The maximum and minimum average velocities for the entire paths tracked were also similar between groups: the anterograde maximum was 14.75 mm/sec and the retrograde maximum was 13.47 mm/sec while the anterograde minimum was 4.11 mm/sec and the retrograde minimum was 3.73 mm/sec. Across shorter distances hemolymph can move even faster, with frame-to-frame maximum velocities of 19.62 mm/sec and 22.38 mm/sec for anterograde and retrograde directions, respectively.

Overall, the bolus-like travel of microspheres through the dorsal vessel confirmed the morphological observations showing that in both directions a peristaltic pump drives hemolymph propulsion. Because the diameters of the dorsal vessel (which can exceed 50 µm) and circulating hemocytes are considerably greater than the diameter of the microspheres tracked (2 µm), we believe that the velocity of particles is an accurate representation of the velocity of hemolymph flow. Furthermore, similar results were obtained when soluble Alexa Fluor dye was injected instead of beads.

Hemolymph flow is accomplished by the sequential contraction of muscle fibers arranged in a helical twist with respect to the lumen of the heart.

Light microscopic visualization of live mosquitoes, sectioned mosquitoes, and mosquitoes that were formaldehyde-fixed and the musculature stained with Alexa Fluor 488-conjugated phalloidin showed that the heart is a muscular tube that spans the length of the abdomen (Figure 3). When viewed from posterior to anterior, cardiac striated muscle fibers form a clockwise helical twist with respect to the lumen of the heart, and it is the directional sequential contraction of these fibers that propels hemolymph from one end of the organism to the other.

Heart contractions are aided by the support of six complete pairs of bilaterally symmetrical alary muscles that span all abdominal sutures with the exception of the junction between the seventh and eight abdominal segments (posterior suture),

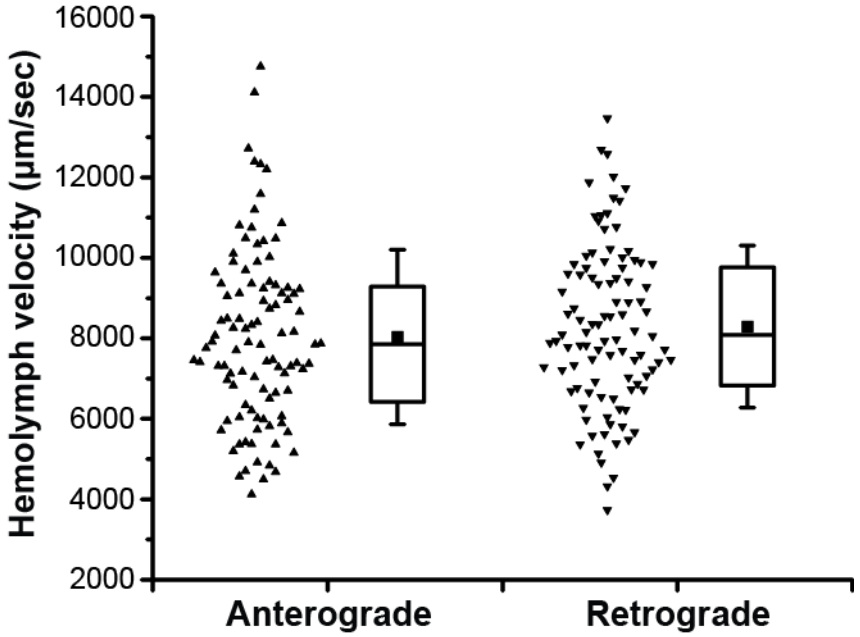

Figure 2. Velocity of hemolymph flow through the heart. Tracking of inoculated red fluorescent microspheres showed that hemolymph travels in anterograde and retrograde directions at an average speed greater than 8 mm/sec. For each flow direction (anterograde and retrograde), raw data are plotted on the left and a summary of the data showing mean (solid square), median (center line), 50% of the data (box), and standard deviation (bars) is plotted on the right.

where musculature resembling the anterior end of two alary muscle pairs attach the posterior end of the heart to the tergum (Fig 3A,C-E). Alary muscles originate in the lateral edge of the tergum (near the junction between the tergites and the pleurites) in the anterior portion of each abdominal segment and initially fan out into two large bundles, each of which promptly subdivides into two bundles, and each divides again into between 10 and greater than 30 myofibers that bind the heart, forming baskets that tether the dorsal vessel to the abdominal cuticle. The end point of alary muscle fibers varies with their location, but they firmly bind the dorsal vessel, with most fibers attaching to the ventral half of the heart (Figure 3A,E). Fibers at the center of the basket bind the heart at a 90° angle before binding myofibers that originate from the paired alary muscle on the opposite side of the heart (Figure 3A). Fibers at the anterior and posterior edges of the basket bind the heart at a sharp angle and continue on to bind myofibers from alary muscles that originate in adjoining abdominal segments (Figure 3A). The tension created by the binding of alary muscles to the heart causes an expansion of the cross-sectional area of the heart, giving the heart a segmented appearance that resembles six chambers joined by tapered segments. In addition to supporting the mosquito heart, alary muscles, along with connective tissue, form an incomplete dorsal diaphragm that delineates the pericardial sinus containing the heart and pericardial cells and separates them from the perivisceral sinus (Figure 3B). It is possible that this dorsal diaphragm may create a filter that limits the size of particles entering the heart.

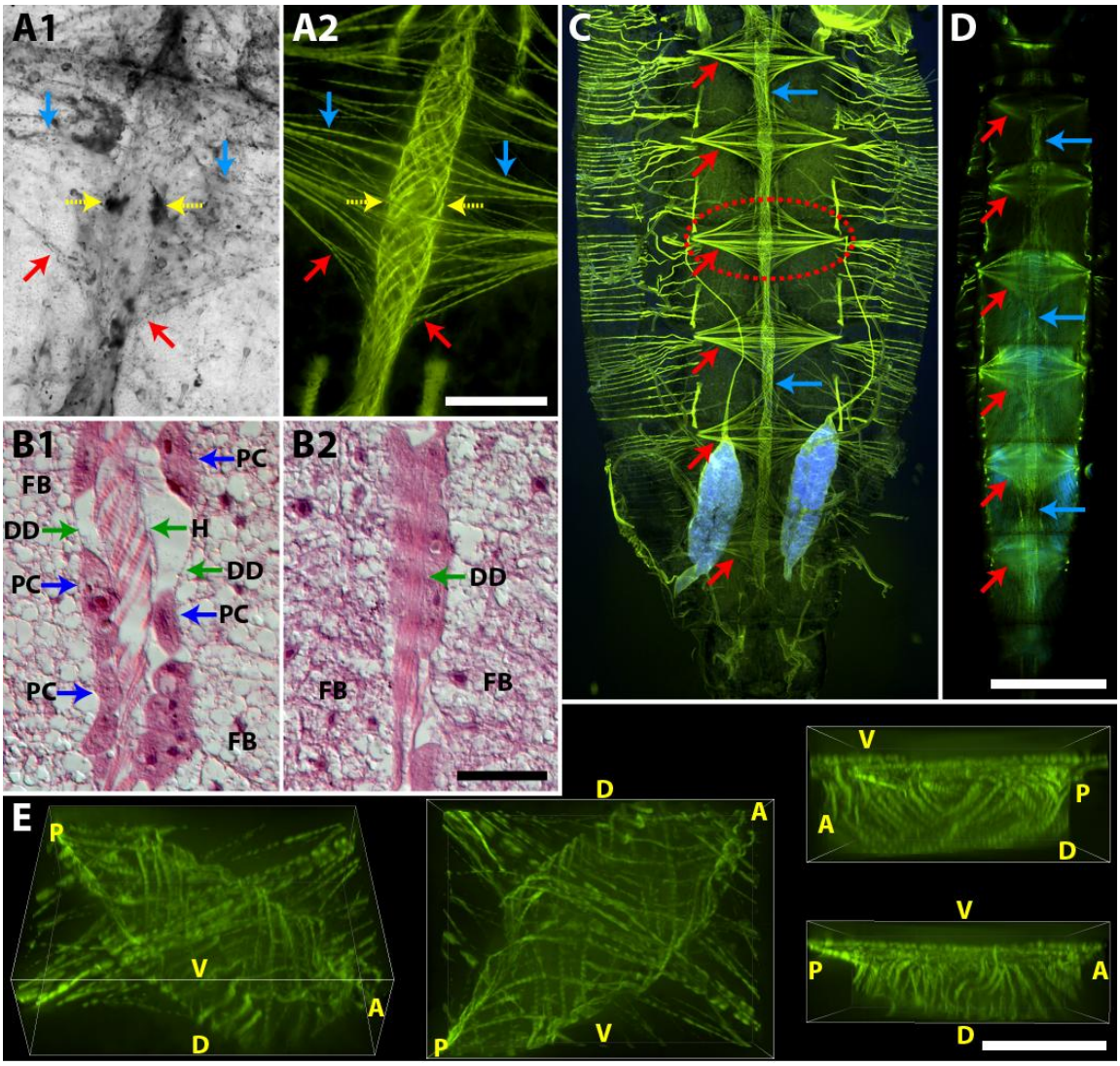
A1
A2
C
D
B1
PC
FB
DD
H
DD
PC
PC
PC
FB
B2
DD
FB
FB
E
P
V
A
D
D
A
P
V
V
A
P
D
V
P
A
D

Figure 3. Musculature associated with the mosquito heart. All images are oriented with anterior side toward the top (with the exception of panel E), and panels A2, C, D and E show muscle fluorescently labeled green with phalloidin-Alexa Fluor 488. (A) Bright field (A1) and fluorescence (A2) imaging of dissected whole mounts showing that muscle fibers are arranged in a clockwise helical twist that extends toward the thorax. Alary muscle fibers bind the heart and either join myofibers that originate from the opposite alary muscle (blue arrows) or join alary muscle fibers that originate in neighboring abdominal segments (red arrows). Paired ostia are labeled with India ink (yellow dotted arrows). (B) Histological sections of mosquito abdomens showing the clockwise helical spiraling of cardiac musculature (heart; H), the dorsal diaphragm (DD), pericardial cells (PC), and fat body (FB). (C) Fluorescence imaging of dissected whole mount showing that the mosquito heart spans the length of the abdomen and contains helically oriented musculature (e.g., blue arrows). Six complete pairs of alary muscles span the abdominal sutures (red arrows; one complete pair inside dotted circle) except the suture between the last two abdominal segments. Ovaries are stained blue with Hoechst 33342. (D) Fluorescence imaging through the cuticle of a fixed mosquito showing that the dorsal vessel is located immediately underneath the dorsal cuticle (e.g., blue arrows) and showing the six complete pairs of alary muscles (red arrows). (E) 3-D rendering of a segment of the mosquito heart, showing the clockwise helical spiraling of muscle fibers and the alary muscles associated with it. A, anterior; P, posterior; D, dorsal; V, ventral. Bars: A = 75 µm; B = 40 µm; C-D = 500 µm; E = 20 µm.

Hemolymph enters the heart through incurrent ostia and thoracic venous channels, and exits through excurrent distal openings.

Tracking of red fluorescent microspheres in hundreds of videos showed that hemolymph enters the heart through 14 abdominal and thoraco-abdominal ostia (Figure 4). During anterograde flow, particles unidirectionally enter the lumen of the heart through ostia while during retrograde flow particles neither enter nor exit, suggesting that abdominal ostia open during the diastole phase of each anterograde contraction while remaining completely closed when the heart is contracting in the retrograde direction (Figure 4). As particles enter the heart through the ostia, their velocity changes from as low as a virtual standstill while in the hemocoel to speeds in excess of 4 mm/sec in the lumen of the heart (Figure 4B).

Abdominal ostia are located as pairs on the lateral wall of the heart near the anterior portion of segments 2, 3, 4, 5, 6, and 7, for a total of 12 abdominal ostia. Each ostium is composed of two muscular funnel-shaped lips that protrude into the lumen of the heart at an anterior angle (Figure 5), and are morphologically similar to the one-way incurrent ostia described in other insects (no excurrent ostia were structurally or functionally observed in *Anopheles* mosquitoes)[6]. The location of the ostia is dorsal of the lateral midline of alary muscles but slightly posterior, and these valves are within the pericardial sinus delineated by the incomplete dorsal diaphragm formed by the alary muscles and accompanying connective tissue (Figure 3A). Visual observation of the alary muscles did not conclusively show that they directly bind each ostium or directly participate in the peristaltic contraction of the vessel. However, because the ostia are located near the center of each alary basket and complete alary muscles are only present in regions surrounding the ostia (complete pairs are not present in the suture

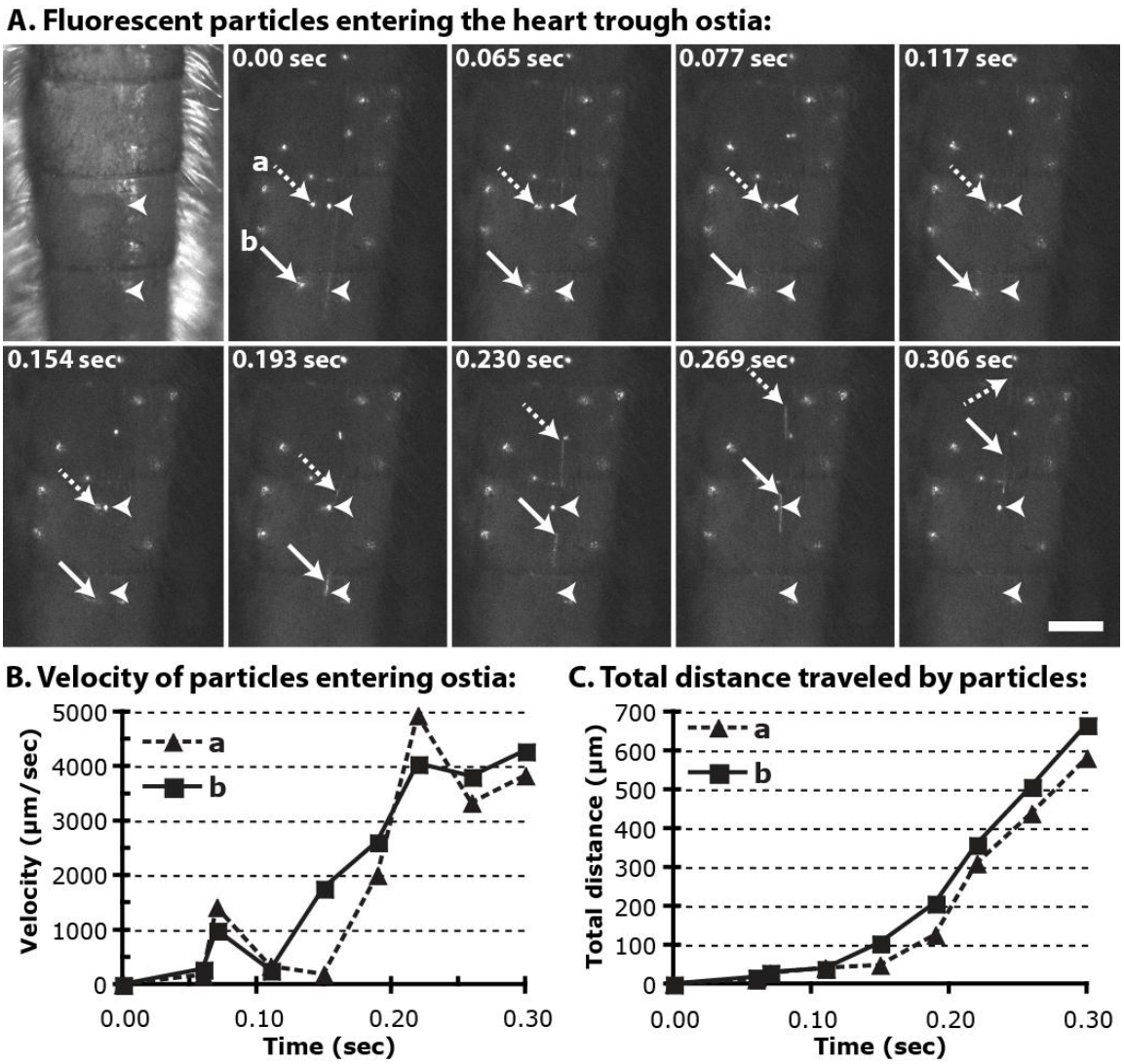

Figure 4. Tracking of particles as they enter the heart through ostia and travel in the anterograde direction. (A) Bright field (top left) and sequence of consecutive fluorescence images tracking two 2 µm diameter red fluorescent microspheres as they enter through ostia (microsphere a, dotted arrow; microsphere b, arrow; ostia, arrowhead). Both particles enter the lumen of the heart at the 0.193 sec mark. Bar = 200µm. (B) Velocity plot showing that while in the hemocoel particles move slowly but once inside the heart they travel at speeds in excess of 4 mm/sec. (C) Distance plot showing that during the 0.193 sec the particles were tracked in the hemocoel they traveled less than 100 µm while during the 0.113 sec they were tracked inside the heart they traveled greater than 500 µm.

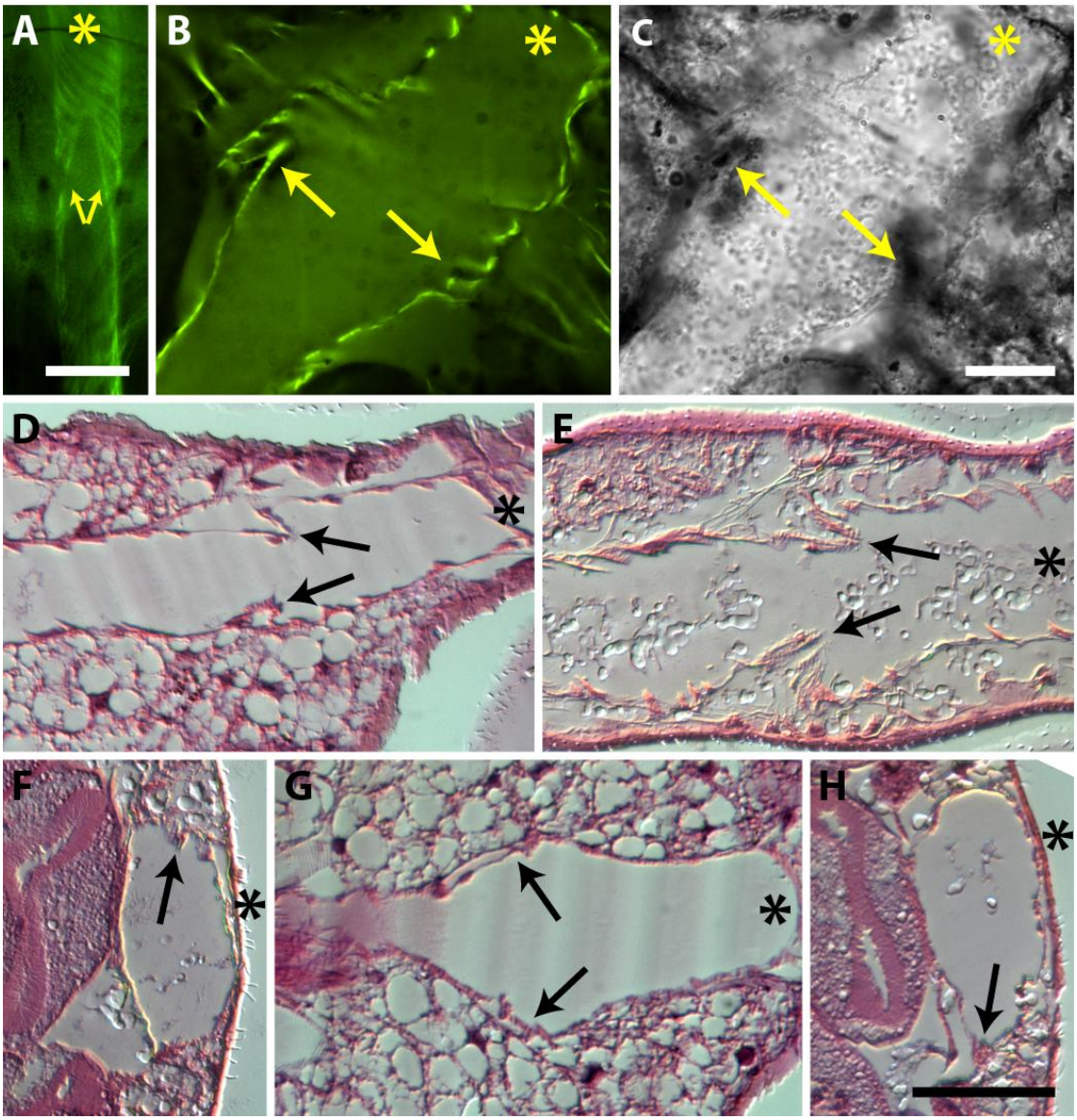

Figure 5. Incurrent abdominal ostia. Asterisk (*) denotes anterior in panels A-E and G, and dorsal in panels F and H. (A) Visualization of labeled muscle through the dorsal cuticle. Ostial lips (arrows) extend from the lateral wall and are angled toward the anterior of the mosquito. (B-C) Fluorescence (B) and bright field (C) parallel images showing incurrent ostia composed of muscle fibers (B; arrows) and counterstained with India ink (C; arrows). (D-F) Longitudinal (D, E) and cross (F) sections of the heart showing muscular ostia in the open position (arrows). Note that muscle is oriented in a helical twist with respect to the lumen of the vessel. (G-H) Longitudinal (G) and cross (H) sections of ostia in the closed position (arrows). Note that in this static view of peristalsis heart regions can be seen dilated as wide as 55 µm in diameter as well as completely constricted. Bars: A = 50 µm; B-C = 20 µm; D-H = 40 µm.

between segments 7 and 8 where there are no ostia; see below), it is possible that the alary muscles may indirectly control the opening and closing of the ostia and pull the heart into diastolic position when the cardiac helical muscles are relaxed. This is not in conflict with the opening of ostia only during anterograde flow as the angular nature of the ostial lips may prevent them from opening when hemolymph is flowing in the retrograde direction.

The heart is attached to the aorta at the thoraco-abdominal junction by musculature resembling the posterior portion of a pair of alary muscles (Figure 6). As mentioned, during retrograde flow hemolymph does not enter the heart through abdominal ostia. Instead, hemolymph flowing through venous channels in the lateral-posterior thorax enters the heart through what appears to be a single pair of ostia located in the anterior end of the heart at the thoraco-abdominal junction (Figure 6A-B). Following entry into the vessel, hemolymph flow is dictated by the direction of the peristaltic contractions of the heart. Mosquito venous channels appear to be homologous to those recently discovered in *Drosophila* [75], and all hemolymph propelled in the retrograde direction appears to originally reach the heart through these newly discovered channels. Further experiments attempted to assess whether hemolymph can also enter the heart through the aorta. Although visualization of flow through the aorta was not possible due to heavy sclerotization, indirect evidence from actin labeling studies showed that the aorta lacks significant musculature and likely collapses during retrograde flow (Figure 6B). Hence, retrograde hemolymph transport through the aorta is unlikely.

Hemolymph exits the dorsal vessel through excurrent openings located at each end of the vessel. During anterograde flow hemolymph exits through the anterior

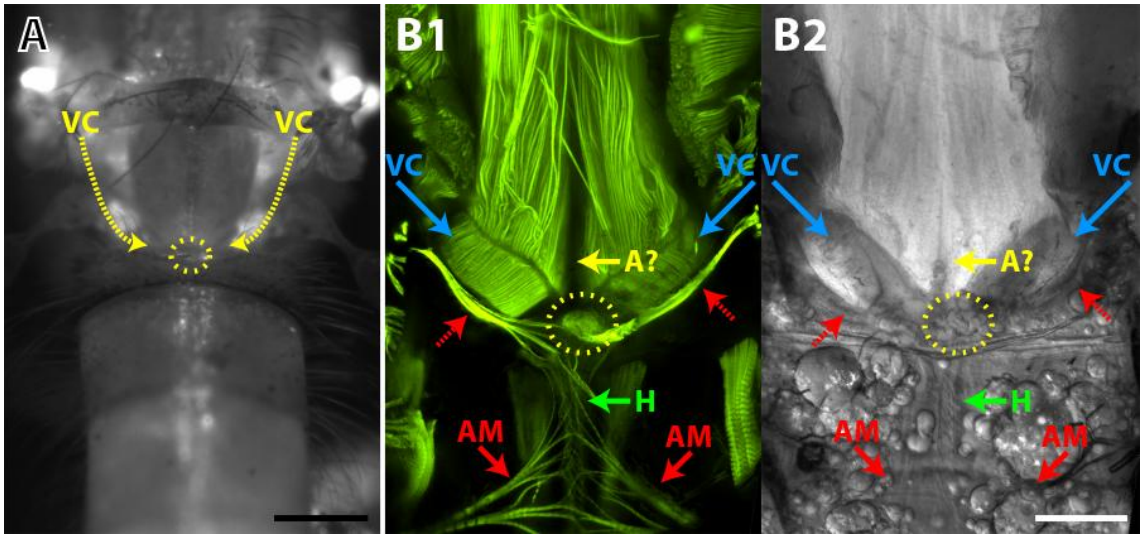

Figure 6. Venous channels and aorta. Mosquitoes were imaged from the dorsal side and images are oriented with the anterior of the mosquito toward the top. (A) Image of a living mosquito injected with red fluorescent microspheres. Fluorescent flow lines in the lateral posterior thorax (arrows) represent venous channels (VC) that collect hemolymph from the thorax and channel it to thoraco-abdominal ostia (dotted circle) before entering the heart. (B) Fluorescence (B1) and bright field (B2) images of a mosquito dissected along a coronal plane. Labeling of muscle with phalloidin-Alexa Fluor 488 (B1) showed that the heart (H) is tethered to the aorta and venous channels by musculature that resembles the posterior portion of a pair of alary muscles (red dotted arrows). Hemolymph traveling through the venous channels (VC) enters the heart through a pair of thoraco-abdominal ostia putatively located at the junction between the heart and the aorta (dotted circle). The lack of muscle in the region where the aorta is located (A?) suggests that no significant musculature is associated with that portion of the dorsal vessel. AM, alary muscles. Bars: A = 200 µm; B = 100 µm.

excurrent opening of the aorta, depositing hemolymph in the head region. This anterior excurrent opening was not directly visualized in this study because of the opacity of the thoracic dorsal cuticle, but flow analysis in the cervix and anterior thorax supports this hypothesis (data not shown). During retrograde flow hemolymph exits through the caudal excurrent opening of the heart (Figure 7). This excurrent opening is located in the anterior portion of the eighth (last) abdominal segment and is tethered to the tergum by two pairs of bilaterally symmetrical muscle bundles that resemble the anterior halves of alary muscle pairs (Figure 7A-D). These muscle bundles emerge from two distinct points in the lateral tergum, with the first pair originating near the junction between the 7^{th} and 8^{th} abdominal segments (nearly parallel to the excurrent opening) and the second originating posterior of the caudal end of the heart. Both pairs extend toward the anterior of the insect before binding the heart, and likely function to prevent the heart from being pulled forward during contractions and to facilitate the opening and closing of the excurrent opening. Detailed analysis of numerous preparations suggests that the excurrent opening is composed of two slits formed by the crisscrossing of cardiac musculature to form a laterally oriented figure eight (Figure 7B-C). The two resultant cavities form the hemolymph exit points, with additional muscle fibers extending toward the posterior of the insect and serve to attach the caudal end of the heart to the tergum. The exact conformation of the excurrent opening varies depending on the contraction state of the heart, but the overall structure more closely resembles the double opening model previously described in Culicidae and Calliphoridae [29, 79, 80] than the single opening model described in Drosophilidae [75]. Tracking of inoculated red fluorescent microspheres showed that the posterior excurrent opening allows small volumes of hemolymph to enter the heart when contracting in the anterograde direction while remaining fully open when contracting in the retrograde direction, allowing the entire contents of the vessel to empty into the posterior abdomen at high velocity (Figure 7E).

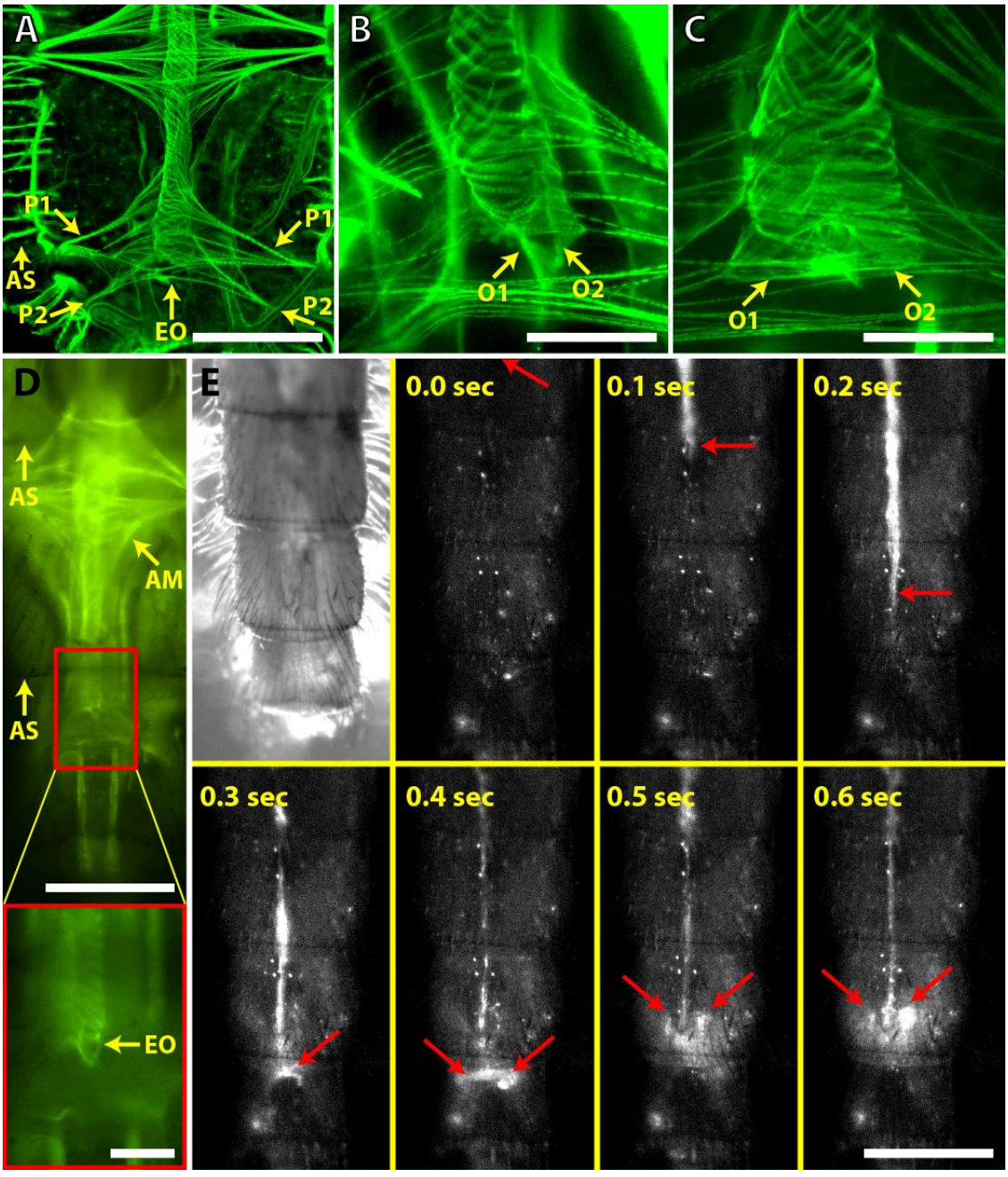
A
P1
P1
AS
P2
EO
P2
B
O1
O2
C
O1
O2
D
AS
AM
AS
EO
E
0.0 sec
0.1 sec
0.2 sec
0.3 sec
0.4 sec
0.5 sec
0.6 sec

Figure 7. Posterior excurrent opening (EO) of the heart. All images are oriented with the anterior of the insect toward the top. (A) Fluorescence micrograph of a dissected whole mount showing the two pairs of bilaterally symmetrical muscle bundles (P1 and P2) that tether the posterior end of the heart to the dorsal cuticle. These muscles resemble the anterior portion of alary muscles. AS, abdominal suture. (B-C) Fluorescence micrographs of dissected whole mounts showing two conformations of the excurrent opening. This opening is formed by the crisscrossing of cardiac musculature, forming two hemolymph exit points (O1 and O2). (D) Fluorescence micrograph through the dorsal cuticle showing attachment of the excurrent opening to the tergum. Area inside the square is magnified in the inset. (E) Tracking of a group of red fluorescent microspheres (arrows) in a sequence of consecutive fluorescence images. Microspheres flow in the retrograde direction and exit through the two lateral slits that constitute the excurrent opening. Bars: A, D, D inset = 200 µm; B, C = 50 µm; E = 400µm.

Discussion:

In this study we used state-of-the-art imaging technologies to characterize the structure of the mosquito heart, describe the mechanisms of hemolymph propulsion, and quantify the directionality and speed of hemolymph flow. To our knowledge, this is the first study that visualized insect heart contractions while at the same time measuring hemolymph flow speed and directionality.

The data presented here are in agreement with some of the earlier data analyzing the *Anopheles* heart [29, 79]. Both this and earlier studies report the relationship between alary muscles and the heart, describe muscle helically oriented around the lumen of the vessel, and maintain that heart contractions reverse direction. However, our quantitative data show that the resting anopheline heart beats at a slower pace than previously reported and clarifies published discrepancies in the number of ostia present. The reason for the discrepancies is unclear but is likely due to the limits of the experimental techniques used in those earlier studies. Our use of fluorescently tagged phalloidin allowed for the conclusive visualization of all dorsal musculature, making the number and location of alary muscles absolutely clear. In addition, the tracking of red fluorescent microspheres allowed for the visualization of hemolymph entry into the heart and the absolute determination of the position and number of abdominal ostia. These data are in agreement with our preliminary observations of the heart of *Aedes aegypti* (not shown), and with published data on the number of alary muscles found in that culicine mosquito [72]. As for the contraction rate, the elevated number of contractions reported by Jones [29] and Iaguzhinskaja [79] is probably due to the unnatural mosquito restraint and quantification methods used or the activity state of the mosquitoes. In the study by Jones [29], for example, *An. quadrimaculatus* were restrained by gluing the body to microscope slides and the contraction rate extrapolated

using the time required for 10 consecutive heart contractions. It is likely that the firm attachment of mosquitoes using glue prevented the natural contraction of abdominal muscles that may be required for proper heart rhythms [29, 81]. In addition, the use of short intervals may not have captured natural pauses during directional switches or brief changes in pulse rates, resulting in an overestimation of contraction velocity. Alternately, the higher heart rates could be attributed to the higher level of activity of the mosquitoes assayed. Our measurements of heart rates of mosquitoes that were more stressfully manipulated by using more forceful restraints or the removal of wings or legs resulted in higher rates (data not shown). With these concerns in mind, our studies used a more natural positioning system that allowed the entire body to rhythmically flex in a natural manner, and measured contractions in each mosquito over a period of 60 consecutive seconds.

Jones [29] also characterized the heart musculature as being formed by double bands spaced 5 to 12 μm apart. Our experimental data do not support the double band model. Contraction of the vessel in conjunction with the tension created by the alary muscles increases and decreases the spacing between individual fibers, meaning that spacing can only be measured relative to location and contraction phase. In addition, Jones [29] reported that severing the alary muscles collapses the abdominal heart chambers, likely impairing hemolymph flow. Although we did not verify this, our observation that the alary muscles physically support the dorsal vessel is in agreement with their hypothesized function in maintaining chamber integrity. Overall, we hypothesize that the morphological data presented in this report are similar across Culicidae, as their general body plan is conserved [82] .

Heartbeat reversals have been observed in multiple insect orders, including Lepidoptera, Orthoptera, Homoptera, Ephemeroptera, Neuroptera, Embioptera,

Coleoptera, Hymenoptera, and Diptera [72, 75, 83, 84], and are thought to be required for (1) the proper dissemination of molecules throughout the body, (2) thermoregulation, (3) the equilibration of hemolymph pressure, and (4) tracheal ventilation. Studies on lepidopterans and brachyceran dipterans have found that the heart spends the majority of the time contracting in the anterograde direction. However, in some insects retrograde contractions occur at a slower pulse rate than anterograde contractions while the opposite occurs in others [74, 75, 80, 85, 86]. In nematoceran moquitoes we also found that the heart spends the majority of time contracting in the anterograde direction but there was no difference in the pulse rate (Hz) of anterograde versus retrograde contractions.

Changes in heart contraction patterns have been described in *Drosophila* using optical and infrared techniques, although the contraction rate and its relation to contraction direction is being debated [75, 87]. Dulcis and Levine [87] also argued that systole and diastole are synonymous with anterograde and retrograde contractions, respectively, an analysis that has since been challenged [75]. While the differences in contraction mechanics seen in *Drosophila* parallel our morphological observations, our studies show that both anterograde and retrograde contractions contain sequential periods of systole and diastole as hemolymph enters the vessel and is propelled in a bolus-like manner. The biological significance of the changes in contraction mechanics is not clear, but we hypothesize that it may be due to the dynamics of hemolymph entry into the heart. During anterograde contractions hemolymph slowly enters the heart through any of the 12 abdominal ostia or the single pair of thoraco-abdominal ostia. In contrast, all hemolymph pumped in the retrograde direction must enter the heart through the thoraco-abdominal ostia, which receive hemolymph from the venous channels. This

distribution may result in differences in hemolymph pressure and volume, necessitating different contraction mechanics.

We also observed that regardless of contraction direction, hemolymph flows through the heart at a velocity greater than 8 mm/sec, indicating that hemolymph can cross the length of the insect in less than one second. The correlative bright field/fluorescence microscopy technique we employed solved the technical limitations faced by researchers who used other direct or indirect techniques to measure either contractions or hemolymph flow, but could not simultaneously measure both. Previous studies using visible light, infrared light, thermography, and electrophysiological recordings quantified heart contractions but could not measure abosolute flow [74, 75, 84, 87, 88]. More recently, a study focusing on the grasshopper *Schistocerca americana* used synchrotron x-ray phase-contrast imaging to measure hemolymph flow speeds by tracking the movement of 10-150 μm diameter buoyant microbubbles [73], but was unable to visualize the dorsal vessel, ostia, or other tissues since this method rendered them transparent. In addition, this latter method employed a restraint system that prevented the natural contraction of abdominal muscles and the ventral diaphragm, likely resulting in altered flow [81]. In contrast, the techniques employed in our study allowed for the simultaneous use of bright field and low-level fluorescence to visualize both heart contractions and hemolymph flow in an insect restrained in a natural position. This system offers temporal and spatial resolutions that are more sensitive than those for synchrotron x-ray phase-contrast and allow for the tracking of smaller particles, although the latter method likely has a higher capability to track particles deep inside the insect.

Mosquitoes are the most important arthropod vectors of human disease and some of the most studied insects. However, our understanding of their circulatory system lags behind that of other physiological systems. This study presents a

comprehensive revision and expansion of our knowledge on the structure and function of the mosquito heart and for the first time quantifies hemolymph flow in an insect while simultaneously observing contracting dorsal vessels. Because of the multifunctional importance of hemolymph flow, we expect that continued studies on the mosquito circulatory system will lead to a better understanding of the interrelation between physiological systems, and the biology of pathogens as they migrate through the hemocoel.

CHAPTER III

INFECTION-INDUCED INTERACTION BETWEEN THE MOSQUITO CIRCULATORY AND IMMUNE SYSTEMS

Preface:

The next two chapters present our research concerning the mosquito immune response following infection. Chapter II is focused almost exclusively on major phagocytic foci that we discovered forming near the incurrent valves of the mosquito heart. We frame our results in an evolutionary context and also discuss implications on mosquito vectorial capacity and general physiology. I was responsible for nearly all of the lab work presented in this chapter. Dr. Hillyer and I worked together extensively on the conceptual aspects of the manuscript, which has been submitted for publication.

Abstract:

Insects counter infection with innate immune responses that rely on cells called hemocytes. Hemocytes exist in association with the insect's open circulatory system and this mode of existence has likely influenced the organization and control of anti-pathogen immune responses. Previous studies reported that pathogens in the hemocoel accumulate on the surface of the insect heart. Using novel cell staining, microdissection and intravital imaging techniques, we investigated the mechanism of pathogen

accumulation in the pericardium of the malaria mosquito, *Anopheles gambiae*, and discovered a novel insect immune tissue, herein named periostial hemocytes, that sequesters pathogens as they flow with the hemolymph. Specifically, we show that there are two types of endocytic cells that flank the heart: periostial hemocytes and pericardial cells. Resident periostial hemocytes engage in the rapid phagocytosis of pathogens, and during the course of a bacterial or *Plasmodium* infection, circulating hemocytes migrate to the periostial regions where they bind the cardiac musculature and each other, and continue the phagocytosis of invaders. Periostial hemocyte aggregation occurs in a time- and infection dose-dependent manner, and once this immune process is triggered, the number of periostial hemocytes remains elevated for the lifetime of the mosquito. Finally, the soluble immune elicitors peptidoglycan and β-1,3-glucan also induce periostial hemocyte aggregation, indicating that this is a generalized and basal immune response that is induced by diverse immune stimuli. These data describe a novel insect cellular immune response that fundamentally relies on the physiological interaction between the insect circulatory and immune systems.

Introduction:

Pathogens transmitted by mosquitoes must traverse the insect's open body cavity (hemocoel) during their journey from the midgut to the salivary glands, and this obligate migration places them in direct conflict with the insect's circulatory and immune systems. The insect circulatory system consists of hemolymph (blood), the hemocoel, and pulsatile organs, of which the dorsal vessel is the most important [25]. The dorsal vessel extends along the dorsal midline of the insect and is anatomically divided into a thoracic aorta and an abdominal heart. In adult mosquitoes, the heart drives hemolymph

propulsion by sequentially contracting in a wave-like manner, with the contractile waves periodically alternating between propagating in the anterograde (toward the head) and retrograde (toward the posterior abdomen) directions [32, 33]. When the heart contracts in the anterograde direction, hemolymph enters the lumen of the vessel through six pairs of incurrent ostia (valves) located in abdominal segments 2 through 7 and exits through an excurrent opening located in the head region [32, 33]. When the heart contracts in the retrograde direction hemolymph enters the vessel through a single ostial pair located at the thoraco-abdominal junction and exits through an excurrent opening located in the terminal abdominal segment. Variants of this arrangement are seen in all insects and similar systems are present in all arthropods [6], conclusively supporting its ancient origin.

While insect circulatory processes have been primarily studied for their role in transporting nutrients, wastes and signaling molecules, one aspect that has been overlooked is the relationship between hemolymph circulation and immune responses. The insect immune system relies on innate reactions to fight pathogens and involves both cellular and humoral components [7, 89, 90]. To date, studies on insect immunity have focused primarily on dissecting the molecular bases of immunity and on understanding the cellular biology of hemocytes (immune cells). These experiments have largely assessed immune responses at single points in time, and have used methods that require insect death during the extraction of hemocytes or other tissues. In the hemocoel, hemocytes, humoral immune factors and pathogens exist in contiguous association with the insect's circulatory organs and have likely shared such an existence throughout the course of arthropod evolution. Because this association occurs in a fluid and dynamic space, we hypothesize that hemolymph currents influence the temporal and spatial control of anti-pathogen responses. Furthermore, given that the closed

circulatory and lymphatic systems of vertebrate animals are integrally associated with immune surveillance [91, 92], we hypothesize that coordinated interactions between the insect's open circulatory system and immune system are essential for effective insect immune responses. Whether this interaction occurs remains unexplored in any insect, and mosquitoes offer an exceptional opportunity for its investigation because: (1) physiological interactions between mosquitoes and a taxonomically diverse array of pathogens have been explored [1, 77, 93, 94], (2) the mosquito circulatory system has been well characterized [32, 33], (3) the phylogenetic distance between mosquitoes and *Drosophila melanogaster* provides a unique perspective on the evolution of the insect immune and circulatory systems, and (4) it has been proposed that mosquito immune responses could be harnessed for the control of mosquito borne disease [95, 96].

We have reported that during the course of an infection in the malaria mosquito, *Anopheles gambiae*, pathogens accumulate in discrete foci along the surface of the mosquito heart [1], and we inferred from more recent experiments that the sites of pathogen accumulation flank the heart's ostia (periostial regions) [33]. Here, we used intravital imaging and microdissection techniques to show that during the course of bacterial and malarial infections, mosquito hemocytes migrate to the periostial regions of the heart where they bind the musculature and each other, and engage in the rapid phagocytosis of pathogens. The scale of the periostial hemocyte aggregation response is unprecedented and represents the formation of an undescribed type of immune tissue. This novel invertebrate cellular immune response integrally involves hemolymph circulation and the heart, and relies on the physiological interaction between the mosquito circulatory and immune systems, supporting their coadaptation to counter pathogens. The fact that this response had not yet been described highlights our fragmentary understanding of insect immunity, and suggests that many studies into

mosquito immune responses have underestimated the role hemocytes play in controlling infection.

Materials and Methods:

Mosquito rearing and maintenance

Anopheles gambiae (G3 strain) were reared and maintained in an environmental chamber as described [33]. Briefly, larvae were hatched in plastic containers and fed a mixture of koi food and yeast. Pupae were separated by size, allowed to develop into adults, and maintained on a 10% sucrose solution at 27°C, 75% relative humidity and a 12 h light/12 h dark photoperiod. Unless stated otherwise, all experiments were carried out on female mosquitoes at 5 days post-eclosion.

Mosquito injections, bacterial infections, and treatment with immune elicitors

For injections, mosquitoes were cold anesthetized and a finely pulled glass needle was inserted through the thoracic anepisternal cleft. A volume of 0.2 µl was slowly injected into the hemocoel and mosquitoes were then placed back in an environmental chamber until assayed.

For bacterial infections, tetracycline-resistant GFP-expressing *E. coli* (modified DH5α) were grown overnight in a shaking incubator at 37° C in Luria-Bertani's rich nutrient medium (LB broth) and, unless otherwise stated, cultures were normalized to OD_{600}=2 or OD_{600}=4 using a BioPhotometer plus spectrophotometer (Eppendorf AG, Hamburg, Germany) prior to injection. To determine the absolute infection dose,

dilutions of each OD_{600}=2 and OD_{600}=4 *E. coli* culture were plated on LB agar with tetracycline, incubated at 37 °C, and the resultant colony forming units were counted 18 h later. On average, OD_{600}=2 and OD_{600}=4 represented infection doses of 38,000 and 131,000 *E. coli* per mosquito, respectively. As a non-living phagocytosis elicitor [1], 1 µm diameter FluoSpheres® carboxylate modified microspheres (Molecular Probes; Eugene, OR) were also injected into mosquitoes. Microspheres were mixed with phosphate buffered saline (PBS; pH 7.0) to a final concentration of 0.08% solids per volume prior to injection.

Three soluble immune elicitors were used in this study: peptidoglycan (PGN) purified from Gram(-) *E. coli*, PGN purified from Gram(+) *Bacillus thuringiensis*, and β-1,3-glucan. For PGN purification, *E. coli* and *B. thuringiensis* were grown overnight in LB broth at 37°C. A volume of 2 ml of each bacterial culture was independently centrifuged for 1 min at 10,000 rcf, and the resulting pellets were suspended in 1 ml of PBS. Bacteria were then lysed, while on ice, by sonication for 1 min using a Branson Sonifier 450 (Branson Ultrasonics; Danbury, CT) equipped with a 3 mm tip that was set to 20% power and 30% duty cycle. Trichloroacetic acid (TCA) was added to the lysed bacteria to a final concentration of 10% v/v, the resultant solutions were incubated for 10 min at 90°C, and the PGNs were extracted by centrifugation for 1 min at 12,000 rcf [97]. The PGN pellets were then washed 3 times by resuspending in 1 mL 75% ethanol and centrifuging for 1 min at 12,000 rcf. After the final centrifugation the PGNs were resuspended in 1 ml PBS, and the purified PGNs were dissociated into soluble fragments while on ice by sonicating for 30 min at 20% power and 30% duty, with 50% rest periods every 40 sec. Following dissociation, all non-soluble material was removed by centrifugation per standard protocol [97], and PGN solutions were normalized to OD_{600}=1 prior to injection.

β-1,3-glucan (microparticulate curdlan), a fungal immune elicitor, was prepared by sonicating 1% w/v curdlan (Sigma-Aldrich; St. Louis MO) in PBS for 5 min at 20% power and 20% duty, while on ice. Particulates remaining in the solution were then allowed to settle for 30 min while on ice, and the clear top phase was removed and used for injections [98]. Finally, although lipopolysaccharide (LPS) is commonly used as an immune elicitor, it was excluded from this study because it has been shown that LPS has little or no immunostimulatory effect in non-mammalian animals [99, 100]. Regardless, preliminary experiments using LPS yielded results that were qualitatively similar to the PGN experiments, but these observations could be due to the residual PGN found in LPS preparations.

Blood feedings and Plasmodium berghei *infections*

Five-day-old female adult mosquitoes were starved for 6 h and then allowed to feed on a *P. berghei*-infected mouse with approximately 10% blood-stage parasitemia and a 1-2% gametocytemia. A control group of mosquitoes originating from the same cohort was allowed to feed, concurrently, on an uninfected mouse. Both groups were then housed in a humidified chamber at 20.5°C for 20 days prior to the assessment of the periostial cellular immune response (see below). The $PbGFP_{CON}$ *P. berghei* strain [101] was used for experiments where periostial hemocyte numbers were counted. The RedStar strain [102] was also used to observe the interaction between hemocytes and sporozoites, as this strain retains a higher level of fluorescence following aldehyde fixation. The infection status of each mosquito was determined by visualizing parasites in the midgut and the salivary glands.

In vivo staining of mosquito hemocytes and hemolymph perfusions

To stain hemocytes inside live mosquitoes, 0.2 µl of a solution consisting of 75 µM CM-DiI (Vybrant® CM-DiI Cell-Labeling Solution, Invitrogen) and 0.75 mM Hoechst 33342 (Invitrogen) in PBS was injected into mosquitoes. It was crucial that this solution be injected within minutes of its preparation, as once the CM-DiI is placed in an aqueous environment its hemocyte-staining effectiveness rapidly decreases, approaching 0% after 10-15 min of mixing. After CM-DiI injection, mosquitoes were immediately returned to 27°C and 75% relative humidity for an incubation period of 20 min.

Circulating hemocytes were collected by perfusing the hemolymph onto the center of 1 cm diameter etched rings on Rite-On (Gold Seal; Portsmouth, N.H.) glass slides [103]. Cells were allowed to adhere to slides for 20 min at room temperature, fixed for 20 min with 4% formaldehyde in PBS, washed 3 times for 5 min with PBS, and coverslips were mounted with Aqua Poly/Mount (Polysciences; Warrington, PA). Visual examination of adherent perfused hemocytes was conducted using a Nikon® 90i compound microscope (Nikon; Tokyo, Japan) equipped with a Nikon® Intensilight C-HGFI fluorescence illumination unit and a CoolSNAP HQ^2 digital camera (Roper Scientific; Ottobrunn, Germany). Cells were counted at 1000x magnification by scanning the slides from the far left to the far right until 50 hemocytes from each individual mosquito were visualized, also keeping track of the number of fat body cells observed. Intact cells were first identified as either hemocytes or fat body by confirming the presence of a nucleus using fluorescence microscopy (Hoechst 33342) and comparing cell morphology by differential interference contrast (DIC) microscopy to the descriptions of previous authors [28]. Then, hemocytes were examined for the presence of phagocytosed GFP-expressing *E. coli*, and all cell types were examined for their incorporation of CM-DiI. Three treatments were performed (naïve, LB injected and *E. coli*

injected), and for each treatment, hemocytes from 15 individual mosquitoes that originated from 5 independent but paired cohorts were examined (i.e., for each treatment, 3 mosquitoes per cohort).

Staining of pericardial cells, heart muscle, and sessile hemocytes

The dorsal portion of mosquito abdomens were analyzed after the labeling of PCs, hemocytes and heart muscle. These tissues were labeled in the presence or absence of an immune challenge, and were labeled in the following combinations: (1) PCs and heart muscle, (2) PCs and hemocytes, and (3) hemocytes and heart muscle. In all experiments, Hoechst 33342 was used as a nuclear stain.

Depending on the experiment, PCs were stained using one of two novel methods. In the first, more permanent method, 0.2 µl of 0.2 mg/ml Alexa Fluor® conjugated IgG (either 488 or 568 nm; Molecular Probes) in PBS was intrathoracically injected and the mosquitoes were placed at 27°C for 1 h to allow the labeled proteins to be pinocytosed by the PCs. The mosquitoes were then placed in PBS and their abdomens were bisected along a coronal plane. The dorsal half of each abdomen, sans any internal organs, was isolated, rinsed, fixed in 4% formaldehyde in PBS for 10 min, washed 3x5 min in 0.1% Tween 20 in PBS (PBST), and mounted on a glass slide using Aqua Poly/Mount. For the second PC staining method, 0.2 µl of a 0.1 mM mixture of Lysotracker® Red (Molecular Probes) in PBS was intrathoracically injected and allowed to incubate for 10 min. Abdomens were then bisected along a coronal plane, rinsed in PBS, and mounted using Aqua Poly/Mount. Because Lysotracker Red stains any region that contains high lysosomal activity, it also serves as a marker for hemocyte-mediated phagocytosis of bacteria. However, Lysotracker Red cannot be aldehyde-fixed, so this

method stains the PCs briefly before the dye diffuses out, and is not useful in combination with most other staining techniques.

To examine and quantify hemocytes that were adhered to tissues, 0.2 µl of a solution consisting of 75 µM CM-DiI and 0.75 mM Hoechst 33342 in PBS was injected into mosquitoes. After allowing this solution to incubate in live mosquitoes for 20 min at 27° C, mosquitoes were injected with 0.2 µl of 16% formaldehyde. Tissues were then allowed to fix for 5 min, the mosquitoes were bisected along a coronal plane, and the dorsal halves were mounted on glass slides using Aqua Poly/Mount. Immediately following mounting, CM-DiI stained hemocytes in the periostial regions were counted through the 90i's oculars at 400x or 1000x total magnification. Hemocytes were only counted if their presence was supported by both CM-DiI and Hoechst 33342 staining, so a small number of cells (<5%) might have been excluded from our counts using this conservative method. Cells were counted as periostial hemocytes only if they were attached directly to the dorsal vessel at the ostia, or formed part of a contiguous mass of hemocytes that were attached to this region. Numbers of periostial hemocytes were recorded on a per mosquito basis, and for each treatment cell counts were conducted on at least 12 mosquitoes that originated from no fewer than 4 independently-reared cohorts. In these experiments, trials were excluded when background staining interfered with the cellular boundaries of hemocyte aggregates in any of the treatment groups.

For the co-staining of PCs and heart muscle, 1 h after the injection of Alexa Fluor-conjugated IgG (568 nm) muscle was stained by injecting a formaldehyde-phalloidin-Hoechst-Triton X 100 mixture as described [33]. Abdomens were then washed by perfusion with PBST 3 times for 5 min each, fixed a second time using 4% formaldehyde, and bisected and mounted as above. For the co-staining of PCs and hemocytes, Alexa Fluor-conjugated IgG (488 nm) was injected to stain the PCs, and

after 1 h the hemocytes were stained with CM-DiI as described above. For the co-staining of hemocytes and heart muscles, CM-DiI was injected and allowed to incubate for 20 min at 27° C, and 0.2 µl of 16% formaldehyde was then intrathoracically injected to kill and preserve the mosquito. Abdomens were then bisected, suspended for 15 min in a Phalloidin-Hoechst-Triton X 100 mixture [33], washed, and mounted on glass slides using Aqua Poly/Mount.

Still image acquisition

Perfused hemocytes and abdominal whole mounts were imaged at 200x-1000x magnification depending on which phenomenon was being captured. Specimens were viewed under differential interference contrast microscopy (DIC) and/or fluorescence illumination using the Nikon 90i microscope ensemble described above, and Z-stack images were captured using a linear encoded Z-motor and Nikon's Advanced Research NIS-Elements software. To display 2 dimensional images, all images within a stack were combined to form a focused image using the Extended Depth of Focus (EDF) module of NIS Elements. For 3 dimensional rendering, Z-stacks were quantitatively deconvolved using the AQ 3D Blind Deconvolution module of NIS Elements and rendered using the volume view feature.

Intravital time-lapse video microscopy

For intravital time-lapse video recording of the interactions between hemocytes, pathogens and the mosquito heart, hemocytes were labeled in vivo using the CM-DiI method described above. Mosquitoes were then restrained on glass slides using small

strips of Parafilm “M” (Pechiney Plastic Packaging, Chicago) to gently adhere the proboscis, legs and wings (extended) to glass slides, and spheres of Parafilm were placed on either side of the abdomen to restrict side-to-side movement. Once mosquitoes were restrained, GFP-expressing *E. coli* were injected and fluorescence-based intravital video recording of the heart region was initiated within 10 sec of treatment. Time-lapse image sequences were captured for green (GFP-*E. coli*) and red (CM-DiI-stained hemocytes) channels at 5 sec intervals using the ND-experiment capture module of NIS Elements. Hemocyte tracking was then done using the manual feature of the Object Tracker module of NIS-Elements, and hemocyte velocity was calculated by dividing the path length by the total time of tracking. To reduce the potential for damage to the mosquito, light shutters were only open while each image was being acquired, and light intensity was greatly reduced by using a neutral density filter of 16.

Statistical analyses

Cell count data was separated by treatment group and tested for normality using the Kolmogorov-Smirnov test. After confirming normality, datasets with one variable and two groups were analyzes by the t-test. Datasets with one variable and more than two groups were analyzed by one-way ANOVA, and multiple comparisons were done using Tukey’s post hoc test. Differences were deemed significant at $P<0.05$.

For statistical evaluation of the co-localization of *E. coli* fluorescence (GFP) and hemocyte fluorescence (CM-DiI) within perfused hemocyte samples or whole mount abdomens, images were analyzed using the Mander’s overlap or Pearson’s correlation coefficient (PCC) features in NIS-Elements. These measures are similar in that they

describe the amount of spatial overlap between two fluorescence channels, with the main difference being that Mander's overlap corrects for differences in signal intensity while PCC does not [104].

Results:

Pericardial cells (PCs) flank the mosquito heart but do not phagocytose pathogens

The initial goal of this study was to investigate whether pathogen accumulation around the dorsal vessel ostia (periostial regions) is due to a physical barrier or due to an active immune response (Figure 1A-B) [1]. Hemolymph in the abdominal cavity flows dorsally toward the ostia [32, 33], and as part of this flow it is possible that pathogens could become stuck in the fenestrated dorsal diaphragm or at the narrow openings of the ostia. Alternately, pathogens could be sequestered as part of an active immune response, and an earlier study suggested that this would most likely be a PC-mediated immune response [1]. To distinguish between these two scenarios we developed two novel methods for the labeling of PCs in vivo. The first employs the injection of AlexaFluor-conjugated IgG and relies on the pinocytic nature of insect PCs, while the second employs LysoTracker Red and relies on the ability of this stain to label cells with high acidic, and presumably lysosomal, content.

Co-staining of PCs and the abdominal musculature showed that PCs are binucleated cells that flank the mosquito heart, including the periostial regions (Figure 1C). However, staining of PCs after infection with GFP-expressing *Escherichia coli* showed that pathogens are not phagocytosed by PCs. Instead, pathogens accumulate between the four PCs that flank the ostia (Figure 1D). Further examination of

Lysotracker Red-stained dorsal abdomens revealed that the accumulated bacteria are inside cells with nuclear and cellular diameters that are considerably smaller than that of PCs, and that these phagocytic cells are similar in size to the phagocytic subpopulation of circulating hemocytes (granulocytes) (Figure 1E). Thus, these data show that pathogen accumulation in the periostial regions is due to an immune response that is not mediated by PCs, and suggest that the phagocytic cells are likely hemocytes.

CM-DiI selectively stains hemocytes in vivo

To determine whether the phagocytic cells identified in the periostial regions are hemocytes, we developed a novel in vivo hemocyte-staining method using the dye chloromethylbenzamido-1,1′-dioctadecyl-3,3,3′,3′-tetramethylindocarbocyanine-perchlorate (CM-DiI). Intrathoracic injection of CM-DiI into live mosquitoes, followed by hemolymph perfusion and ex vivo analysis of cell staining efficiencies showed that CM-DiI stains greater than 97% of the hemocytes collected from naïve (99%), injured (sterile injection with LB broth; 99%) and *E. coli* infected (97%) mosquitoes (Figure 2A-D). Quantitative co-localization of CM-DiI staining and the phagocytosis of GFP-*E. coli* by circulating hemocytes yielded a Mander's overlap of 70%, illustrating the high hemocyte-staining efficacy of CM-DiI. Further qualitative analyses suggested that the slightly lower hemocyte-staining efficiency seen in *E. coli* infected mosquitoes is due to lower incorporation of CM-DiI in hemocytes that have phagocytosed extremely large numbers of bacteria.

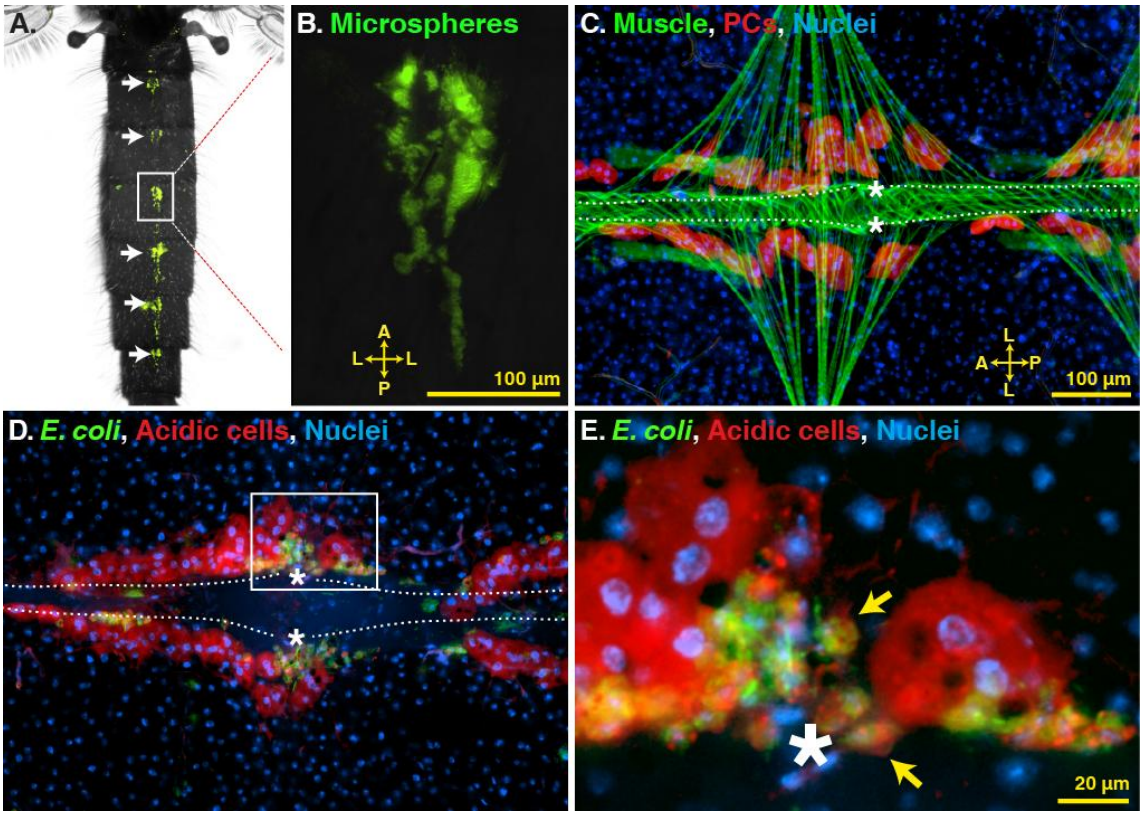

Figure 1. Identification of periostial immune foci. (A-B) Top down view of a mosquito injected with green fluorescent microspheres 24 h earlier. Microspheres accumulate in the periostial regions of each abdominal segment (arrows and rectangle, which is magnified in B). (C) Pericardial cells (568nm-IgG; red) flank the heart (phalloidin; green tube that extends horizontally), including the periostial regions (asterisks). (D-E) At 24 h post-infection with GFP-*E. coli*, numerous acidic cells (Lysotracker Red; red) are associated with the heart. PCs do not phagocytose pathogens. Instead, smaller acidic cells located at the periostial regions intensely phagocytose bacteria (e.g., rectangle in D, which is magnified in E). A, anterior; P, posterior; L, lateral; asterisks, location of the ostia; dotted lines, outline of the heart. In panels C-E, Hoechst 33342 (blue) was used as a nuclear stain.

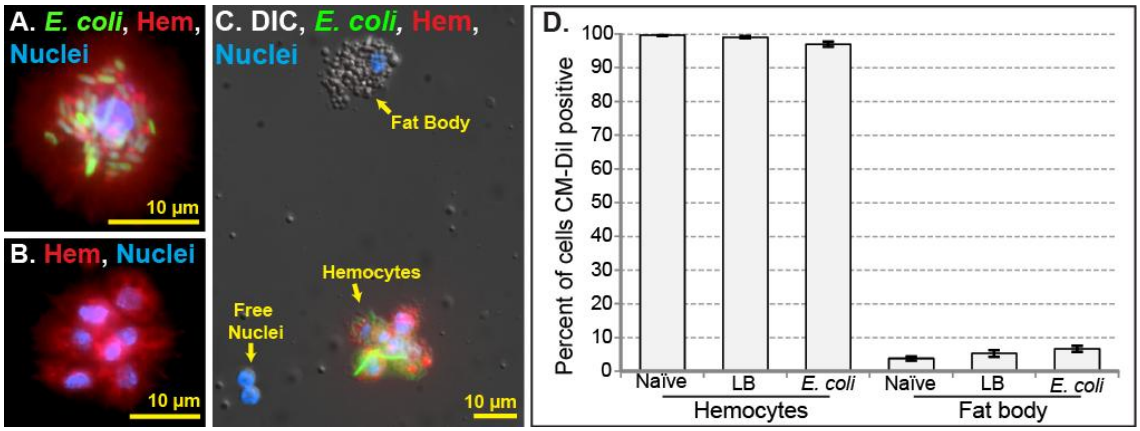

Figure 2. CM-DiI selectively stains hemocytes in vivo. (A-B) Perfused hemocytes from mosquitoes injected with CM-DiI (red) and Hoechst 33342 (blue; nuclear stain). CM-DiI stains individual hemocytes (B) and hemocyte aggregates (A) from both naïve (A) and *E. coli*-infected (B) mosquitoes. (C) Bright field and fluorescence overlay of hemocytes, fat body and free nuclei collected by perfusion. Only hemocytes stain with CM-DiI. (D) Quantitative analysis of in vivo CM-DiI staining in perfused cells from naïve, injured (LB) and *E. coli*-infected mosquitoes. Greater than 97% of hemocytes stain with CM-DiI, fewer than 5% of fat body cells stain with CM-DiI, and free nuclei do not stain with CM-DiI. Columns, mean; bars; standard error of the mean.

In addition to hemocytes, hemolymph perfusion results in the collection of small amounts of fat body as well as free nuclei from lysed cells. Visual analysis of all cellular components collected by perfusion revealed that CM-DiI only stains hemocytes (Fig 2C-D), and analysis of carcasses and other tissues from CM-DiI injected mosquitoes conclusively showed that cells other than hemocytes do not incorporate CM-DiI.

Hemocytes form periostial immune foci, which occur in close proximity to the pericardial cells

With the knowledge that a major cellular immune response occurs in the periostial regions, we then aimed to determine whether this immune response is mediated by hemocytes. Complementary hemocyte, PC, and muscle staining confirmed that this indeed is the case. Co-labeling of hemocytes and muscle showed that hemocytes laterally flank the heart at the periostial regions in both naïve and *E. coli*-infected mosquitoes (Figure 3A). Infection with GFP-*E. coli*, followed by CM-DiI injection 24 h later, revealed strong spatial overlap between GFP-fluorescence and hemocytes (Figure 3B), and suggested that hundreds of hemocytes phagocytose pathogens in the periostial regions during an active infection. Then, examination of abdomens from mosquitoes infected with non-fluorescent *E. coli* confirmed that PCs and hemocytes are two distinct cell populations, and that hemocytes occur in aggregates positioned between the 4 PCs that flank each ostial pair (Figure 3C). Finally, comparisons of cellular and nuclear diameters confirmed that hemocytes are identical in size to (1) the phagocytic cells previously detected using LysoTracker Red staining (Figure 1E), and (2) the circulating population of granulocytes (Figure 2A-C).

Because immune processes within the mosquito hemocoel occur in three-dimensional space, we then performed a series of experiments where heart muscle was labeled along with PCs, phagocytosis foci, or hemocytes. Analysis of deconvolved and volume rendered Z-stacks showed that PCs intertwine with the alary muscles while phagocytosis foci and periostial hemocytes are located dorsal of the alary muscles and in the vicinity of the ostia (Fig 3D). Taken altogether, these data describe a novel mosquito immune response, where hemocytes in the periostial regions of the heart phagocytose and degrade pathogens.

Infection induces the migration of hemocytes to the periostial regions.

Because periostial hemocytes appeared to represent a substantial proportion of the total number of hemocytes present in mosquitoes [46-48, 50, 51, 105], and because their positioning suggested a strong interaction between the mosquito circulatory and immune systems, we then investigated whether hemocytes are recruited to the periostial regions during the course of an infection. Intravital video imaging of periostial hemocytes during the first 15 min post-infection revealed that resident sessile hemocytes phagocytose *E. coli* within seconds of their injection into the hemocoel (Figure 4A-C). Pearson's correlation coefficient measurements of movies quantitatively showed this, as the fluorescence overlap of periostial hemocytes and *E. coli* increased within the first few frames of the video and began to plateau at a correlation near 60% by 3 min post-infection (Figure 4D). Longer video recordings confirmed these findings, and in addition showed that during the first hour post-infection circulating hemocytes migrate to the periostial regions (4E-G). These migrating hemocytes move into the pericardial space by slowly gliding over the alary muscles and other heart-associated musculature, and not

via a process that is exclusively driven by hemolymph flow; the median velocity of the hemocytes tracked was 1.2 μm/sec (Figure 4G), which is orders of magnitude slower than the 200-1,000 μm/sec hemolymph flow velocity at the periostial regions [33]. Overall, while most hemocytes migrate to the periostial regions as individual cells, some arrive at the pericardium in small cellular aggregates. Many of these migrating hemocytes contain phagocytosed *E. coli* prior to entering the pericardial space, indicating that they have been immune activated elsewhere in the mosquito.

To further elucidate the process of periostial hemocyte aggregation, naïve mosquitoes, mosquitoes that had been injured 24 h earlier, and mosquitoes that had been infected with various doses of GFP-*E. coli* for 24 h were injected with CM-DiI and the number of periostial hemocytes were counted. On average, 5-day-old naïve mosquitoes contain 43 periostial hemocytes, distributed among the 6 periostial regions of the abdomen (Figure 5A, C). Injury does not result in an increase in the number of periostial hemocytes, but infection with large numbers of *E. coli* for 24 h leads to a >4-fold increase in the number of periostial hemocytes (Figure 5A). Hemocyte aggregation in the periostial regions is induced in an infection dose-dependent manner (Figure 5A), with the increases in mean number of periostial hemocytes per mosquito being nearly linear for *E. coli* infection intensities of OD_{600}=1 through OD_{600}=5 (R^2=0.92; means of 69, 89, 106, 138, and 188, respectively). Then, quantitative analysis of periostial hemocyte numbers during the course of an infection revealed that hemocyte numbers in the periostial regions approximately double within the first hour, and plateau at 4 h post infection (Figure 5B). Depending on the bacterial dose and the time following infection, periostial hemocyte aggregates vary from small and dispersed groups of hemocytes to expansive and contiguous aggregates of hemocytes (Figure 5C-E).

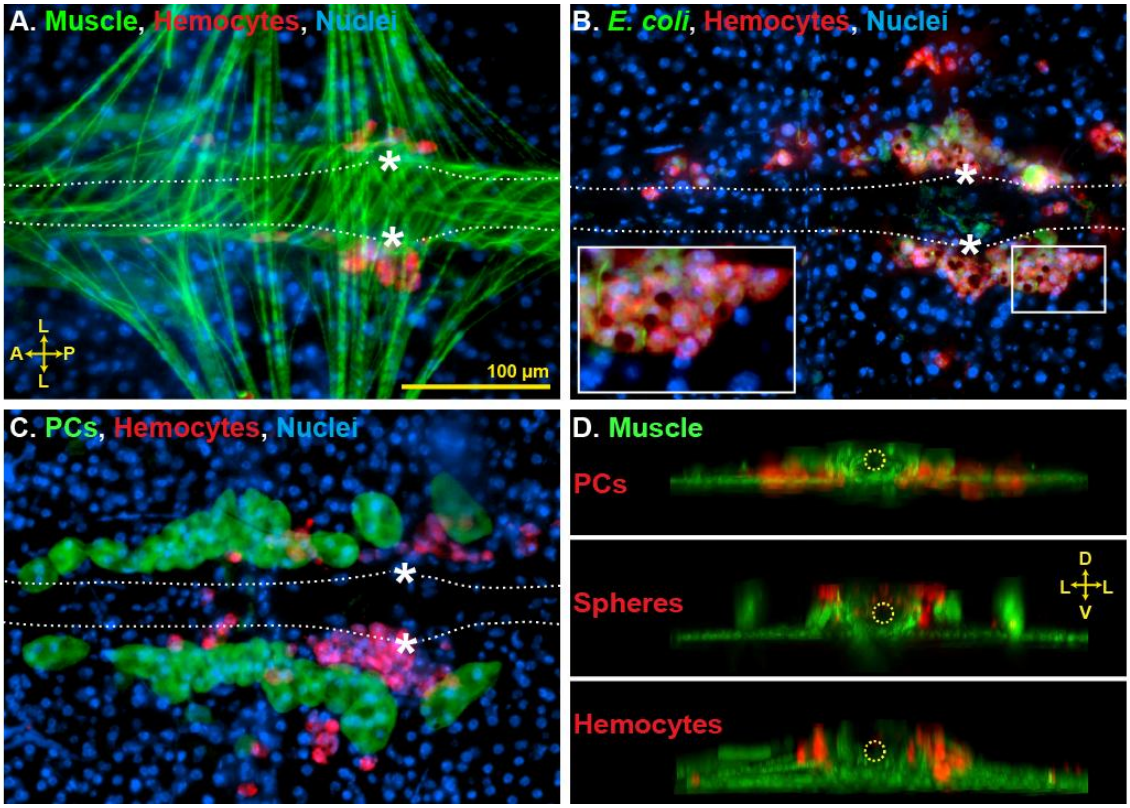

Figure 3. Hemocytes form periostial phagocytic foci, which occur in close proximity to the pericardial cells (PCs). (A) Heart musculature (phalloidin; green) and hemocytes (CM-DiI; red) 24 h following infection with non-fluorescent *E. coli*, showing hemocytes at the periostial regions. (B) Periostial hemocytes (red) 24 h after GFP-*E. coli* (green) infection, showing phagocytosis and melanization (dark spots) reactions. (C) Pericardial cells (488nm-IgG; green) and hemocytes (red) following infection with non-fluorescent *E. coli*, showing that PCs and periostial hemocytes are structurally distinct. (D) 3D-rendered volume views illustrating the spatial separation of periostial hemocytes and PCs. The point of view is looking through the lumen of the vessel (yellow circle), with the heart located dorsally and the alary muscles extending laterally in the ventral portion of the image. The PCs (red; 568nm-IgG) occur within the fan-like alary muscles (green horizontal line; phalloidin), while phagocytosis (red microspheres) and hemocytes (red; CM-DiI) occur toward the dorsal edge of the heart. D, dorsal; V, ventral; A, anterior; P, posterior; L, lateral; asterisks, location of the ostia; dotted lines; outline of the heart. In panels A-C, Hoechst 33342 (blue) was used as a nuclear stain.

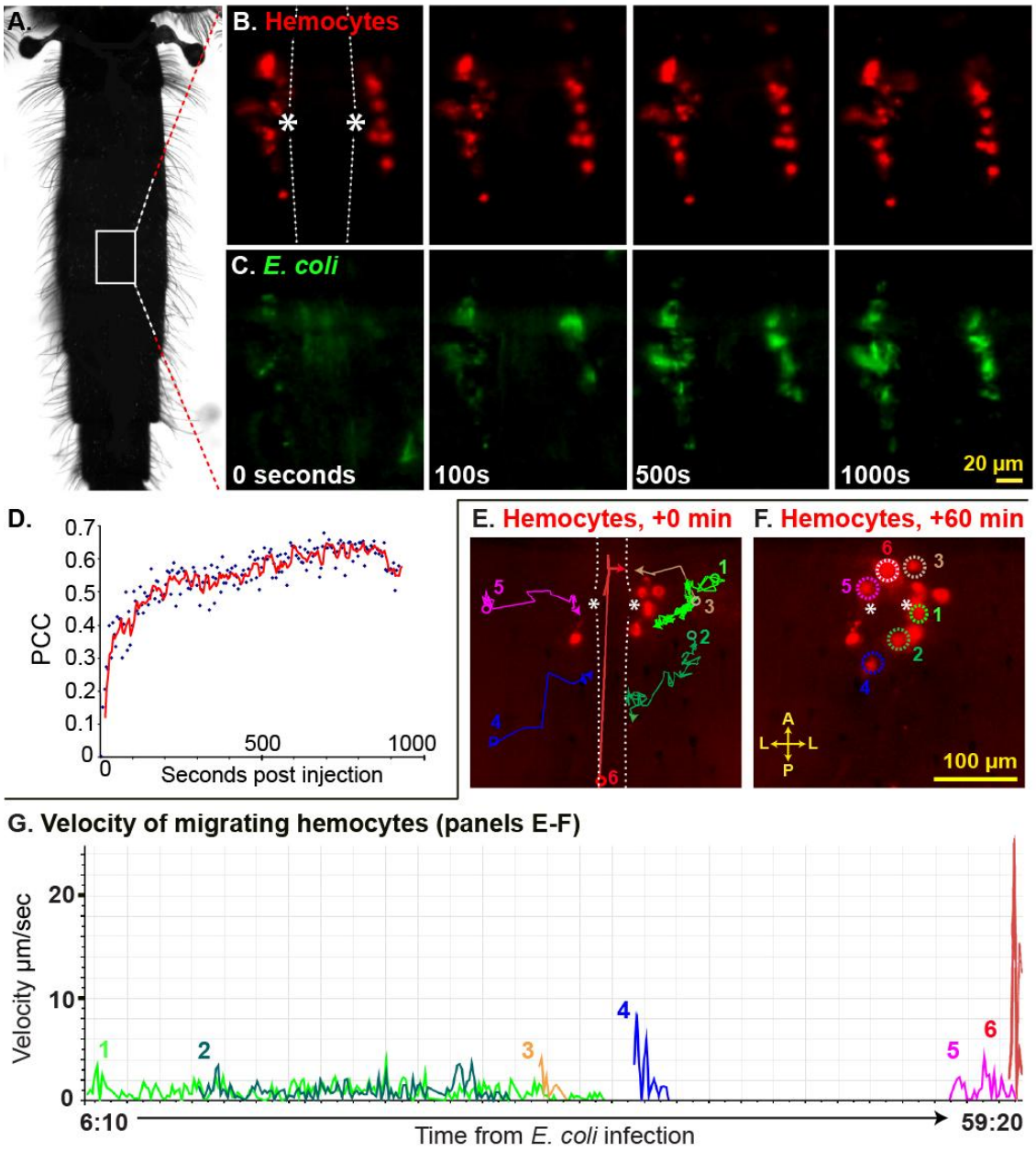
A.
B. Hemocytes
C. E. coli
0 seconds
100s
500s
1000s
20 µm
D.
PCC
0.7
0.6
0.5
0.4
0.3
0.2
0.1
0
0
500
1000
Seconds post injection
E. Hemocytes, +0 min
F. Hemocytes, +60 min
A
L
L
P
100 µm
G. Velocity of migrating hemocytes (panels E-F)
Velocity µm/sec
20
10
0
6:10
59:20
Time from E. coli infection

Figure 4. Periostial hemocytes rapidly phagocytose pathogens and infection induces the recruitment of hemocytes to the periostial regions. (A) Top-down view of a mosquito, outlining the region observed in panels B, C, E and F. (B-C) Time-lapse images of a periostial region of a mosquito whose hemocytes had been labeled with CM-DiI prior to infection. The heart is outlined by dotted lines and the asterisks denote the ostia. During the first 1,000 sec post-infection with *E. coli* little hemocyte (red) movement is observed (B), but phagocytosis of *E. coli* (green) by resident periostial hemocytes begins within seconds of infection (C). (D) Pearson's correlation coefficient analysis (A-B), quantitatively showing the rapid co-localization of hemocytes and *E. coli*. (E-F) Time-lapse images showing the migration of hemocytes (red) to the periostial regions during the first hour post-infection with *E. coli*. At the time of infection, 6 CM-DiI stained hemocytes flank the heart (E), and during the first hour of infection at least 6 additional hemocytes attach at the periostial region (F; dotted circles). The movement of each migrating hemocyte is shown in panel E using colored lines, with the circles marking the points of first observance and the arrows marking the points of attachment. (G) Velocity and acceleration of the hemocytes tracked in panels E and F as they migrate to the periostial regions, showing that hemocytes glide across the alary muscles at a median velocity of 1.2 µm/sec. A, anterior; P, posterior; L, lateral.

Infected mosquitoes at times contain more than 300 periostial hemocytes (Figure 5E), even when counting is done using our conservative protocol, which favors the exclusion of a small number of hemocytes rather than the inclusion of non-hemocytes.

While infection induces the migration of hemocytes to the periostial regions, their numbers decrease once the acute stage of infection has passed. Infection of mosquitoes with large numbers of *E. coli* (OD_{600}=4) revealed that hemocytes are recruited to the periostial regions within the first 24 h post-infection, but that the number of periostial hemocytes decreases by day 3 post-infection (not shown). Infection of mosquitoes with fewer *E. coli* (OD_{600}=2) revealed a similar trend: the number of periostial hemocytes decreases significantly by 3 days post-infection, but remains elevated for the lifetime of the mosquito, relative to similarly aged naïve controls (Figure 6A). Surprisingly, all mosquitoes assayed at 12 days post challenge had live *E. coli* in their hemocoels (and periostial regions; Fig. 6B), and the amount of melanin deposition in the periostial regions also increased as mosquitoes aged. Thus, the maintenance of elevated numbers of periostial hemocytes may be due to the continued need of cellular antimicrobial activity, as mosquitoes appear to be incapable of completely clearing an *E. coli* bacterial infection [103, 106]. Finally, based on the number of circulating hemocyte [46-48, 50, 51, 105], the periostial hemocyte population represents between 10% and 25% of the total hemocyte population post-infection, which highlights the importance of pathogen sequestration in these areas of high hemolymph flow.

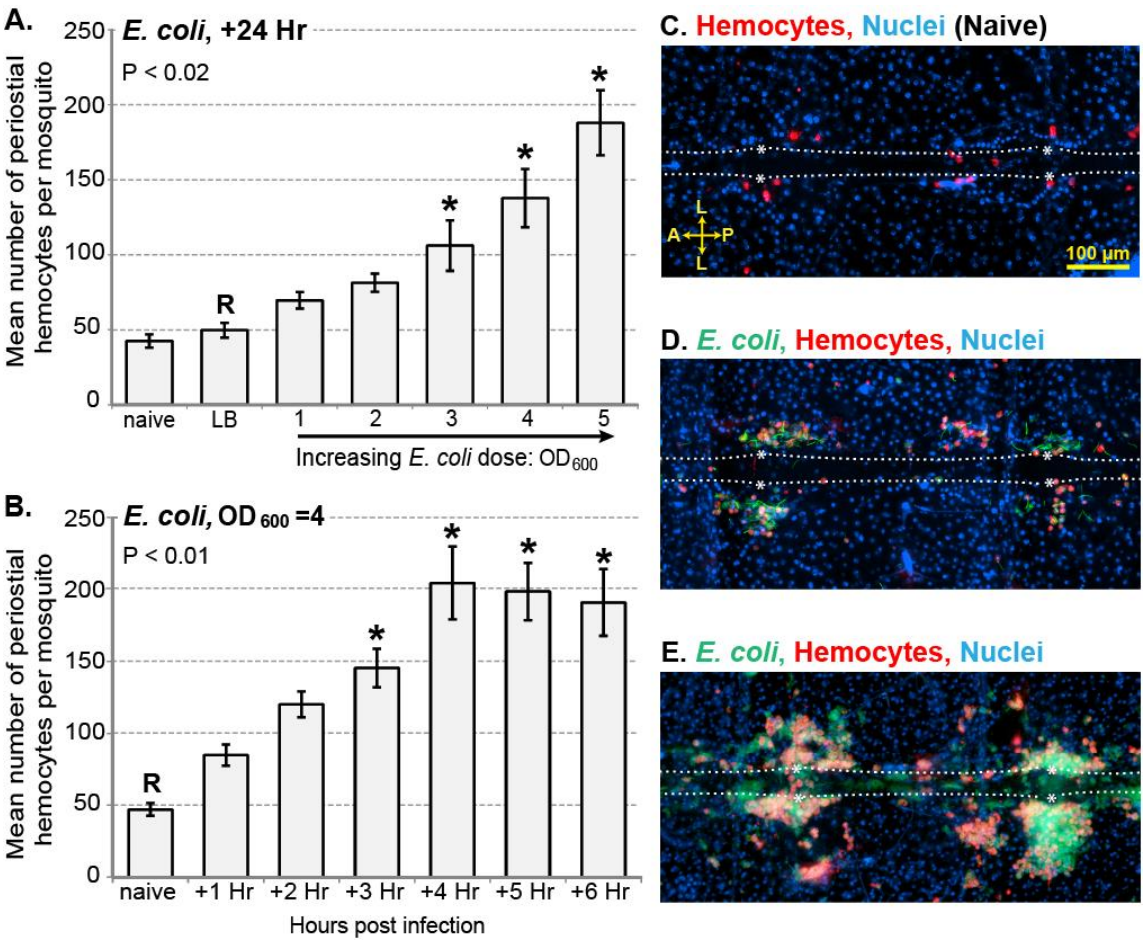

Figure 5. Periostial hemocyte aggregation occurs in a dose and time dependent manner. (A) Periostial hemocytes numbers in naïve mosquitoes, injured mosquitoes (LB), and mosquitoes infected for 24 h with *E. coli* (OD1-OD5). Resident periostial hemocytes are present in naïve mosquitoes and injury does not trigger hemocyte recruitment, but infection triggers hemocyte migration to the periostial regions in a dose-dependent manner. (B) Dynamics of periostial hemocyte numbers in naïve and *E. coli* (OD4)-infected mosquitoes. Following high-intensity infection, hemocyte recruitment to the periostial regions is complete by 4 h post-infection. Columns mark the mean and bars denote the standard error of the mean. P-values result from one-way ANOVA, and asterisks denote treatment groups that are significantly different from the reference group (R; Tukey's test). (C-E) Resident periostial hemocytes (red) in naïve mosquitoes (C), and both small (D) and large (E) periostial hemocyte aggregates in GFP-*E. coli* (green)-infected mosquitoes. A, anterior; P, posterior; L, lateral; asterisk, location of the ostia; dotted lines, outline of the heart. Hoechst 33342 (blue) was used as a nuclear stain.

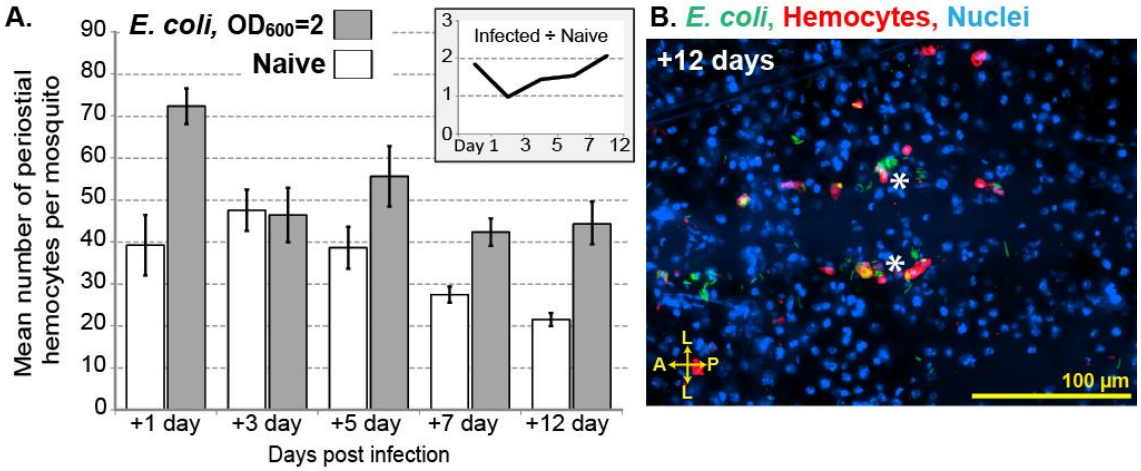

Figure 6. Periostial hemocyte aggregates begin to disperse several days after infection. (A) Periostial hemocyte numbers in naïve mosquitoes and mosquitoes infected with low levels of *E. coli* (OD2) for 1, 3, 5, 7, and 12 days. Columns mark the mean and bars denote the standard error of the mean. The numbers of hemocytes in infected mosquitoes returns to pre-infection levels by 3 days post-infection, but are maintained at higher levels relative to naïve mosquitoes for the lifetime of the mosquito. (A, inset) Ratio of hemocytes in infected vs. naïve mosquitoes at different times post-treatment. (B) *E. coli* infection (green) persists at 12 days post infection, with hemocytes (red; CM-DiI) remaining immunologically active in the periostial regions. A, anterior; P, posterior; L, lateral; asterisk, location of the ostia; dotted lines, outline of the heart. Hoechst 33342 (blue) was used as a nuclear stain.

Soluble immune elicitors induce periostial hemocyte aggregation

Phagocytosis of 1 µm diameter microspheres triggers the recruitment of hemocytes to the periostial regions (Figs. 1A-B, 2D), suggesting that immune activation via phagocytosis pathways induces hemocyte migration to the pericardial space. We tested whether several soluble immune elicitors also induce hemocyte aggregation in the periostial regions. Being solubilized, these microbial components are outside of the size range that induces phagocytosis. Examination of dorsal abdomens 24 h after injection with peptidoglycan and β-1,3-glucan revealed that soluble immune elicitors also induce the aggregation of hemocytes in the periostial regions (Figure 7A-E). Interestingly, melanization in the periostial regions was prevalent following injection with peptidoglycan and β-1,3-glucan (Figure 7B, D), and this melanization response was considerably stronger than that observed following infection with *E. coli*. These data suggest that periostial hemocyte aggregation is a basal immune response that is induced by a broad range of immune stimuli.

Plasmodium *infection induces periostial hemocyte aggregation*

Mosquitoes are vectors of disease-causing pathogens. Among the most important mosquito-borne pathogens are *Plasmodium* parasites, which are the etiological agents of malaria. *Plasmodium* infection represents a complex and long-term immune stimulus for mosquitoes [1, 107, 108], and we have previously observed *Plasmodium* sporozoites near the heart's ostia [1]. For these reasons, and because *Plasmodium* infection occurs without breaching the outer cuticle, we analyzed whether *Plasmodium* infection induces periostial hemocyte aggregation. Examination of the periostial regions of mosquitoes that had received a normal blood meal and mosquitoes

that had received a *Plasmodium*-infected blood meal revealed that the process of sporozoite migration to the salivary glands induces the aggregation of hemocytes in the periostial regions: mean numbers of periostial hemocytes increased from 72 in the non-infected group to 106 in the infected group (Figure 7F). Moreover, periostial hemocytes phagocytose *Plasmodium* sporozoites (Figure 7G-I). In some cases, multiple *Plasmodium* nuclei were observed within an individual hemocyte, with sporozoite cell bodies fragmented and their fluorescence largely degraded. Finally, melanization was occasionally observed within the periostial aggregates (Figure 7G). Overall, these data show that *Plasmodium* infection induces the recruitment of hemocytes to the periostial regions, and suggest that the cellular immune response against *Plasmodium* may be stronger than what was reported in an earlier study [1] that assayed circulating hemocytes alone.

Discussion:

Based largely on practical constraints, the insect immune and circulatory systems have been conceptually divided into discrete elements, and the immune system further dissected into cellular and humoral components [109]. However, these entities are physiologically interrelated and have apparently evolved in integral association since the beginning of animal evolution [34, 109-112]. The cellular immune response remains only partially understood in mosquitoes as well as in other adult insects [7, 90]. Likewise, interactions between major circulatory elements and immune cells are virtually unknown and have received little attention.

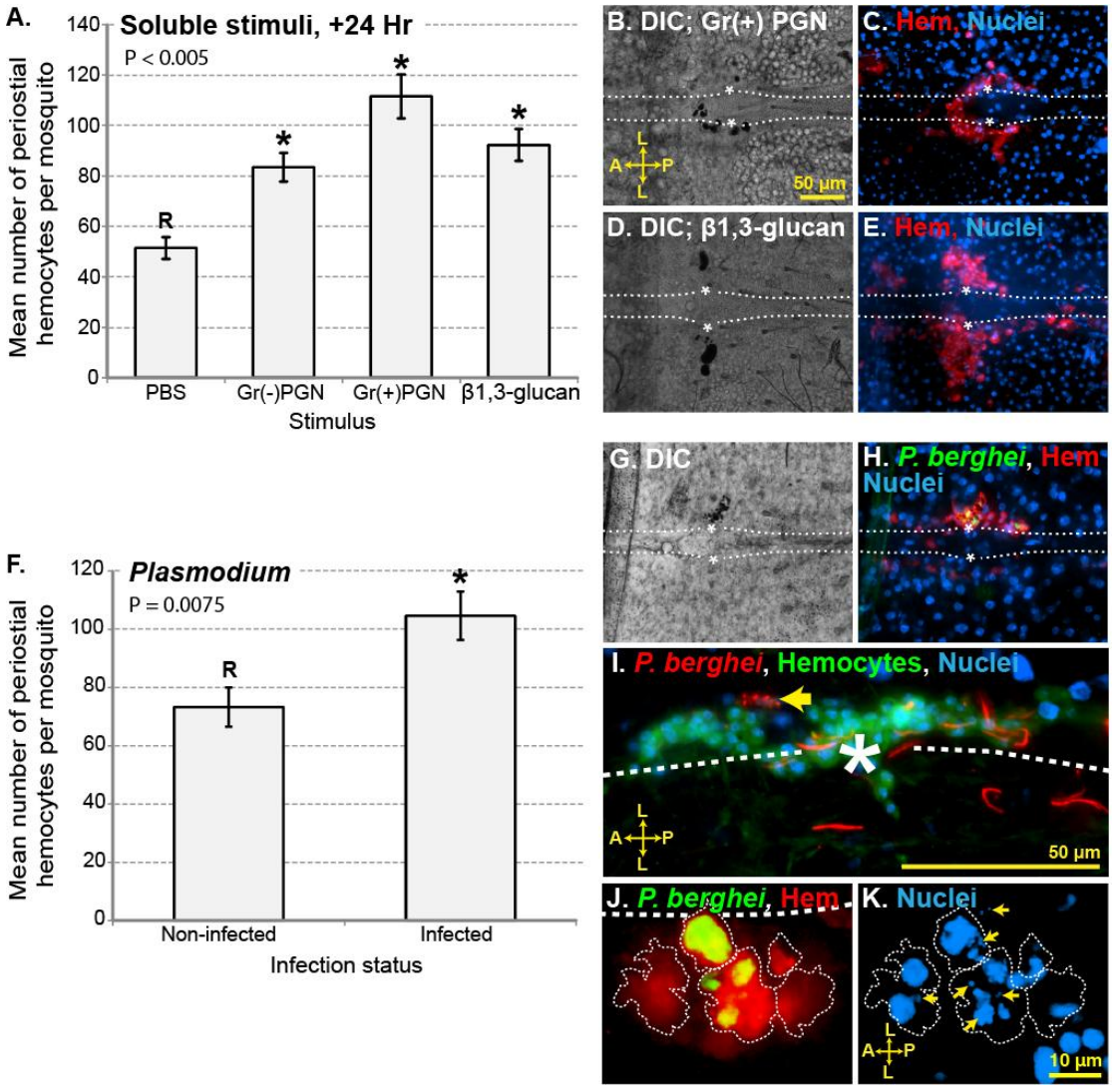
A.
Soluble stimuli, +24 Hr
P < 0.005
Mean number of periostial hemocytes per mosquito
140
120
100
80
60
40
20
0
R
*
PBS
Gr(-)PGN
Gr(+)PGN
β1,3-glucan
Stimulus
B. DIC; Gr(+) PGN
C. Hem, Nuclei
D. DIC; β1,3-glucan
E. Hem, Nuclei
L
A
P
50 µm
F.
Plasmodium
P = 0.0075
120
100
80
60
40
20
0
Non-infected
Infected
Infection status
G. DIC
H. P. berghei, Hem
Nuclei
I. P. berghei, Hemocytes, Nuclei
J. P. berghei, Hem
K. Nuclei
10 µm

Figure 7. Soluble immune elicitors and *Plasmodium berghei* infection induce periostial hemocyte aggregation. (A) Hemocyte numbers in the periostial regions following treatment with soluble immune elicitors. Columns mark the mean and bars denote the standard error of the mean. P-values result from one-way ANOVA, and asterisks denote treatment groups that are significantly different from the reference group (R; Tukey's test). Peptidoglycan (PGN) from both Gram (-) and Gram (+) bacteria, as well as β-1,3-glucan, elicit the migration of hemocytes to the periostial regions. (B-E) DIC and fluorescence images of a periostial region 24 h after Gram (+) peptidoglycan injection (B-C) and β-1,3-glucan injection (D-E). Large hemocyte aggregates (CM-DiI; red) and melanin deposits (black) are observed. (F) Periostial hemocyte numbers 20 days after mosquitoes received a normal (non-infected) or *Plasmodium berghei*-infected blood meal. *Plasmodium* sporozoite migration induces hemocyte aggregation in the periostial regions (P=0.0075). (G-H) DIC and fluorescence images of a periostial region at 20 days following infection with *Plasmodium berghei*. Signs of melanization (black) were sometimes present and overlap was often seen between periostial hemocytes (CM-DiI; red) and green puncta, which represent the remnants of destroyed sporozoites ($PbGFP_{CON}$; green). (I) Interactions between *P. berghei* sporozoites (Pb RedStar; red) and periostial hemocytes (CM-DiO, a CM-DiI analog; green), with arrow pointing to hemocyte-mediated *Plasmodium* fragmentation. (J) Hemocyte (CM-DiI; red; cell boundaries are outlined) and *Plasmodium* (PbGFPCON; green) fluorescence overlay, showing the phagocytosis of multiple sporozoites by periostial hemocytes. (K) Hoechst 33342 fluorescence channel of the image in panel J, showing that the nuclei of *Plasmodium* sporozoites (arrows) are contained within periostial hemocytes. A, anterior; P, posterior; L, lateral; asterisk, location of the ostia; dotted lines, outline of the heart. Hoechst 33342 (blue) was used as a nuclear stain.

Using methods we previously developed for the study of hemolymph circulation [32, 33], along with novel techniques for the in vivo investigation of hemocyte biology, we analyzed the cellular immune response in the pericardial region of the malaria mosquito, *Anopheles gambiae*. We discovered that during an active infection, hemocytes migrate to the periostial regions, where they form a major component of the cellular immune response. Exemplifying the interrelationship of cellular immunity and circulatory processes, periostial hemocytes form phagocytic foci in regions of high hemolymph flow, which are also in the direct vicinity of the mosquito's major nephrocytes, the pericardial cells. Together, the data presented herein describe a novel immune mechanism and the formation of a novel immune tissue in mosquitoes. Because previous mosquito studies did not recognize sessile hemocyte aggregations as a major player in immunity, they failed to examine a large proportion of the cellular immune response, and thus, underestimated the relative contribution of hemocytes in anti-pathogen responses.

Using a correlative imaging approach, we scrutinized what appeared to be major phagocytic foci forming in the periostial regions of the mosquito heart. We previously reported that these foci form in response to infection, but their cellular composition and their functional role remained unknown [1]. Similar foci form in other insects, although they have never been directly studied [35, 113]. Here, we report that these immune foci are composed of periostial hemocytes that rapidly and efficiently phagocytose pathogens. Rapid phagocytosis is believed to be an essential immune process, which culminates in pathogen death and the production of humoral immune components [36, 114, 115]. Furthermore, the large number of periostial hemocytes present in infected mosquitoes, when compared to the total number of circulating hemocytes [46-48, 50, 51, 105], suggests that this response involves between 10% and 25% of the hemocytes

present in mosquitoes, which highlights the importance of pathogen sequestration in areas of high hemolymph flow.

Periostial immune aggregates are composed of a mixture of resident hemocytes and circulating hemocytes that settle in the pericardial regions in response to infection. Given that bacterial infection induces an increase in the number of circulating hemocytes in *An. gambiae* [48], and that *Ae. aegypti* hemocytes can replicate in response to various stimuli [46, 51], we hypothesize that some of the migrating hemocytes seen in this study are the products of hemocyte replication in response to infection. While the origin of periostial hemocytes seems clear, the molecular trigger that induces hemocyte aggregation in the periostial regions is unknown. The finding that hemocyte recruitment is induced by bacteria, latex microspheres and soluble immune elicitors suggests that multiple pathways of immune activation can induce periostial hemocyte aggregation. Finally, our data from the first hour post-infection showed that hemocytes most often slowly move into the periostial regions as single cells. This, along with reports that there are several mechanisms of hemocyte chemotaxis [42, 116], suggests that the formation of pericardial aggregates involves a specific, spatially directed response to infection. But hemocytes sometimes arrive into the pericardial regions as small aggregates. Thus, there remains the possibility that hemocyte aggregation in circulation, or increases in hemocyte size post-infection [103, 117], are physical mechanisms for an evolutionarily pragmatic response to infection.

What is perhaps most interesting about periostial hemocyte aggregates is their location. In dipterans, the cardiac ostia are the major incurrent valves for hemolymph entry into the heart [32, 33, 75]. Thus, hemocyte aggregation in these regions greatly increases the likelihood that hemocytes encounter circulating pathogens, and that toxic products produced during pathogen breakdown are either immediately diluted as they

are swept into the rapidly flowing hemolymph or are captured by the nephrocytic PCs that flank the heart. PCs filter proteins and colloids from the hemolymph [112], and thus, it is likely that the proximity of the PCs to the periostial hemocytes is essential for the quick absorption of pathogen breakdown products. We speculate that, during the course of arthropod evolution, periostial hemocytes and PCs adapted to their current locations because of their proximity to each other in an area of high hemolymph flow.

In a manner comparable to what we describe in mosquitoes, the macrophages of many lower vertebrates aggregate in areas of high blood flow in response to infection [118, 119]. These aggregates assemble in the spleen and liver, where they concentrate the destruction and recycling of exogenous and endogenous material. Likewise, the tissue macrophages of higher vertebrates (e.g., stellate cells and Kupffer cells) are believed to have originated from the same cellular ancestors as the phagocytes found in all animals, and are also commonly located in areas of high blood flow [120]. It seems parsimonious to speculate that such phylogenetically disparate phagocyte aggregation responses are entirely based on functional analogy. However, mounting evidence suggests that these aggregation responses rely on conserved molecular and physiological components that were present in an ancient bilaterian [34, 110-112, 120, 121]. From a physiological perspective, we believe the data presented here exemplifies the taxonomically widespread importance of evolutionary constraints imposed on the cellular branch of the immune system as a consequence of its long history of evolution in close association with the circulatory system.

Although it is known that most *Plasmodium* sporozoites rapidly die during their migration through the mosquito hemocoel [1], the specific interactions between sporozoites and hemocytes remain largely unknown. Earlier reports showed that phagocytosis of *Plasmodium* by hemocytes occasionally occurs [1, 36]. Our data show

the in vivo interaction between *Plasmodium* and hemocytes, along with the first evidence of a systemic cellular immune response to late-stage malaria infection (increase in periostial hemocyte numbers). While the large number of sporozoites released by each oocyst makes it unlikely that phagocytosis is the primary component of the anti-*Plasmodium* response in the hemocoel, increases in melanization and periostial hemocyte aggregation suggest that hemocyte activation leads to the production of humoral factors that target *Plasmodium* via lytic and melanization pathways. Evidence from others supports this idea, as *Plasmodium* development in mosquitoes induces the transcriptional regulation of immune genes in hemocytes [122, 123], and our data on melanin deposition near hemocyte-*Plasmodium* interactions are in agreement with studies on the anti-sporozoite response in mosquitoes [36, 124].

In other insects, phenomena that involve hemocyte aggregates interacting with foreign entities have been labeled as nodulation or encapsulation [7]. Although the nomenclature for these responses is not consistent across taxa, they involve the aggregation of hemocytes and melanin around the periphery of a large organism or a clump of bacteria. Nodulation, however, requires types of hemocytes for which no functional analogs exist in mosquitoes (i.e., lepidopteran plasmatocytes and *Drosophila* lamellocytes) [7]. Likewise, encapsulation has been described as a walling off by hemocytes of objects too large to be phagocytosed [25, 125]. This stands in stark contrast with the periostial hemocyte response, which is heavily associated with phagocytosis. Thus, while periostial immune foci share with nodulation and encapsulation the process of hemocyte aggregation, the phagocytic nature of periostial hemocytes makes this a distinct and new insect immune response. Furthermore, because nodulation and cellular encapsulation do not commonly occur in mosquitoes,

periostial hemocyte aggregation is the primary hemocyte aggregation immune response in the culicid lineage.

In most insects, one problem foiling hemocyte research is that no effective means of specifically staining hemocytes in vivo exists [47, 123]. As part of this investigation, we developed a CM-DiI based method that fluorescently labels hemocytes in vivo. Several lines of evidence support the specificity and efficiency of CM-DiI hemocyte labeling. First, CM-DiI stains virtually all circulating hemocytes and also stains cells attached to tissues in a random pattern (sessile hemocytes). Second, CM-DiI stains cells that fit the morphological description of hemocytes given by previous authors [28, 36, 47]. Finally, the vast majority of cells that stain with CM-DiI exhibit the characteristic phagocytic signature of mosquito granulocytes. Although the mechanism by which CM-DiI specifically stains hemocytes remains unknown, our data suggest that CM-DiI is unable to cross the basal lamina surrounding internal tissues, and that it initially stains hemocytes through phagocytosis and then diffuses throughout the cellular membrane. Evidence supporting this mechanism of labeling includes: (1) injection of carbon particles prior to CM-DiI treatment blocks hemocyte staining; (2) CM-DiI staining appears most brightly as puncta within the hemocytes but over time spreads over the entire cell membrane; and (3) upon mixture with PBS, CM-DiI precipitates out of solution. Taken altogether, this suggests that CM-DiI could be categorized as a functional marker that stains only hemocoelic phagocytes in vivo. Techniques based on similar principles have been used for the study of macrophage biology in mammals [126], and thus, this approach for the first time allows the study of mosquito hemocyte cell biology in vivo and in real time.

In conclusion, there remain deficits in our current knowledge of hemocyte biology in adult insects, as well as in our understanding of the direct interactions between the

insect circulatory and immune systems. Here, we developed new methods for the in vivo study of mosquito hemocytes and pericardial cells (nephrocytes), and applied these methods to discover a novel mosquito immune response. Namely, we uncovered periostial hemocyte aggregates, an immune tissue that is located on the surface of the mosquito heart and represents a basal component of the cellular immune response against bacteria and malaria parasites.

CHAPTER IV

SYSTEMIC ANALYSIS OF POST-INFECTION HEMOCYTE ACTIVITY IN THE MALARIA MOSQUITO, *ANOPHELES GAMBIAE*

Preface:

This chapter continues the work presented in Chapter III, but takes a systemic approach. I was responsible for nearly all of the lab work presented and Dr. Hillyer and I again worked together on the techniques and concepts pertinent to this study. The work presented in this chapter will be submitted for publication.

Abstract:

Insect immune cells (hemocytes) mediate the immune response to a variety of insect pathogens. Major gaps still exist in our basic knowledge of hemocyte biology, even in insects that greatly effect human wellbeing. As one example, the types, numbers and responses to infection of hemocytes in mosquitoes remain vaguely understood. Here we used novel methods to assay the numbers and activities of circulating and sessile hemocytes throughout the body of *Anopheles gambiae* at various ages and at different states of infection. Qualitative studies showed that sessile hemocytes are prevalent, occur throughout the mosquito's body, and tend to concentrate in specific

regions of the abdomen following immune challenge or aging. These sessile cells are heavily involved in phagocytosing foreign pathogens. Quantitative analyses showed that total hemocyte numbers in *An. gambiae* typically range from approximately 1500 to 9000 depending on age and infection status, and that sessile hemocytes form approximately 25% of the total hemocyte population. We also found that total systemic hemocytes increase significantly following infection and decrease during the first six days post-emergence. After finding that total hemocyte number changes following infection and with aging, we used tubulin staining to show that mitosis occurs in circulating hemocytes, and that mitotic indices increased following infection. Together, these data show that sessile hemocytes form a major component of the mosquito immune system and that hemocyte numbers and activities change with age and in response to infection. These data also show autonomous division by circulating hemocytes.

Introduction:

The insect immune response relies upon innate reactions and involves both cellular and humoral components [35, 36, 39]. The immune cells (hemocytes) exist within an open circulatory cavity (hemocoel), where they phagocytose and encapsulate foreign elements and coordinate the humoral response to infection. In disease vectors, immune cells help maintain vectorial capacity by allowing the insect to survive infection, but also act to reduce the numbers of some human pathogens [1, 40]. Understanding the basic physiology of the mosquito immune response will help advance our knowledge of the effect immune factors have on vector competence. It has also been demonstrated that specific mosquito immune responses could be harnessed for the control of mosquito borne disease [95].

Most modern studies of mosquito immunity have focused on phagocytosis or signaling pathways that lead to the release of humoral factors [107, 108], or on the ex vivo examination of fixed cells [28, 36, 37, 94]. However, basic activities such as hemocyte proliferation, or attachment tissues to form sessile populations, remain poorly understood in dipterans. In mosquitoes, microscopic studies of hemocyte morphology have shown that there are several distinct classes of hemocytes. These routinely include phagocytic granulocytes and oenocytoids, which are involved in the melanization response [28, 47]. Many authors also describe a small type of cell (<5 µM diameter when spread) called prohemocytes [28, 47, 49, 127], which are normally reported to resemble small granulocytes. Prohemocytes are often claimed to develop into larger cells upon certain stimuli, although there is little modern evidence of this in mosquitoes. Mosquito hemocyte numbers have also been counted in previous studies, although similar techniques have sometimes led to dissimilar counts [46, 47, 49]. Nevertheless, the general consensus is that mature adult mosquitoes have between approximately 1000 and 3000 cells [46-48, 51, 128], similar to the number estimated in *Drosophila* [129].

While the dynamics of hemocyte aggregation, sessile hemocyte activity, and hemocyte proliferation are just beginning to be uncovered in mosquitoes, it has been documented in other insects that circulating hemocyte numbers change in response to immune challenge and it has often been hypothesized that this change is due to either a release of sessile hemocytes into circulation, or the replication of a progenitor cell type known as prohemocytes [35, 47, 49, 115, 130]. The hypotheses that sessile hemocyte detachment or a prohemocyte replication is responsible for the increases seen in circulating hemocyte numbers is based largely on the fact that neither a hematopoietic organ, nor hemocyte mitosis, has been observed in adult insects [25]. Another possibility

is that hemocytes divide autonomously, an idea which has been suggested but never conclusively shown [46, 51, 131]. In support of this theory of hemocyte replication, it has been documented that hemocytes proliferate somewhere in the body of adult *Aedes* mosquitoes in response to blood feeding or infection with filarial nematodes [46, 51].

Here we present the first counts of hemocyte numbers throughout the entire body of the malaria mosquito, *Anopheles gambiae,* including both circulating and sessile hemocytes. We found that total hemocyte numbers range between 1421 and 8890 cells depending on age and infection status. Namely, systemic hemocyte populations increase in response to infection and decrease within days of adult emergence. Sessile hemocytes were found to represent approximately 25% of the total hemocyte population and were heavily phagocytic in infected mosquitoes. Finally, we for the first time present direct evidence of mitosis in circulating hemocytes.

Materials and methods:

Mosquito rearing and maintenance

Anopheles gambiae (G3 strain) were reared and maintained as described [33]. Briefly, larvae were hatched in deionized water in plastic containers and fed a blend of koi food and yeast. Pupae were separated by size, allowed to emerge into adults in plastic buckets, and fed a 10% sucrose solution *ad libitum.* Rearing and maintenance was done in an environmental chamber at 27°C, 75% relative humidity and a 12 h light/12 h dark photoperiod.

Mosquito injections and bacterial infections

For injections, mosquitoes were cold-anesthetized and a finely pulled glass needle was shallowly inserted into the thoracic anepisternal cleft. A volume of 0.2 µl was injected into the hemocoel and mosquitoes were then returned to an environmental chamber until assayed.

For bacterial infections, GFP-expressing *Escherichia coli* (modified DH5α) were grown overnight at 37° C in Luria-Bertani's rich nutrient medium (LB broth), and cultures were normalized to OD_{600}=4 using a BioPhotometer plus spectrophotometer (Eppendorf AG, Hamburg, Germany) prior to being injected into mosquitoes. To quantify the infection dose, 1:2000 dilutions of OD_{600}=4 *E. coli* culture were plated on LB agar with tetracycline, incubated at 37 °C, and the colony forming units were counted 18 h later. On average, OD_{600}=4 represented infection doses of 103,000 (SD= 29,000) cells per mosquito. Female mosquitoes were infected at 1, 5 and 15 days post-eclosion. Hemocytes were counted in naïve, LB injected, and infected mosquitoes at 2, 6 and 16 days post eclosion.

Hemocyte labeling and visualization

A sequence of procedures, performed in a series, was used to analyze systemic hemocyte numbers in individual mosquitoes. For each individual, all steps were completed on the same day with the exception of the counting of perfused cells, as perfused preparations remained useful for several days. As a brief overview, hemocytes inside individual mosquitoes were labeled with CM-DiI, collected by perfusion, and allowed to adhere to glass slides. While perfused cells were adhering, the mosquito

carcass was fixed, dissected and mounted on glass slides. The perfused hemocytes were then fixed and mounted, and sessile and circulating numbers were then counted, starting with the sessile cells. For each age group, 3 treatments were performed (naïve, LB injected and *E. coli* injected), and for each treatment, hemocytes from 10 individual mosquitoes that originated from 10 independent but paired cohorts were examined (3 mosquitoes per cohort). Each step will now be presented in detail.

In vivo hemocyte staining was achieved as we have described (King and Hillyer, 2012). Briefly, each female mosquito was injected with 0.2 µl of a freshly prepared solution consisting of 75 µM CM-DiI (Vybrant® CM-DiI Cell-Labeling Solution, Invitrogen) and 0.75 mM Hoechst 33342 (Invitrogen) in 25°C PBS. After CM-DiI injection, mosquitoes were immediately returned to 27°C for 20 min, prior to hemolymph collection.

Circulating cells were collected by perfusing the hemolymph [51, 103]. Concisely, a slit was cut through the lateral edge of the last abdominal segment using a feather blade and the mosquito was placed on a vacuum restraint with the tip of its abdomen pointing downwards. A glass microinjection needle was then inserted into the mosquito's cervix, 200 µL of Schneider's *Drosophila* Medium was injected, and the hemolymph that exited the posterior abdomen was collected onto the center of two 1 cm diameter etched rings on Rite-On glass slides (Gold Seal; Portsmouth, N.H.). This was done at a rate of 20 seconds per mosquito, with the first 100 µL collected in one etched ring and the second in the other. Cells were allowed to adhere to slides for 20 min at room temperature, fixed for 10 min with 4% paraformaldehyde in PBS, washed 3 times for 5 min with PBS, and coverslips were mounted with Aqua Poly/Mount (Polysciences; Warrington, PA). Circulating hemocytes were counted within three days of perfusion.

Immediately following perfusion, a 16% paraformaldehyde solution was injected into the carcass as described, and the tissues were allowed to fix for 10 minutes on ice. The mosquito was then submersed in 0.2% Tween 20 in PBS, placed in PBS without Tween and a cracked feather blade and 0.20 mm minuten pins were used to slice and separate the ventral and dorsal abdomens along the ventral pleural suture (coronal plane). The midgut and Malpighian tubules were then extracted and the legs and wings cut from the body. The thorax was cut in half along a sagittal plane and the head and cephalic appendages were detached as a single unit and left intact. All disarticulated mosquito fragments were then mounted in Aqua Poly/Mount under a coverslip and sessile hemocytes were counted within two hours of CM-DiI staining.

Visual examination and imaging of hemocytes was conducted using a Nikon® 90i compound microscope (Nikon; Tokyo, Japan) equipped with a Nikon® Intensilight C-HGFI fluorescence illumination unit and a CoolSNAP HQ^2 (Roper Scientific; Ottobrunn, Germany) and Nikon DS-Qi1Mc digital cameras. Nikon's NIS-Elements software was used for on-screen viewing and image acquisition. Specimens were viewed under differential interference contrast microscopy (DIC), bright field, and/or fluorescence illumination, and Z-stack images were captured using a linear encoded Z-motor and Nikon's Advanced Research NIS-Elements software. To produce 2 dimensional images, image stacks were combined to form a focused image using the Extended Depth of Focus (EDF) module of NIS Elements.

Sessile hemocytes were examined in all tissues of the mosquito following infection and at 2, 6, and 16 days post-emergence. Mosquitoes were only used for total body counts after ensuring that >95% of the perfused hemocytes had been stained by CM-DiI and that background staining was not present in whole-mounts. Sessile hemocyte counts were conducted on the abdomens, thoraces, heads, palps, wings,

legs, midguts and Malpighian tubules, and the antennae and halteres were scanned for the possible presence of stained hemocytes. Hemocytes on each tissue were counted through the oculars using 400x-1000x magnification. Hemocytes inside the heads, palps, wings and legs were counted through the transparent cuticle using 400x-1000x magnification. When high cell densities were present on large pieces of tissue, we confirmed the accuracy of our ocular counts using 200x or 400x magnification images, along with NIS Elements manual particle counting function. Hemocytes were only counted if their presence was supported by both CM-DiI and Hoechst 33342 staining. Cells were counted as periostial hemocytes only if they were attached directly to the ostia of the heart, or formed part of a contiguous association with such hemocytes. Perfused hemocytes were counted and imaged under 1000x magnification.

Because background staining was common on the side of the thorax where CM-DiI was injected, hemocytes were only counted on the side of the thorax with less background and this number was doubled to extrapolate hemocyte numbers in each thorax. A small confirmatory study of thoracic hemocytes was conducted in which CM-DiI was injected into the abdomens of naïve, LB injected and infected mosquitoes. This study showed that similar numbers were obtained in this manner to those obtained by extrapolating the numbers obtained from unilateral counts.

Mitosis and mitotic index

Concentrations of 10 nM, 100 nM, 1µM, 10 µM and 100 µM of Nocodazole, Taxol and Colchicine, or 20 µM of MG-132 (Acros Organics; Geel, Belgium), were used in attempts to enrich the number of observed hemocytes undergoing mitosis post-infection. Each drug was either co-injected along with bacteria prior to hemocyte collection or was

included with the perfusion buffer during collection. Colchicine (1µM) injected 1 h prior to perfusion was chosen for qualitative studies of hemocytes as it slightly enriched the number of mitotic cells and the spindle bodies were ideal for interpretation of mitotic stages. Taxol (1µM) administered during perfusion was chosen for quantitative studies because it is known to rapidly arrest mitosis with relatively low cytotoxicity, resulting in highly condensed asters that are confidently recognized [128, 132]. MG-132 was found ineffective, suggesting that the mitotic checkpoint might be atypical, or absent in hemocytes [133].

Mitosis was directly detected using immunohistochemical staining of tubulin along with Hoechst staining. During qualitative mitotic analyses, hemocytes from Colchicine injected mosquitoes were perfused with 10 µL of 1 µM Colchicine in Schneider's medium. For quantifying mitotic indices, hemocytes were perfused with 10 µL of Schneider's medium onto an etched ring containing a Taxol solution that was instantly diluted to a final concentration of 1µM. Cells were then allowed to adhere for 20 minutes at room temperature and fixed as described. Cells were permiabilized by addition of 0.5% Triton X 100 for 5 min followed by 3 x 5 min washes in cold PBS. Slides were then blocked in 5% fetal bovine serum in PBS for 1 hour at room temperature. Mouse anti-tubulin antibody (4 µg/mL final concentration) was applied in blocking solution, gently agitated, and incubated for 1 hour at 25°C. Three 5 min washes were then performed before incubation in 4 µg/mL AlexaFluor™ 568, or Cy2 Goat-anti-mouse antibody (Molecular Probes; Eugene, Oregon) in 5% FBS for 1 hour at 25°C. Slides were then incubated in 30 µg/mL Hoechst 33342 for 10 min, washed 3 x 5 min and mounted using Aqua Poly/Mount. Proboscis snips and low injection/recovery were also included in qualitative analyses, and successfully verified that dividing cells were observed using other collection methods [47, 123].

Mitotic bodies were identified under 1000x magnification using images of *Drosophila S2* macrophage-like cell lines as a reference [127, 132, 134]. Mitotic cells were verified as hemocytes by morphology and by phagocytosis of *E. coli*. Mitotic indices were calculated by determining the percentage of dividing hemocytes in each mosquito after inspecting 800-1000 cells. Multinucleated cells with no apparent spindles were not counted as they likely arise from cell fusion or abnormal mitosis [135, 136].

Statistical analyses

Hemocyte count data was separated by age and treatment group and tested for normality using the Kolmogorov-Smirnov test. After confirming normality, datasets were analyzed by one-way ANOVA. When significant intersample variation was found, post hoc comparisons were done using Tukey's test. Kruskal-Wallis analysis of variance and Dunn's post tests were used to analyze datasets that contained one or more group that did not assume a normal distribution. Differences were deemed significant at $P<0.05$.

Results:

Validation of hemocyte counting method

Using our exhaustive perfusion technique, no significant change in periostial hemocyte numbers were found when compared to a previous study in which no perfusion was conducted prior to dissection (King and Hillyer, 2012). This shows that while our technique washes out all possible circulating cells, it does not significantly affect sessile cells. Efficacy was further supported by our counts in which an average of

only 11% of the total circulating cells were found in the second 100 µL of diluted hemolymph to be collected during hemolymph perfusion. Although it is hard to positively identify non-adherent bodies as cells, we also consistently observed a negligible amount of cells (<10) per mosquito that could be interpreted as hemocytes in the liquid that escaped during dissection of fixed mosquitoes or the diluted hemolymph that remained after the 20 minute adherence period.

Total counts: sessile hemocytes form a major component of the systemic phagocytic response to infection

We obtained counts for both sessile and circulating cells from the same individual mosquitoes (Figures 1-2). Circulating hemocytes in naïve mosquitoes decreased significantly between 2 and 6 days post-emergence, by an average of 41% (Figure 2A). Circulating numbers were also found to increase significantly following infection in 6 and 16 day-old mosquitoes; by an average of 56% in 6 day-olds and more than doubling, on average, in 16 day-olds (Figure 2A).

After hemolymph perfusion, hemocytes were found attached at varying frequencies to visceral organs and inside of all major appendages, except the antennae and halteres (Figures 1-2). Quantitative analyses showed that sessile hemocyte numbers decreased by an average of 34% between 2 days post-eclosion and 6 days post-eclosion (Figure 2B). The average numbers of total hemocytes in 2 and 6 day old naïve mosquitoes were 4902 and 2381, respectively (Figure 2C). When all three treatment groups were considered, the absolute hemocyte totals ranged from 2789 to 8890 in 2 day-olds, 1421 to 6782 in 6 day olds and from 1423 to 6988 in 16 day olds (Figure 2C).

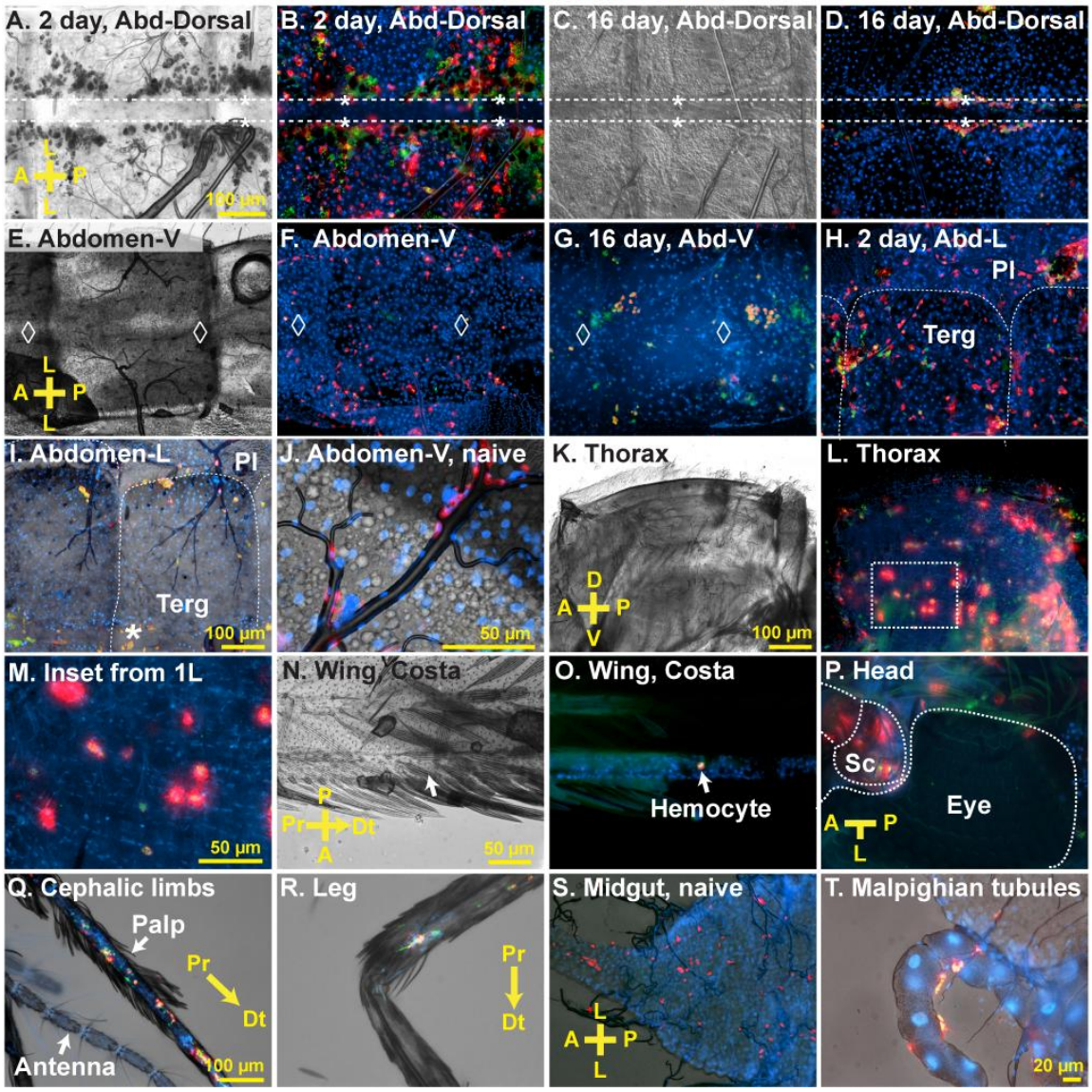
A-T. Brightfield or DIC, Hemocytes, E. coli, Nuclei
A. 2 day, Abd-Dorsal
B. 2 day, Abd-Dorsal
C. 16 day, Abd-Dorsal
D. 16 day, Abd-Dorsal
E. Abdomen-V
F. Abdomen-V
G. 16 day, Abd-V
H. 2 day, Abd-L
Pl
Terg
I. Abdomen-L
J. Abdomen-V, naive
K. Thorax
L. Thorax
M. Inset from 1L
N. Wing, Costa
O. Wing, Costa
Hemocyte
P. Head
Sc
Eye
Q. Cephalic limbs
Palp
Pr
Dt
Antenna
R. Leg
S. Midgut, naive
T. Malpighian tubules
100 µm
50 µm
20 µm

Figure 1. Sessile hemocytes occur throughout the body of infected and naïve mosquitoes. (A-B) Bright field and fluorescence overlay of widely spread sessile phagocytic hemocytes in the dorsal abdomen of mosquitoes infected at 1 day post-emergence (Red, CM-DiI stained hemocytes; Green, GFP-*E. coli*; Blue; Hoechst stained nuclei). Note the dark melanization products taken up by the pinocytic pericardial cells that flank the heart (dotted lines, outline of the heart; Asterisks, ostia). (C-D) DIC and fluorescence overlay of concentrated phagocytic hemocytes in the dorsal abdomen of mosquitoes infected at 15 day post-emergence. (E-G) Bright field and fluorescence of phagocytic hemocytes in the ventral abdomens of mosquitoes infected at 1 day and 15 days post-emergence (Diamonds, ventral abdominal ganglia). (H-J) Overlay of sessile hemocytes adhering to the abdominal walls and tracheae in the abdominal pleura (Terg, Tergite; Pl, Pleurite). (K-L) Bright field and fluorescence images of sessile phagocytic hemocytes in thoracic flight muscles. (M) High magnification image of boxed area in figure 1L. The rows of small, densely packed nuclei belong to the flight muscles. (N-R) Overlay images of hemocytes in the major appendages (Sc, scape). (S-L) Overlay images of hemocytes bound to the midgut and Malpighian tubules. Unless otherwise stated, samples shown are from adults infected at 5 days and imaged at 6 days post-emergence. Orientation guides and scale bars apply to the image they appear in and each subsequent image, until new guides are encountered. A, anterior; P, posterior; D, dorsal; V, ventral; L, lateral; Pr, proximal; Dt, distal.

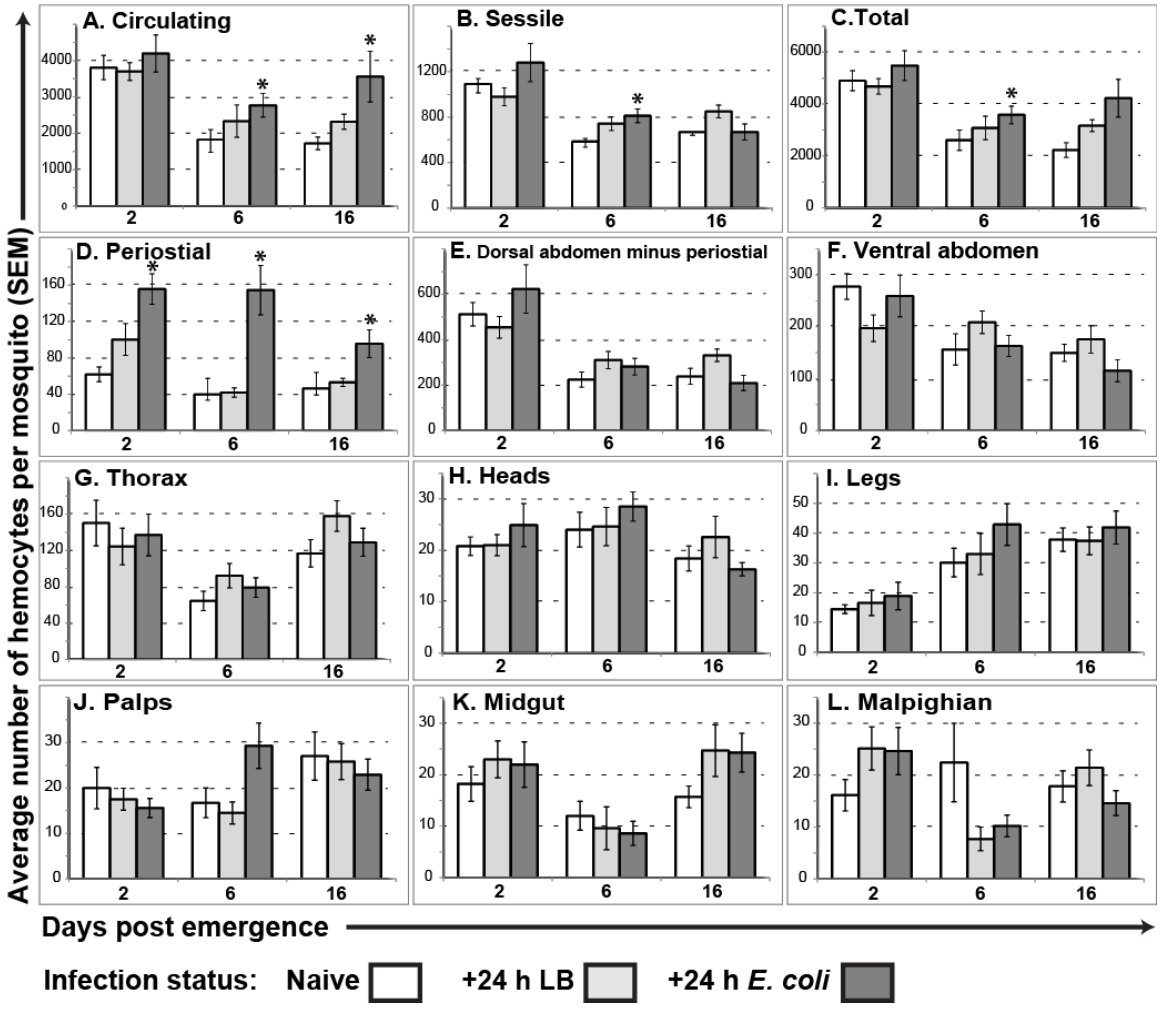

Figure 2. Systemic hemocyte numbers increase following infection and decrease during the first 6 days post-emergence. (A-B) Separate counts of sessile and circulating populations. (C) Total hemocyte numbers including all sessile and circulating cells. (D-F) Abdominal sessile hemocyte numbers separated into: cells attached to the ostia (periostial), the remainder of the dorsal abdomen minus the periostial cells, and the cells attached in the ventral abdomen. (G-L) Sessile cells attached within the appendages and to the major visceral organs. Whiskers represent standard error. Small asterisks indicate significantly higher sample means, versus the naïve control, within an age group.

Total systemic hemocyte numbers were found to decrease significantly between 2 and 6 days post emergence for all treatment groups (K-W test P= 0.0135), and to increase significantly between naïve and infected 6 day olds (K-W test P<0.01). While total numbers decrease between 2 and 6 days post-emergence, we found that proportions of sessile hemocytes remain relatively constant between all age groups at an average of 23.4% of total hemocytes (SD=3.5%; Figure 2-3). We also confirmed our previous observation that sessile cells preferentially adhere to specific areas of high hemolymph flow following infection, especially the heart's ostia (Figure 1A-D; King and Hillyer, 2012). Whether attached in areas of high flow or spread throughout the body, the sessile population is heavily involved in the phagocytosis and the breakdown of pathogens.

A large number of sessile hemocytes were normally bound to the inner surfaces of the abdominal walls on both the dorsal and ventral halves (Figure 1A-I, 2D-F). In younger insects these abdominal sessile hemocytes were more widely distributed than in older insects (Compare Figures 1B to 1D, and 1F to 1G). Infection in younger insects was also more commonly coupled with uptake of melanization products by the pericardial cells that line the heart (dark matter in Figure 1A, compare to 1C). In the abdominal pleurae hemocytes were often found in sessile aggregates that were either attached to the wall of the abdomen, or to tracheae, in both infected and uninfected insects (Figures 1H-J). Quantitative analyses showed that periostial cells increase significantly following infection in all age groups, from an average of 62 to 156 in 2 day-olds, 40 to 151 in 6 day-olds and from 47 to 96 in 16 day-olds (Figure 2D). Hemocyte numbers in the remainder of the dorsal abdomen, excluding periostial cells, decreased by approximately 50% between days 2 and 6 in all treatment groups and numbers did not significantly change following infection.

The thorax is dominated by the flight muscles and hemocytes were found distributed throughout them and around their periphery in what appeared to be a random fashion (Figure 1K-M, 2G). The flight muscles obscured the details of the activity of many of these sessile cells, but most appeared to have phagocytosed bacteria following infection (Figure 1M). No significant changes in thoracic hemocyte numbers were found between age groups or treatments during quantitative analyses and the average number of thoracic hemocytes between all groups was 120 (SD=55) per mosquito.

Sessile hemocytes were found in all major appendages in relatively small numbers (Figures 1N-R, 2H-J), except for the antennae and halteres. Hemocytes were only clearly observed in the wings in 17% of 2 day-olds, 10% of 6 day-olds and 26% of 16 day olds (Figure 1O). When observed, the average number of wing hemocytes was 3.25 or less, per mosquito, for all age groups and treatments. Hemocytes were occasionally found at the base of the antennae and halters (see Figure 1P), but were included in with numbers for the head or thorax, respectively. This was done because it was hard to clearly identify whether these cells were truly inside these appendages. Hemocytes were present in the legs, heads and palps of all individuals (Figures 1P-R, 2H-J). Numbers did not change significantly between any groups for the heads and palp. The head and palps each usually contained approximately 20 hemocytes. The hemocytes in the head were usually more prevalent at the base of the head and near the antennal bases. The hemocytes in the legs were found to increase significantly between days 2 and 6, basically doubling in number (Figure 2I). In all appendages, the observed hemocytes had normally phagocytosed bacteria following infection, even when found inside the distal extremities.

The midgut and Malpighian tubules had a small but highly variable number of attached sessile hemocytes and no significant differences were found between any

groups (Figures 1S-T, 2K-L). This normally included approximately 20 cells that were widely scattered along the basal side of each organ. Nearly all of these cells were found to have phagocytosed bacteria following infection.

Sessile hemocytes become more concentrated in major body cavities and more prevalent in appendages as mosquitoes age

Observational data suggested that sessile hemocytes are more dispersed in 2 day-old mosquitoes than in older adults, especially on both the dorsal and ventral walls of the abdomen (see Figures 1A-I). They also suggested that their drop in numbers from days 2-6 post-emergence coincided with a stark increase in periostial clumping in response to infection (compare Figures 1B to 1D). Analysis of the proportions of hemocytes supported this observation and show that the proportion of periostial cells responding to infection relative to the remainder of sessile abdominal cells tripled in older mosquitoes, from 11% to 31%, but only doubled (from 8% to 17%) in 2 day-olds (Figure 3B).

The number of cells in the legs and palps also increased with age, especially when considered in proportion to changes in total hemocyte numbers (Figure 3C). Hemocytes in 2 day-olds were only seen near the very base of the legs and palps, while in older mosquitoes it was not uncommon to see hemocytes near the distal ends of the legs and palps. It was also observed that in 2 day old mosquitoes, hemocytes were localized heavily near the larval swimming muscles in the abdomen (Figure 3D-E). We used muscle staining [33] to confirm that histolysis of larval swimming muscles is still underway during the first two days following emergence (Figures 3D-F;[82]).

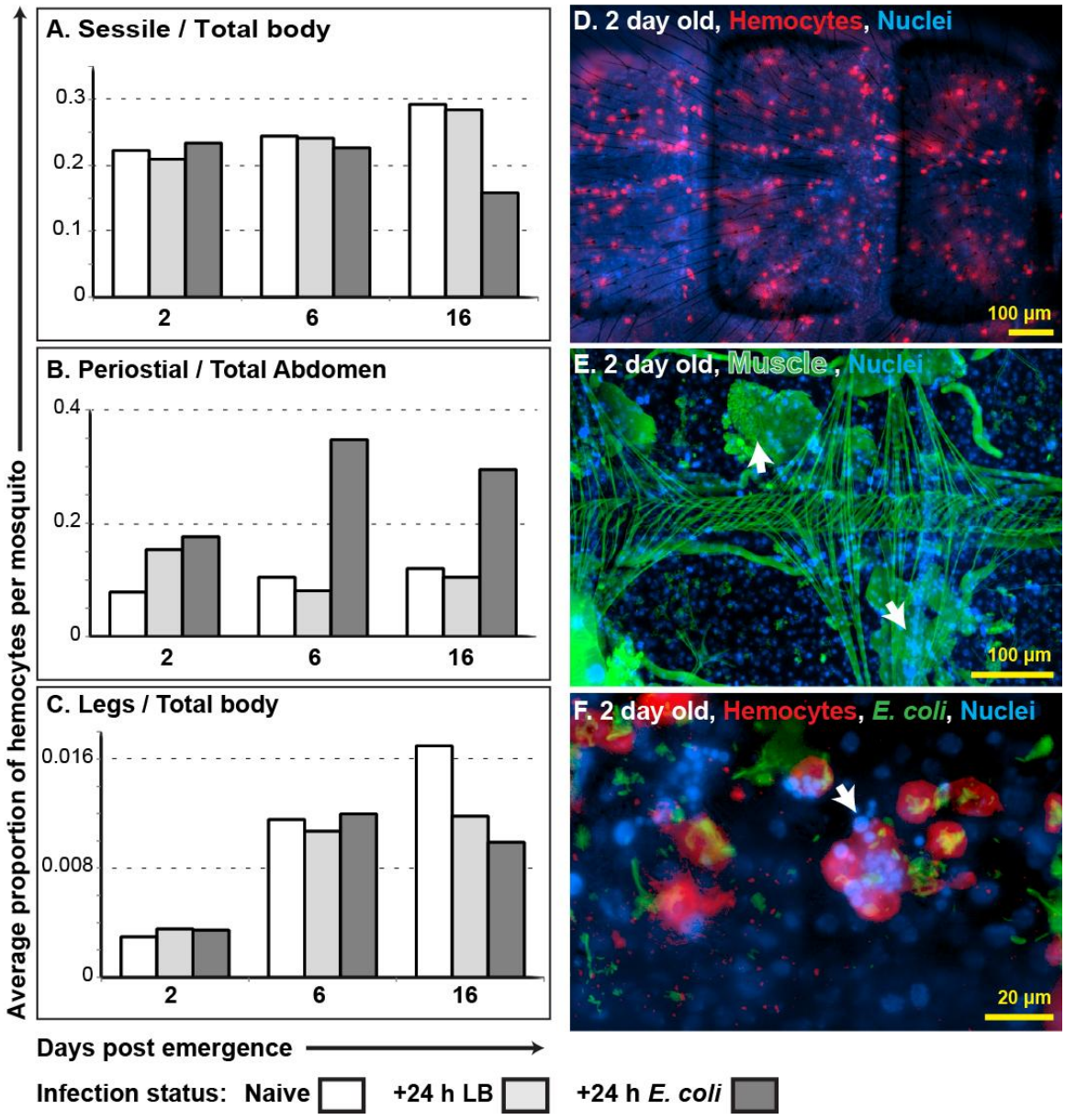
A. Sessile / Total body
0.3
0.2
0.1
0
2
6
16
B. Periostial / Total Abdomen
0.4
0.2
0
2
6
16
C. Legs / Total body
0.016
0.008
0
2
6
16
Average proportion of hemocytes per mosquito
Days post emergence
Infection status: Naive
+24 h LB
+24 h E. coli
D. 2 day old, Hemocytes, Nuclei
100 µm
E. 2 day old, Muscle, Nuclei
100 µm
F. 2 day old, Hemocytes, E. coli, Nuclei
20 µm

Figure 3. Sessile hemocytes are more widespread within the major hemocoelic cavity of young mosquitoes, but are less spread throughout the appendages. (A-C) Graphs depicting proportional levels of sessile hemocytes in select tissues. (A) Sessile hemocytes relative to systemic hemocyte numbers. Sessile hemocytes represent between 15 and 30 percent of total hemocytes. (B) Periostial hemocytes relative to the remainder of hemocytes in the abdomen. Periostial hemocyte aggregation responses are much more dramatic in 6 and 16 day-old mosquitoes, demonstrating the widespread nature of abdominal sessile hemocytes in 3 day-olds. (C) Sessile hemocyte numbers from legs relative to total systemic hemocyte numbers, highlighting their dramatic migration into the appendages during maturation. (D) Fluorescence overlay showing widespread hemocytes through the cuticle of a 2 day-old naïve mosquito. (E) Fluorescence overlay of Phalloidin staining of abdominal muscles in a 2 day-old adult. Arrowheads highlight the remnants of larval swimming muscles undergoing autolysis. (F) High magnification fluorescence overlay of hemocytes engaged in an apparent interaction with the condensed nuclear material (arrow) of autolysed abdominal muscles in a 2 day-old mosquito.

We also found that the sessile hemocytes in these regions were capable of phagocytosing foreign particles, along with evidence of the uptake and breakdown of condensed nuclear materials from the remnants of autolysed muscle cells (Figure 3F).

Hemocyte aggregates displaying low-level phagocytosis were often seen in 2 day-olds, but not older adults (Figure 4A). We hypothesize that these aggregates represent either a remnant population of larval hemocytes, or dispersing clumps of newly produced adult cells. In 2 day-olds we occasionally observed phagocytic cells that were heavily melanized (Figures 4B-C) and large perfused melanized aggregates (Figure 4D-E). These cells did not spread dramatically and usually contained a small number of bacteria. It seems likely that carry-over of larval immune cells, or sensitivity of differing immune activation pathways, explain why these occurrences are limited to recently emerged adults.

Phagocytic hemocytes occur in a range of sizes

Using CM-DiI staining and the internalization of fluorescent *E. coli* to distinguish hemocytes, we found phagocytic hemocytes with spread diameters ranging from less than 5 µM, to greater than 25 µM. Within each perfused sample, a great diversity of spread diameters was normally seen and there was no distinct cutoff in size between intrasample hemocyte size-variants. Other than size, these hemocytes were similar in general appearance using our staining methods or DIC microscopy, and did not appear to form distinct morphological classes. Smaller phagocytic hemocytes (≤5 µM) were commonly seen in all age groups (Figure 4F) and appeared to be similar to what others have termed prohemocytes [7, 47]. Our observations suggest that this class of cell likely represents a size-variant of granulocytes.

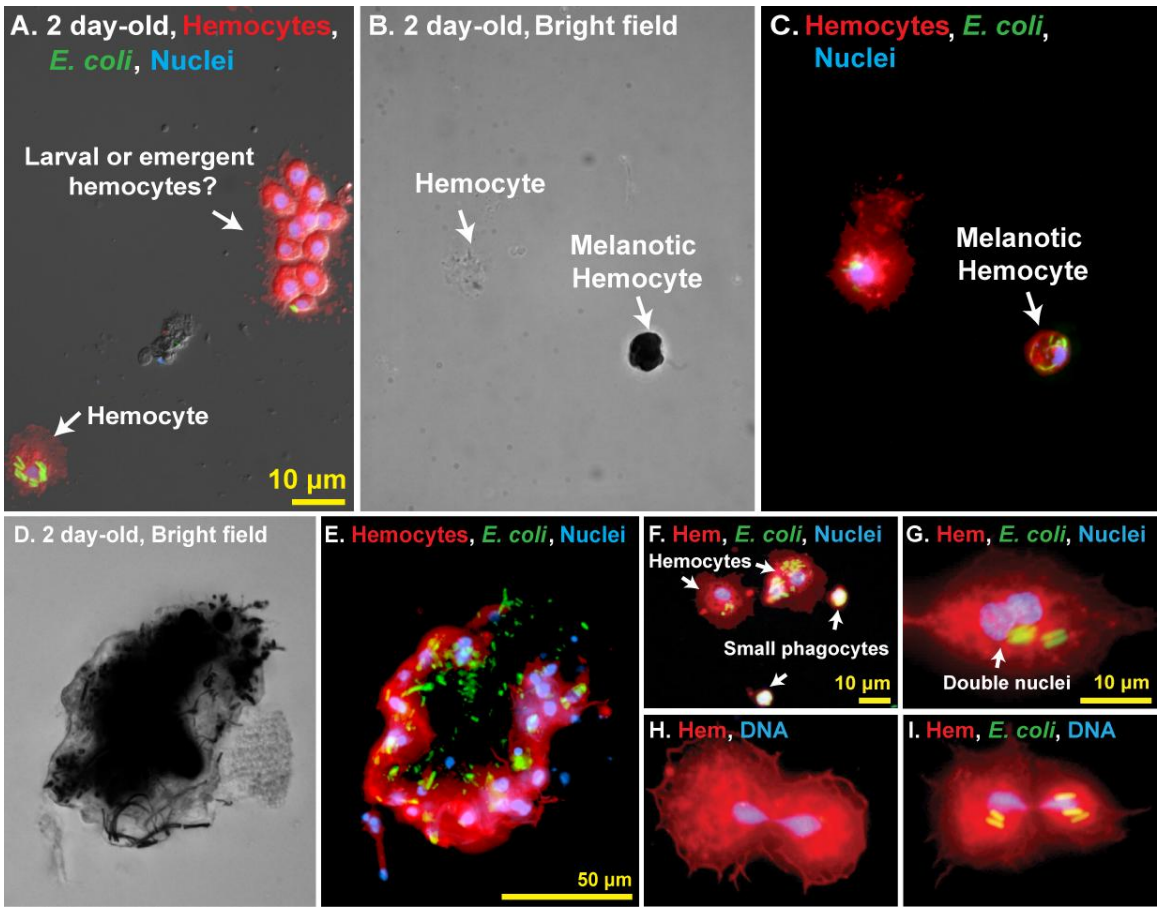

Figure 4. Morphological variance of circulating hemocytes is pronounced in younger mosquitoes. (A) DIC and fluorescence overlay showing the clusters of lightly phagocytic hemocytes seen in 2 day-olds alongside a fully phagocytic hemocyte. (B-C) Bright field and fluorescence overlay of a heavily melanized hemocyte alongside a typical hemocyte. (D-E) Bright field and fluorescence overlay showing a large multicellular melanotic body from a 2 day-old mosquito. (F) Fluorescence overlay showing small hemocytes (~5 µm diameter) alongside typical hemocytes (Hem, Hemocyte). Note that the white color signifies overlap of all three fluorescent channels, indicating the high level of phagocytosis these cells are capable of. (G-I) Fluorescence overlay of evidence of autonomous division in adult hemocytes using CM-DiI and nuclear staining.

Infection induces mitosis in circulating hemocytes

Mitosis has never been directly recorded in an adult insect. During the initial stages of this study, we occasionally noticed cells that appeared to be undergoing various stages of cell division using our CM-DiI staining technique (Figure 4G-I). We then used a direct measure of mitosis based on tubulin and nuclear staining, and found mitotic cells in 85% of 6 day-old mosquitoes assayed following immune challenge. We attempted to use several drugs to improve the qualitative observations of spindle dynamics and the measurements of mitotic indices. For all drugs except MG-132, concentrations above 10 µM affected the number of adherent cells, suggesting that these doses are cytotoxic or that tubulin dynamics are important for adherence. Concentrations of 100 nM or less generally did not yield mitotic cells. Lack of mitotic cells from untreated samples, or samples treated with 100 nM or less showed that the duration of hemocyte mitosis is likely ≤20 min and that, without an arresting agent, most cells completed cytokinesis during the 20 min adhering process.

Injections of 1 µM Colchicine followed by perfusion in Schneider's with 1 µM Colchicine were found to enrich the population of mitotic hemocytes and to be ideal for qualitative analyses and imaging. Using Colchicine, all stages of mitosis were observed (Figure 5A). Mitotic hemocytes were also commonly observed alongside a variety of non-mitotic cells, and tubulin staining in these cells suggested that cytoskeleton dynamics might be important during the hemocyte response (Figure 5B). Specifically, larger phagocytic hemocytes were observed to have a more rounded shape and contained a dense ring of tubulin around their margins (Figure 5B "rounded hemocyte"), whereas most hemocytes under 10 µm in diameter had a cytoskeleton that was crosshatched or radial in appearance (Figure 5B).

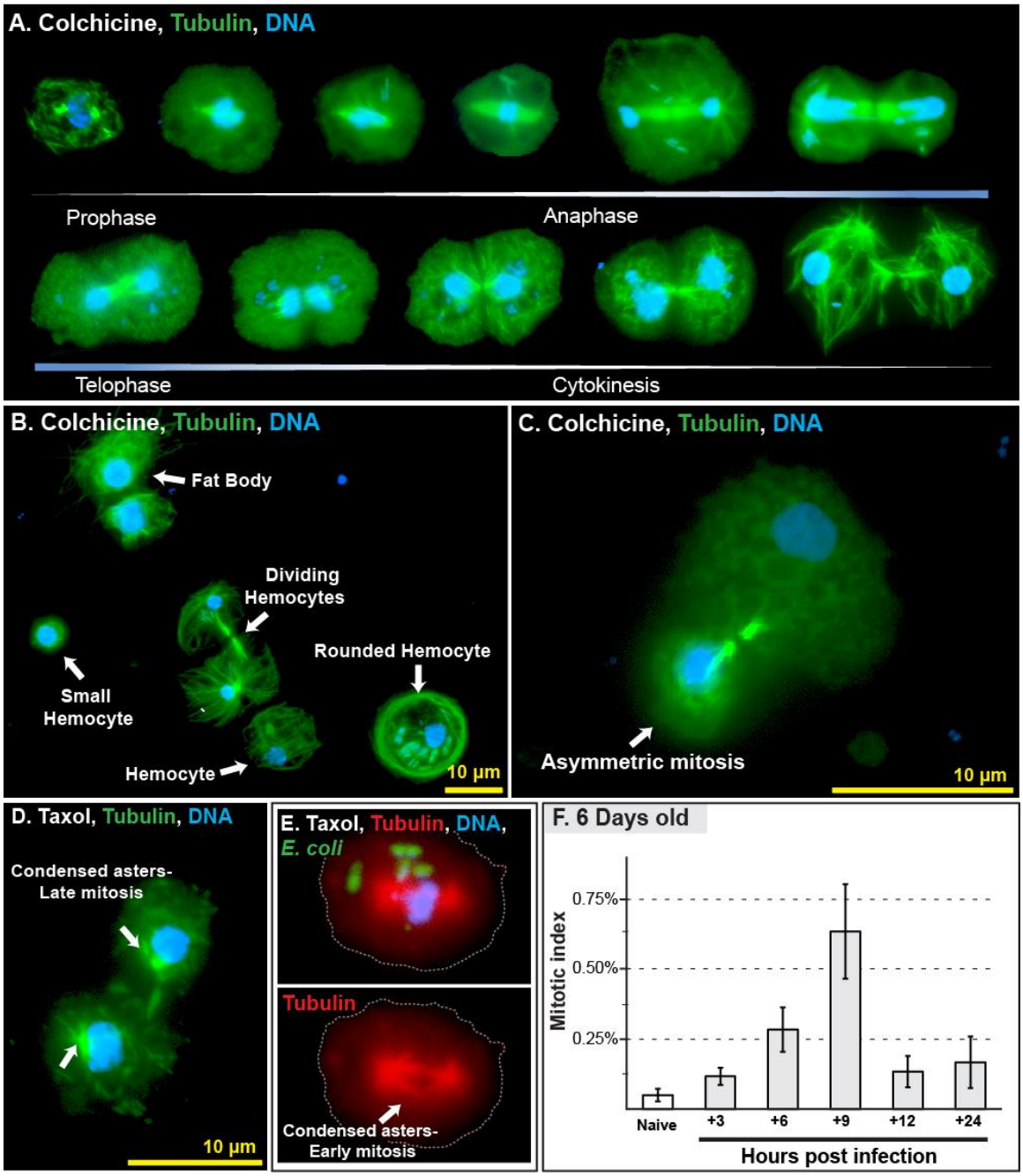
A. Colchicine, Tubulin, DNA
Prophase
Anaphase
Telophase
Cytokinesis
B. Colchicine, Tubulin, DNA
Fat Body
Dividing Hemocytes
Rounded Hemocyte
Small Hemocyte
Hemocyte
10 µm
C. Colchicine, Tubulin, DNA
Asymmetric mitosis
10 µm
D. Taxol, Tubulin, DNA
Condensed asters- Late mitosis
10 µm
E. Taxol, Tubulin, DNA, E. coli
Tubulin
Condensed asters- Early mitosis
F. 6 Days old
Mitotic index
0.75%
0.50%
0.25%
Naive
+3
+6
+9
+12
+24
Hours post infection

Figure 5. Hemocytes undergo mitosis in the hemocoel. (A) Fluorescence overlay showing all stages of mitosis observed in 6 day-old mosquitoes. (B) Fluorescence overlay of tubulin stained perfused cells along with other cell types, showing clear and direct evidence of mitosis in the circulating hemocytes of an adult insect. Note the crosshatched cytoskeleton in the normal hemocyte and the rounded tubulin border of the "rounded" hemocyte. It is also apparent that small hemocytes contain extensive cytoskeletons within their small cytoplasm. (C) Asymmetric mitosis of hemocytes resulting in one prohemocyte-sized daughter cell. (D-E) Taxol treatment results in spindle contraction. Triple fluorescence results, like those used to quantify mitotic indices, are shown in panel D. Dotted line denotes cell boundary. (F) Graph of mitotic indices over time points following infection. By this measure, proliferation peaked at 9 hours post-infection.

Fat body was easy distinguished from hemocytes by tubulin staining because their cytoskeleton had a much more tangled appearance (Figure 5B).

Interestingly, during qualitative analyses grossly asymmetric cytokinesis was occasionally observed (Figure 5C). The smaller cells resulting from these divisions are similar in size to the small hemocytes (possible “prohemocytes”) described above (Figures 4F and 5B). Supporting the idea that what have been called prohemocytes could represent a small form of granulocyte.

A 1 µM dose of taxol was found to be ideal for halting mitosis when applied during perfusion (Figures 5D-E). Under these conditions, the mitotic index was found to increase to greater than 0.5% at 9 h post infection before dropping back to around 0.1% by 12 hours post-infection (Figure 5F). Mitosis was observed in 100% of infected mosquitoes at 6 and 9 hours post-infection and was observed in 50% of naïve mosquitoes. The average mitotic index of all samples counted post infection was approximately 0.24%. Assuming that these cells undergo mitosis at roughly the same speed as similar *Drosophila* S2 cells (20-30 min [134]), and that our direct methods only allowed for reliable identification of mitotic cells from pro-metaphase onward (≤20 min), this would explain a ≈10% increase in hemocyte numbers within 12 hours based on autonomous proliferation.

Discussion:

Insects lack an adaptive immune response. However, with an exclusively innate immune system they have filled virtually every imaginable terrestrial and freshwater niche and, by many measures have become the most successful group of multicellular

organisms [8, 109]. This immune system is composed of both cellular and humoral factors and relies upon the actions of several types of immune cells called hemocytes [25]. These cells exist within the open circulatory cavity (hemocoel) of the insect, where they phagocytose and encapsulate foreign elements and help coordinate the initiation of humoral responses [35, 36, 94]. Because insects are such an integral part of life on earth, it is unfortunate that major gaps still exist in our basic knowledge of hemocyte biology; especially when some types of insect are of paramount economic and medical importance to humans. As one outstanding example, the reported numbers, types, and activity of hemocytes present in adults of disease-vector mosquitoes remain incongruous.

A variety of techniques have been employed to study hemocytes. Hemocytes are usually collected from circulating populations by some variation of hemolymph perfusion or extraction [47, 51, 103]. Most prior studies have relied on ex vivo examination of static cells, although flow cytometry has been used on ex vivo living cells [137, 138]. In vivo studies have also been conducted in larval *Drosophila,* but focus on cell classes that don't occur in mosquitoes of any age [139]. In mosquitoes, even very similar techniques have produced incongruent hemocyte counts [46, 47, 49], although the general consensus is that adult mosquitoes have between approximately 1000 and 3000 cells [46-48, 51, 128]. Regardless of discrepancies in assessing hemocyte numbers, all mosquito studies have focused on relative numbers of circulating hemocytes, rather than total body hemocyte numbers, which are believed to include a large number of sessile hemocytes.

Changes in circulating hemocyte numbers are known to occur in multiple insect species in response to various immune stimuli and aging [7, 125], and have been reported in mosquitoes [46-48, 50, 51]. It has often been assumed that release of

hemocytes from a discrete hematopoietic organ, or the replication of a progenitor cell type known as prohemocytes, lead to these increases in circulating hemocyte numbers following stimulus. However, no adult hematopoietic organ has been found in any insect, nor has release of sessile hemocytes or mitosis of circulating hemocytes been observed in adults [25]. Using novel techniques, we herein present the first report of total hemocyte numbers and sessile/circulating numbers in *Anopheles gambiae* mosquitoes. Along with an increase in hemocyte numbers following infection and a sharp drop between 2 and 6 days post-emergence in adult mosquitoes, we also report the first direct evidence of mitosis in circulating hemocytes.

Using CM-DiI staining we quantified the number of perfused cells and the distribution of sessile cells within the entire mosquito. We found that sessile hemocytes form a substantial proportion (16-30%) of the total population and are heavily involved in phagocytosis. Many of the sessile hemocytes in the abdomen, the compartment of the hemocoel where they are most prevalent, are found attached to trachea or near the ostia of the heart. Attachment near the ostia is especially pronounced, and these sessile aggregates form the largest groups of sessile cells in the body. We believe that aggregation near the ostia represents an adaptation for either increasing the oxygen supply of the cell, or to increasing chances that they will intercept circulating or invading pathogens. This type of attachment activity is common to most free living amoeboid cells and metazoan immune cells [120] and shear-flow (i.e. hemolymph currents) is known to modulate migration and attachment in a wide phylogenetic range of eukaryotes [140, 141]. We believe that the age-dependent shift from widespread single hemocytes into aggregates within the major body cavities, along with the age-dependent dispersal of hemocytes into the appendages, suggests that a large number of hemocytes are

produced in the major cavity of the hemocoel during metamorphosis. This is in agreement with the general model of hematopoiesis in immature *Drosophila* [142].

We also observed that total hemocyte numbers decline over the first 6 days of an adult mosquito's life, and this change corresponds to changes in the morphology of some of the hemocytes. Specifically, in the 6 and 16 day-old adults the vast majority of the cells appeared to be granulocytes as typically described, although there was high variation in size. These cells are characterized by being highly phagocytic, spreading on a glass surface and including granules in their cytoplasm. Tubulin staining also revealed that these cells often have a "cross-hatched" or radial appearance to their cytoskeleton. In 2 day-old mosquitoes, we occasionally observed heavily melanized cells in perfused samples from 2 day-olds, along with clusters of hemocyte aggregates displaying low phagocytic activity relative to many of the other hemocytes in the sample. We speculate that these represent activities specific to larval or newly produced adult hemocytes. Tubulin staining showed that heavily phagocytic hemocytes sometimes undergo cytoskeletal changes and begin becoming more rounded and reminiscent of the heavily melanotic cells we observed (compare Figures 4B-C and 5B "rounding hemocyte"). It is possible that this could represent a series of changes leading from a heavily phagocytic cell to a rounded melanotic cell.

Because mosquitoes pupate so rapidly, histolysis of immature tissue occurs on a large scale within the body of the newly emerged adult (see Figure 3E;[82]). While our results are in agreement with reports that hemocytes are not directly involved in histolysis [82], we showed that sessile hemocytes attached near autolyzing tissues were capable of phagocytosis and there was evidence that they were involved in the uptake of debris from autolyzed cells. This suggests another possible role for hemocytes in adult insects and could help explain a function for the higher hemocyte numbers present in

newly emerged mosquitoes; specifically, the breakdown of dead tissues that result from histolysis.

It was previously known that circulating hemocytes increase in number following immune stimulation [46-48, 51, 128]. We corroborated these reports while also showing that sessile hemocytes increase in number along with their circulating counterparts, thus demonstrating that total hemocyte numbers increase. During our analyses of hemocyte numbers, we occasionally observed evidence of mitosis in circulating cells and further pursued this possibility. Our data from tubulin staining show that a small proportion of circulating granulocytes undergo mitosis, and that this proportion increases following infection. As stated by Wieder (1999), this type of assay represents the “one true direct measure of cellular proliferation” [132], although it may undercount the level of mitosis. Therefore, these data should be viewed as a conservative measure of mitosis. Regardless, we believe our results suggest that hemocytes are capable of propagation by autonomous division, although the possibility that these dividing cells emerged from a specialized tissue cannot be completely ruled out. The strongest piece of evidence supporting autonomous division is that early stages of mitosis were often seen in circulating granulocytes, suggesting that these cells began mitosis while in circulation. Based on the likely division time of hemocytes, and our measured mitotic indices, proliferation in circulating hemocytes is ≈10% per 12 hours and could easily account for the entire amount of proliferation seen in our systemic measures.

It has been proposed that prohemocytes mature into adult hemocytes upon activation (for review see: [7]). Our evidence of smaller (≤ 5 µm) hemocytes with a high nuclear to cytoplasm ratio “budding” from larger ones (asymmetric cytokinesis) suggests that the opposite might be true and that small granulocytes are produced from mature hemocytes. Phagocytosis by 4 µm diameter cells which stain identically to granulocytes

with CM-DiI and anti-tubulin was also observed regularly. This differs from both the classical definition of prohemocytes [131] and more modern analyses in mosquitoes [47]. We therefore speculate that what have been termed prohemocytes could simply be a size variant of granulocytes. Older evidence from electron microscopy studies supports this hypothesis, although it is often overlooked [128]. Hemocytes are bathed in a nutrient rich medium and are known to increase in size upon immune stimulus [36]. Therefore, it would not be surprising if these smaller daughter cells were produced with a minimum of sacrifice to the mother cell but were able to mature into capable immune cells in a relatively short time. Recent data from mammalian cells shows that asymmetric partitioning of cellular components between daughter cells is common and purposeful in certain cases [143]. It was also found that partitioning of cellular “garbage” was especially high, and the authors propose that certain types of asymmetric mitosis might represent a physiological mechanism for producing a “pristine” daughter cell from a mother cell that contains undegraded substances and are destined to undergo apoptosis. Apoptosis is known to occur in insect hemocytes during aging or following infection [144, 145], asymmetric mitosis could play a role in maintaining a healthy hemocyte population following a phagocytic response to infection.

In conclusion, these data represent three major advancements in our understanding of hemocyte biology. First, we show that sessile hemocytes form a major component of the mosquito immune system. Second, systemic analyses show that the number and activities of hemocytes change dramatically with age and in response to infection. Lastly, we show strong direct evidence of mitosis in circulating hemocytes, suggesting that hemocyte proliferation in adult mosquitoes does not require a discrete organ or progenitor cell type.

CHAPTER V

MEMBERS OF THE SALIVARY GLAND SURFACE PROTEIN (SGS) FAMILY ARE MAJOR IMMUNOGENIC COMPONENTS OF MOSQUITO SALIVA

Preface:

The research presented in Chapter V was initially aimed at investigating the role a family of mosquito salivary gland proteins (SGS) plays during salivary gland invasion by *Plasmodium*. Despite our efforts, we were unable to gather any conclusive data regarding involvement of SGSs in the *Plasmodium* life cycle. However, we did make exciting discoveries towards understanding the role SGS proteins play as a component of the saliva. I inherited this project from Dr. Hillyer, who had begun working on SGS during his postdoctoral studies. I conducted a large part of the lab work presented here, and we worked together on interpreting the often perplexing results of our bench work and bioinformatic analyses. The chapter, as presented, was published in late 2011, in the *Journal of Biological Chemistry [146]*. I was first author of this paper.

Abstract:

Mosquitoes transmit *Plasmodium* and certain arboviruses during blood feeding, when they are injected along with saliva. Mosquito saliva interferes with the host's hemostasis and inflammation response, and influences the transmission success of some pathogens. One family of mosquito salivary gland proteins, named SGS, is composed of large bacterial-type proteins that in *Aedes aegypti* were implicated as

receptors for *Plasmodium* on the basal salivary gland surface. Here, we characterize the biology of two SGS proteins in the malaria mosquito, *Anopheles gambiae*, and demonstrate their involvement in blood feeding. Western blots and RT-PCR showed that SGS4 and SGS5 are produced exclusively in female salivary glands, that expression increases with age and after blood feeding, and that protein levels fluctuate in a circadian manner. Immunohistochemistry showed that SGSs are present in the acinar cells of the distal lateral lobes and in the salivary ducts of the proximal lobes. SDS-PAGE, Western blots, bite blots, and immunization via mosquito bites showed that SGSs are highly immunogenic and form major components of mosquito saliva. Lastly, Western and bioinformatic analyses suggest that SGSs are secreted via a non-classical pathway that involves cleavage into a 300 kDa soluble fragment and a smaller membrane bound fragment. Combined, these data strongly suggest that SGSs play an important role in blood feeding. Together with their role in malaria transmission, we propose that SGSs could be used as markers of human exposure to mosquito bites and in the development of disease control strategies.

Introduction:

The saliva of hematophagous arthropods is a cocktail of proteins and small molecules that assists in the acquisition of a blood meal by interfering with the host's hemostasis and inflammation response [5, 147]. The injection of arthropod saliva into the vertebrate body also elicits an adaptive immune response that produces antibodies against some salivary constituents. For these reasons, the salivary components of blood feeding arthropods have been proposed as markers used for surveying exposure to vector bites [61], as targets for transmission blocking vaccines [3], and as a

pharmacopeia of novel therapeutic agents [5]. Before such applications can be developed, a better understanding of the "sialomes" of major disease vectors is necessary so that the best candidates for any of these uses can be identified. This task is compounded by the fact that functionally analogous salivary proteins are often not orthologous between groups of arthropods, so it is important to identify proteins from each relevant organism [5].

Mosquitoes are the most menacing arthropod disease vectors, transmitting a broad range of viral, protozoan, and metazoan pathogens. Perhaps the most practical use for mosquito saliva is as a tool for surveying human exposure to mosquito bites [61]. A large percentage of the world's population lives in areas where the rate of mosquito-borne disease transmission is not accurately reflected by standard entomological measures of mosquito activity [148, 149]. Recent efforts have aimed to improve the sensitivity of vector exposure methods by identifying mosquito-specific saliva proteins that are immunogenic following delivery via bite. A candidate is gSG6, a protein found only in mosquitoes of the genus *Anopheles* that has shown promise in several lab and field studies [67, 149]. The identification of other mosquito specific (and genus specific) salivary immunogens should improve this epidemiological method, and published data suggest that there are other yet unidentified saliva proteins that are more immunogenic than gSG6 [150, 151].

The saliva of mosquitoes and other arthropods has also been shown to modulate vertebrate immune responses, resulting in the enhanced transmission of certain pathogens [3, 63]. Accordingly, vaccines which help incite the host antibody response against salivary immunomodulatory factors have been shown to lower the transmission rates of *Leishmania* parasites, and have been proposed for use against other arthropod-vectored diseases [3, 65]. While mosquito saliva has conclusively been shown to

enhance the transmission of several viruses [63], its role in the transmission of malaria parasites remains a point of contention [152-154]. Thus, the identification of novel immunomodulatory components of mosquito saliva may aid in the development of disease control strategies.

In the past decade, transcriptomic and proteomic studies have greatly increased our knowledge of the sialomes of a number of arthropod vectors [5, 147], with transcriptomic studies in *An. gambiae, Aedes aegypti* and *Culex pipiens* specifically increasing our understanding of the mixture of proteins found in mosquito salivary glands [155-157]. During a transcriptomic analysis of female *An. gambiae* salivary glands, Arca *et al.* [156] identified a contiguous series of large genes of unknown function (Vector base IDs: ENSANGP00000027299, ENSANGP00000027791 and ENSANGP00000029569; later named “SGS” by Korochkina et al. [68]) that had not been predicted during earlier genome scans and which appear to have been horizontally transferred into the mosquito genome from a bacterial source whose only known living relatives are *Wolbachia* Proteobacteria [158]. A member of this gene family was independently identified while screening a panel of monoclonal antibodies produced against *Ae. aegypti* salivary gland surface proteins. This protein, named aaSGS1 (GenBank: AAV28546), was shown to be required for the successful invasion of *Ae. aegypti* salivary glands by *Plasmodium gallinaceum* sporozoites [68]. Thus, the biology of SGS proteins is intriguing, as they have been implicated in the *Plasmodium* life cycle and in mosquito-*Wolbachia* interactions.

Using an array of complementary techniques, we conclusively show that two members of the *An. gambiae* SGS gene family, SGS4 and SGS5, are associated with blood feeding behavior, form prevalent components of mosquito saliva, and are major salivary immunogens. Further, we show that SGSs are not restricted to *An. gambiae*

saliva, as they are primary saliva constituents in both the anopheline and culicine lineages. Based on these and other data [159], we propose a putative role for SGS proteins as major immunomodulatory factors in mosquito saliva, and offer an explanation as for why SGSs have largely been overlooked in previous sialomic studies.

Materials and Methods:

Animal rearing and tissue collection

*An. gambi*ae (G3) and *Ae. aegypti* (LVP) mosquitoes were reared as described [117]. Briefly, larvae were hatched in plastic water containers and fed a mixture of koi food and yeast. Pupae were separated by size, allowed to eclose in 4.73 L plastic containers with marquisette tops, and the adults were maintained on a 10% sugar solution at 27°C, 75% relative humidity, and a 12 h light/12 h dark photoperiod with 30 min crepuscular periods that precede and follow each light cycle. Unless otherwise stated, 5-day-old adult female mosquitoes were used for all experiments.

Salivary glands were collected by submerging mosquitoes in phosphate buffered saline (PBS) and pulling the heads off with watchmaker's forceps. Minuten pins held by pin vices were then used to separate the glands from the head or to search through the anterior thorax, in the cases when the glands did not pull cleanly from the thorax.

Mosquito saliva was collected by inducing salivation using pilocarpine. For *An. gambiae*, this was done in a manner similar to that of Remoue *et al.* [61], except that topical application of 1% W/V Pilocarpine with 0.2% TWEEN 20 in PBS [160] was used instead of malathion, and saliva was collected into mineral oil rather than water. Because *Ae. aegypti* are more heavily pubescent, salivation in this mosquito was instead

induced by intrathoracic injection of 0.2 µl of a 0.01% W/V solution of pilocarpine in PBS. Only saliva from mosquitoes that visibly produced small droplets of saliva and appeared healthy after the end of the procedure was used in these experiments.

An. gambiae bite blots were done by attaching a nitrocellulose membrane to the bottom of a water-filled glass bottle heated to 58°C, and pressing the membrane against the freshly replaced marquisette cover of a mosquito cage. Within seconds, female mosquitoes were attracted to the heat and began probing the membrane with their proboscis, and this was allowed to continue in the dark for 10 min. Because heat is a principal cue for blood feeding [161], we believe that this method stimulates the production of saliva in a manner similar to natural blood feeding, as opposed to the sugar-based collection methods used in prior studies [162].

Following early suspicions that SGS protein levels might be affected by feeding behavior or circadian changes in expression, tissue collections were done between hours 6 and 8 of the light photoperiod, unless otherwise stated, and collection began at exactly the same times within each experiment.

Protocols used in this study for the maintenance and use of vertebrate animals were approved by Vanderbilt University's Institutional Animal Care and Use Committee (IACUC). Vanderbilt University's Division of Animal Care oversaw and provided veterinary care for this study, and is accredited by the Association for Assessment and Accreditation of Laboratory Animal Care (AAALAC).

Gene expression analyses

For non-salivary gland tissues, RNA from 10 mosquitoes was isolated using Trizol Reagent (Invitrogen, Carlsbad, CA) and repurified using the Purelink ™ Micro-to-Midi Total RNA Purification system (Invitrogen). For salivary gland samples, RNA from 50 glands was isolated directly using the Purelink system, per manufacturer's protocol for animal tissue samples. Up to 5 µg of RNA per sample was then treated with RQ1 RNase-Free DNase (Promega, Madison, WI), and first strand cDNA was synthesized from poly(A) + RNA using the SuperScript® III First-Strand Synthesis System (Invitrogen). A standard phenol/ chloroform extraction was used to purify the cDNA, and samples were then quantified and normalized. Standard PCR was conducted on a BioRad DNA Engine® Thermal Cycler using Choice-Taq™ DNA Polymerase (Denville Scientific, Metuchen, NJ). Real-time quantitative PCR (qPCR) was done using Power SYBR® Green PCR Master Mix (Applied Biosystems, Foster City, CA) on an ABI 7300 Real-Time PCR System, and relative quantification was carried out using the $2^{-\Delta\Delta C}{}_{T}$ method [163]. For both standard PCR and qPCR, *rpS7* was used as the reference gene. Primers used for standard PCR were: SGS4_d_F 5'-GCTGTTCCTTCGAAACTTGC-3', SGS4_d_R 5'-TCGCCGTGTATACCAATGAA-3'; SGS5_d_F 5'-ACCGCAACCGTAGCAATAAC-3', SGS5_d_R 5'-TCGAACAATCTGGGAGGTTC-3'; rpS7_01F 5'-CGTGAGGTCGAGTTCAACAA-3', rpS7_01R 5'-GCTGCAAACTTCGGCTATTC-3'. Primers used for qPCR were: SGS4_q01F 5'-TAACAACCCGCAGGAGATTC-3', SGS4_q01R 5'-GCTGCTGAATCGTTTCCTTC-3'; SGS5_q01F 5'-GCATCGGATCGTGGAACTAT-3', SGS5_q01R 5'-GTGGTGCTTGGGATGAAACT-3'; rpS7_02F 5'-GACGGATCCCAGCTGATAAA-3', rpS7_02R 5'-GTTCTCTGGGAATTCGAACG-3'.

Antibody production

Anti-SGS antibodies were produced by challenging rabbits with recombinant fragments of SGS4 and SGS5. Three polyclonal antibodies were developed. The first, referred throughout this manuscript as α-SGS_{RHS}, recognizes both SGS4 and SGS5 and was produced against a region of SGS4 that shares 96% amino acid identity with SGS5. This region, residues 2248-2571 of SGS4, is located directly N-terminal of the predicted transmembrane domain and includes the RHS domain. The other two antibodies, referred throughout this manuscript as α-SGS4 and α-SGS5, specifically recognize SGS4 or SGS5 by targeting unique regions located 88-549 and 512-822 residues from the N-terminus, respectively. Briefly, the SGS regions detailed above were amplified by PCR using Accuprime Pfx SuperMix (Invitrogen). Resulting amplicons were cloned into the pET-46 Ek/LIC expression vector (Novagen, Madison, WI) and proteins were expressed in BL21(DE3) *E. coli* cells. N-terminal His-tagged protein fragments were purified using BD TALON Metal Affinity Resin (Clontech, Mountain View, CA), and polyclonal antibodies were produced in rabbits (Affinity Bioreagents, Golden, CO). The IgG fraction of immune and pre-immune sera was purified using a KPL Protein A Agarose kit (KPL, Gaithersburg, MD), concentrated using a 30 kDa cutoff Microcon filter (Millipore, Billerica, MA), and buffer exchanged to PBS. Antibody concentrations were determined by measuring OD_{280} [164]. Primers used to amplify the cloned fragments were: for α-SGS_{RHS}, SGS4&5Pos_VS 5' GACGACGACAAGATGTGTGGAAAACGACTCGCTCTGAAT-3', SGS4&5Neg_VS 5'-GAGGAGAAGCCCGGTCTTACCCCGAACCTGCTTGAATGT-3'; for α-SGS4, SGS4_5P2_F 5'-GACGACGACAAGATCAAGGTGAAAGGGTTCGTGT-3', SGS4_5P2_R 5'- GAGGAGAAGCCCGGTCGTCGCTTGCTCAAGTTTTCC -3'; for α-SGS5, SGS5_Pos_VS

5’-GACGACGACAAGATGCGACAAACGCAAACCTTCACATCG-3’, SGS5Neg_VS 5’-GAGGAGAAGCCCGGTTGCTTTCACGGTTACCCATTCTCC-3’ (vector sequences are underlined).

Antibodies against *An. gambiae* saliva were produced in female Swiss Webster mice via exposure to mosquito bites. Mice were placed on top of cages containing approximately 150 starved female mosquitoes and fed upon for 5 min. Halfway through the procedure, mice were lifted off the cage and quickly repositioned, which induced the mosquitoes to re-probe. Blood was collected by cardiac puncture and sera was purified [164] at the end of each of three bite regimens: one week after a single bite exposure, one week after the last of three weekly bite exposures, and one week after the last of six weekly bite exposures. Non-immune control sera were purified from age- and cage-matched naïve mice.

SDS-PAGE, immunoblots, and total protein staining

In order to accommodate SGS’s large size, a variety of gels and protein standards were used throughout the study. These varied depending on the level of resolution and the protein mass inclusion best suited for an individual experiment. Whole tissues (salivary glands, thoraces, etc.) were either homogenized in 1% NP-40 buffer containing cOmplete® protease inhibitors (Roche, Penzberg, Germany) prior to mixing with denaturing NuPage© LDS loading buffer (Invitrogen) containing 2.5% β-mercaptoethanol (BME), or were homogenized directly in denaturing buffer with BME. Collected saliva was pooled, vigorously mixed with LDS sample buffer, and separated from the mineral oil by centrifugation at 8,600 rcf for 5 min. Whole tissue or saliva samples were then electrophoresed in either 4% Tris-Glycine polyacrylamide gels for 2 h

at 125 V, 3-8% Tris-Acetate polyacrylamide gels for 1 h at 150 V, or 4-12% Bis-Tris polyacrylamide gels for 1 h at 200 V, and separated proteins were transferred to PVDF membranes (Invitrogen) using the manufacturer's protocol. Western blotting was subsequently performed using KPL's Protein Detector™ LumiGLO Western Blotting Kit (Gaithersburg, Maryland, USA).

Bite-blots of mosquito saliva were treated in a similar manner to our Western blots, and the bite blots of previous authors [162]. A step similar to a standard transfer was included to ensure that saliva proteins were strongly bound to the membrane.

In order to assess the presence of total proteins in salivary samples, an imidazole-zinc negative detection protocol was used [165]. Although imidazole-zinc staining is very sensitive, it does not allow for the quantification of relative band content. When this was necessary, a quantitative coomassie staining protocol was used [166]. Gels were digitally scanned in a manner that avoided signal saturation, and densitograms were produced in ImageJ (National Institutes of Health, Bethesda, MD).

Immunohistochemistry

Salivary glands were dissected, fixed for 1 min in 100% acetone, and washed 3 times for 5 min each in PBS. Washed samples were blocked with 2% bovine serum albumin in PBS (B-PBS) for 1 h, rinsed 3 times for 5 min each in PBS, and incubated in rabbit α-SGS4, α-SGS5 or pre-immune IgG in B-PBS for 1 h. Samples were then washed as above, incubated in goat α-rabbit Alexa Fluor 568 (Invitrogen) with 0.01 mg/mL Hoescht 33342 in B-PBS for 1 h, washed, and mounted on slides using Aqua-Poly/Mount (Polysciences Inc., Warrington, PA). Salivary glands were imaged using DIC and fluorescence illumination on a Nikon 90i light microscope (Nikon Corp., Tokyo,

Japan) connected to a Photometrics CoolSNAP HQ2 high sensitivity monochrome CCD camera (Roper Scientific, Ottobrunn, Germany), and Z-stack images were captured and analyzed using Nikon's Advanced Research NIS-Elements software. To determine the precise location of SGS staining, Z-stacks were processed using the AQ 3D Blind Deconvolution module of NIS-Elements, and for the purpose of publication Z-stacks were flattened into 2 dimensions using the Maximum Intensity Projection module of NIS-Elements. Throughout, protein-A purified primary (immune and preimmune) and secondary antibodies were used at concentrations of 10 and 2.6 µg/ml, respectively.

Bioinformatic analyses

SGS sequences were scanned for functional sites that occur in non-structured regions using the Eukaryotic Linear Motif server (ELM; http://elm.eu.org), applying *An. gambiae* as the taxonomic range filter. ExPASy PeptideCutter tool was used to scan for putative Caspase-1 family cleavage sites (http://expasy.org), and SignalP 3.0 and SecretomeP 2.0 (both at http://www.cbs.dtu.dk) were used to search for classical and non-classical signal peptide cleavage sites, respectively. Following prediction of protease cleavage sites, the predicted molecular weights of SGS fragments were calculated using the Compute pI/Mw tool in ExPASy, and ExPASy ProtScale was used to plot hydrophobicity using the Rao & Argos scale [167].

Results:

SGS4 and SGS5 are expressed exclusively in the salivary glands

To determine the tissue-specific transcription of *Anopheles* SGSs, cDNA synthesized from salivary glands, heads, thoraces, thoraces from which the salivary glands had been removed, or abdomens of female mosquitoes was used as template for PCR using gene-specific primers. PCR revealed that *sgs4* (GenBank: AAV28544) and *sgs5* (GenBank: AAV28545) are only transcribed in the salivary glands and in the thorax, but that when the salivary glands are removed from the thorax this signal disappears (Figure 1A). Quantitative PCR confirmed this finding, and further showed that mRNA levels of *sgs4* and *sgs5* are 120 and 143 fold higher, respectively, in the salivary glands when compared to the whole body (Figure 1B). When mRNA levels of *sgs2* and *sgs3* were assayed, expression was inconsistently detected, and only in non-salivary gland tissues (not shown). For this reason, SGS2 and SGS3 were not studied further.

Given the salivary gland specificity of *sgs4* and *sgs5*, a polyclonal antibody that recognizes both SGS4 and SGS5 was developed (α-SGS_{RHS}). Western analyses revealed that, much like the transcription data, SGS4 and SGS5 are salivary gland-specific (Figure 1C), and interestingly, SGS4 and SGS5 are present exclusively in the salivary glands of female mosquitoes (Figure 1D). Within female salivary glands, SGS4 and SGS5 levels are minimal in freshly eclosed mosquitoes and peak around 10 days of age (Figure 1E). When a blood meal is provided, levels of SGS4 and SGS5 immediately increase and remain elevated for the lifetime of the mosquito (Figure 1F). Given that these data suggest that SGS4 and SGS5 are involved in some aspect of blood feeding, antibodies that selectively recognize SGS4 or SGS5 were constructed.

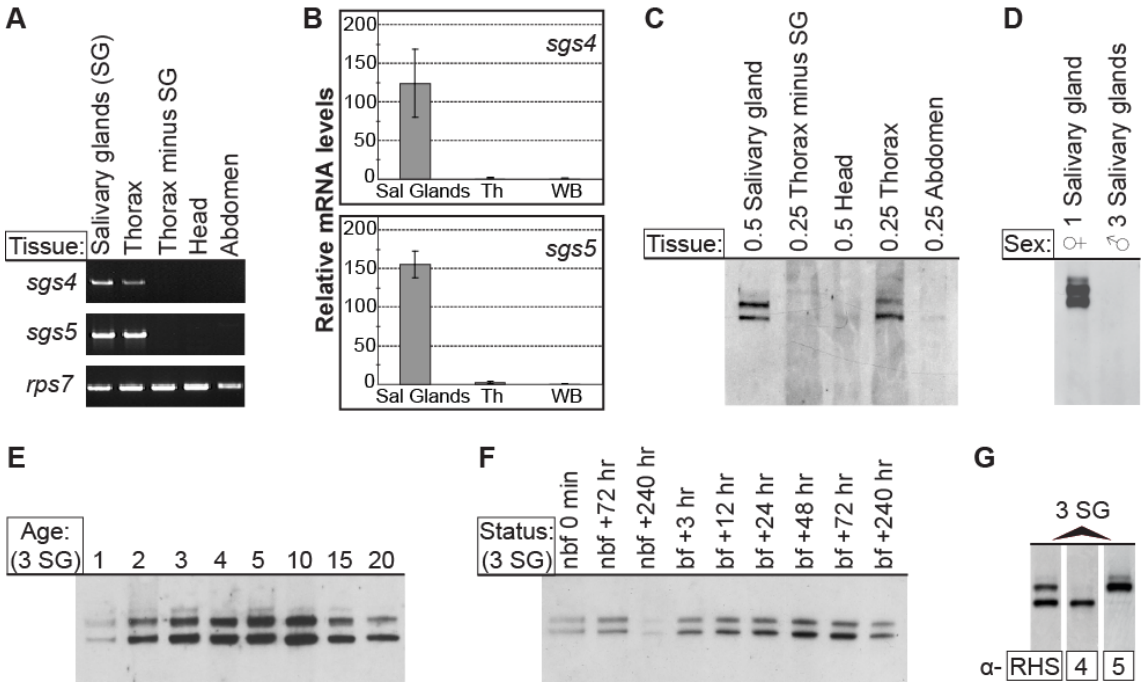

Figure 1. SGS4 and SGS5 are produced specifically in the salivary glands of adult female *Anopheles gambiae* and their production is associated with blood feeding. (A-B) Conventional PCR (A) and real-time quantitative PCR (B) comparing *sgs* transcript levels in tissues from 5-day-old adult mosquitoes. *sgs4* and *sgs5* are only transcribed in the salivary glands. (C-D) Western-blots of tissue samples from 5-day-old adult *An. gambiae*, showing that SGS4 and SGS5 are only present in the salivary glands of female mosquitoes. (E) Western blot of *An. gambiae* salivary glands at different times post-eclosion, showing that SGS levels are minimal in newly emerged adults and peak around 10 days of age. (F) Western blot of *An. gambiae* salivary glands at different times following blood feeding (bf), along with non-blood fed controls (nbf), showing that blood-feeding enhances SGS production. (G) The same lane of a Western blot stripped and reprobed with each of the antibodies produced against recombinant SGSs, showing their binding specificities and that SGS5 is slightly more massive than SGS4. Western blots in panels C-F were probed using α-SGS_{RHS} (recognizes both SGS4 and SGS5) and were performed after electrophoresing samples in 4% Tris-Glycine SDS-PAGE gels. For an explanation of SGS mass size, see figure 6.

Stripping and reprobing of the same Western blot with each of the three α-SGS antibodies confirmed the band identities and showed that SGS5 is slightly more massive than SGS4 (Figure 1G).

SGS4 and 5 are present in the distal-lateral acinar cells and the salivary ducts

Analysis of quantitatively deconvolved Z-stacks acquired from salivary glands immunolabeled with α-SGS4 or α-SGS5 revealed that both of these proteins are present on the basal and apical cellular surfaces of the distal lateral lobes (Figure 2A-J). Lower intensity staining was also detected in the salivary ducts of the proximal lateral lobes, a pattern that also suggests a role in blood feeding. Preimmune controls (Figure 2G-I) and midguts labeled with α-SGS4 and α-SGS5 showed no staining.

Because of the unexpected finding that *Anopheles* SGSs are present in the salivary ducts, Western blots were conducted in salivary glands that were disarticulated into their three anatomical regions: the distal lateral lobes, the proximal lateral lobes, and the median lobes. Western analyses confirmed the immunolabeling results, and suggest that both SGS4 and 5 are subjected to processing in the proximal lateral region of the salivary glands, as in these regions their weight is reduced by approximately 10 kDa (Figs. 2K).

Finally, during the immunolabeling experiments, unambiguous differences between α-SGS samples and pre-immune controls were only obtained after fixation with organic solvents (acetone or ethanol) and not following fixation with formaldehyde, regardless of permeabilization with Triton-X 100 or heat induced antigen retrieval.

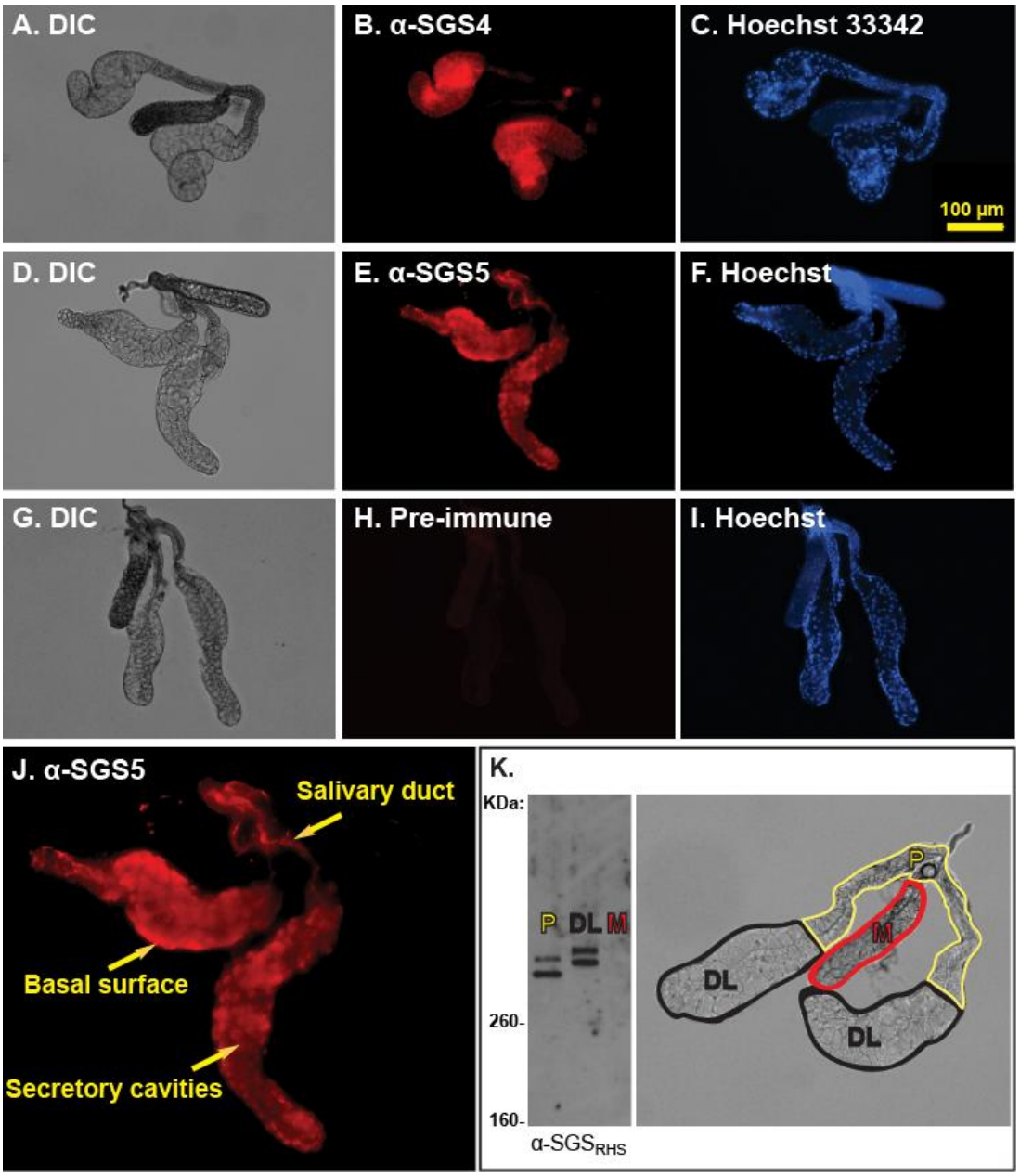

Figure 2. SGS4 and 5 are present in the distal-lateral acinar cells and the salivary ducts. (A-I) Immunohistochemistry of female salivary glands using α-SGS4 (A-C), α-SGS5 (D-F), or pre-immune antibodies (G-I; from mouse later immunized with SGS4). Serial micrographs show imaging through DIC (A, D, G), Texas Red (B, E, H; antibody labeling), and Hoechst 33342 (C, F, I; DNA stain) channels. (J) Close-up of panel E showing labeling of the acinar cells of the distal lateral lobes and the salivary ducts of the proximal lobes. (K) Western blot of disarticulated salivary glands, confirming that SGS4 (bottom bands) and SGS5 (top bands) are present only in the lateral lobes, and showing that both are slightly less massive in the proximal lateral lobes than they are in the distal lateral lobes (4% Tris-Glycine SDS-PAGE).

This suggests that SGSs are either located in a region inaccessible to the antibodies following aldehyde fixation or that the antibodies do not efficiently bind the native proteins.

SGSs form a major component of An. gambiae *and* Ae. aegypti *saliva*

Because expression and localization data suggested that SGS4 and 5 may be involved in blood feeding, mosquito salivation was artificially induced, and the collected saliva was analyzed for the presence of SGS4 and SGS5. Western analyses conclusively detected both SGS4 and 5 in mosquito saliva (Figure 3A-B). In order to ensure that the presence of SGSs in saliva was not the result of pilocarpine treatment, we used heat to entice mosquitoes to probe a nitrocellulose membrane and performed "bite blots" using α-SGS antibodies. Bite blots revealed that SGS4 and SGS5 are released with the saliva during probing. SGS4 and SGS5 were only detected at the probing sites; no staining was observed outside the probing areas or when 3 times as much preimmune antibody was used instead of α-SGS antibodies (Figure 3C). Like SGSs found in the proximal lateral salivary lobes (Figure 2K), SGSs in saliva are approximately 10 kDa less massive than SGSs found in the distal lateral lobes.

To determine the relative levels of SGSs in mosquito saliva we first stained 4% SDS-PAGE gels with Zinc-imidazole and assessed protein bands in the range of 200-500 kDa (Figure 3D). This experiment yielded two distinct results. First, it showed that SGSs are the only detectable proteins in this size range. Second, it showed that soaking salivary glands in detergent prior to denaturation results in a 10 kDa size reduction.

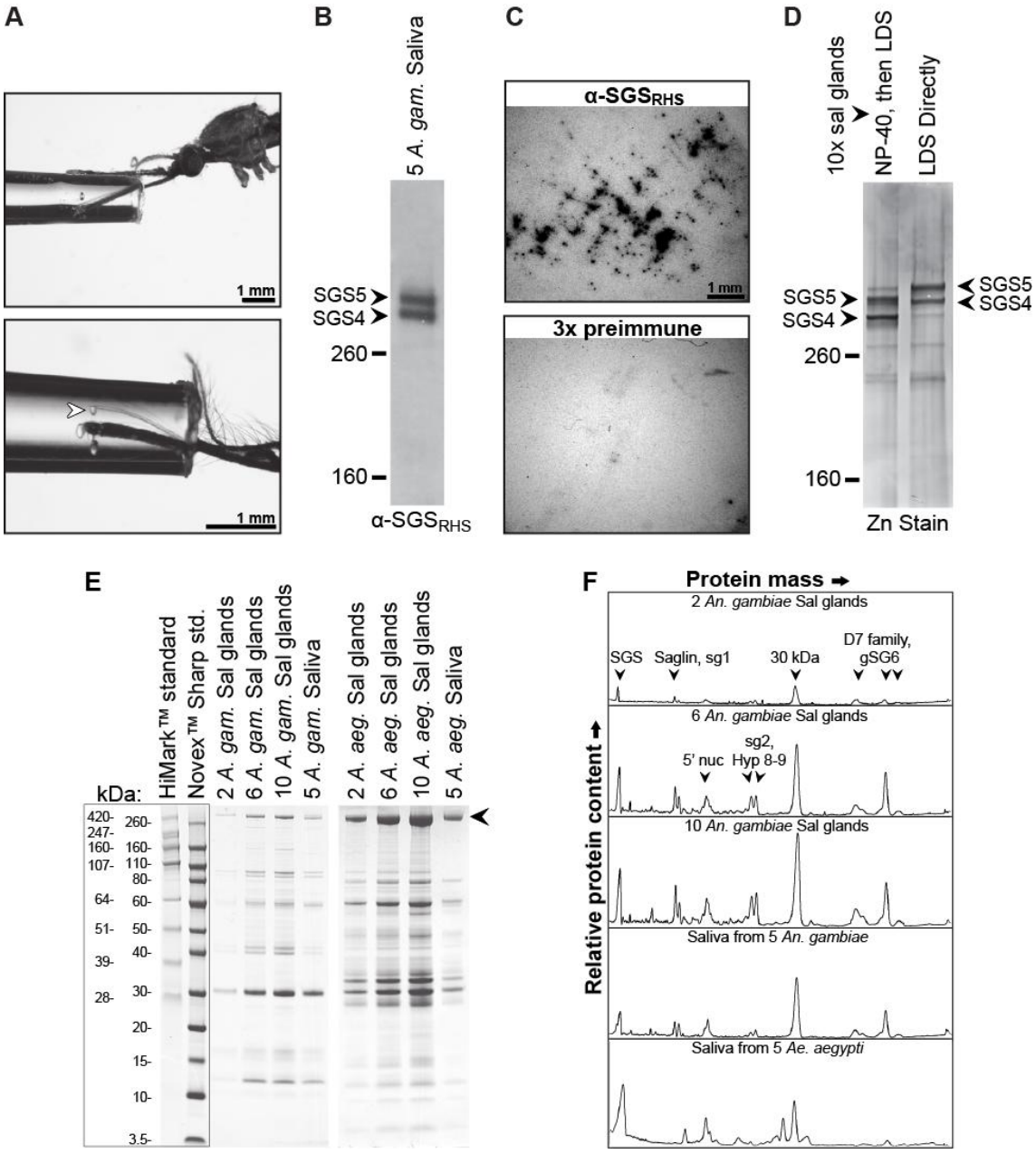
A
1 mm
1 mm
B
5 A. gam. Saliva
SGS5
SGS4
260
160
α-SGSRHS
C
α-SGSRHS
1 mm
3x preimmune
D
10x sal glands
NP-40, then LDS
LDS Directly
SGS5
SGS4
260
160
SGS5
SGS4
Zn Stain
E
kDa:
HiMark™ standard
Novex™ Sharp std.
2 A. gam. Sal glands
6 A. gam. Sal glands
10 A. gam. Sal glands
5 A. gam. Saliva
2 A. aeg. Sal glands
6 A. aeg. Sal glands
10 A. aeg. Sal glands
5 A. aeg. Saliva
420-
247-
160-
107-
64-
51-
39-
28-
260-
160-
110-
80-
60-
50-
40-
30-
20-
15-
10-
3.5-
F
Protein mass ➡
2 An. gambiae Sal glands
SGS
Saglin, sg1
30 kDa
D7 family, gSG6
6 An. gambiae Sal glands
sg2, 5' nuc
Hyp 8-9
10 An. gambiae Sal glands
Saliva from 5 An. gambiae
Saliva from 5 Ae. aegypti
Relative protein content ➡

Figure 3. SGS4 and 5 are the only prevalent proteins in their size range found in mosquito salivary glands and form major constituents of mosquito saliva. (A) Saliva collection in *An. gambiae* (top) and *Ae. aegypti* (bottom). Droplet formation can be seen in both images, with the *Ae. aegypti* image showing saliva being ejected from the hypopharynx (arrowhead). (B) Western blot of *An. gambiae* saliva collected following pilocarpine treatment, showing that SGS4 and SGS5 are a component of mosquito saliva. (C) Bite-blots probed with α-SGS_{RHS} (top) or 3 times the amount of pre-immune serum (bottom), showing that SGSs are released with the saliva during probing. (D) 4% Tris-Glycine SDS-PAGE gel stained with Zn-imidazole, showing that SGS4 and SGS5 are the only proteins in their size range present in mosquito salivary glands. Note that when glands were immediately immersed in denaturing LDS buffer their size is approximately 10 kDa more massive than when they were incubated in NP-40 detergent prior to denaturation. SGS4 and 5 in the saliva match the smaller SGS forms seen in whole salivary glands initially soaked in non-denaturing buffer. (E) Coomassie stained 4-12% SDS-PAGE of salivary glands and saliva from *An. gambiae* and *Ae. aegypti*. The combined SGS bands are marked by an arrowhead. (F) Densitogram of select lanes from gel in panel D, showing relative protein content. In both salivary glands and saliva, SGSs form one of three major peaks in *An. gambiae* and is the major peak in *Ae. aegypti*. Peak identities, other than SGS, are inferred using data from a previous study [168].

Next, proteins from salivary glands as well as saliva collected by pilocarpine treatment were separated by SDS-PAGE on 4-12 Bis-tris gradient gels and relative protein mass content was quantified by coomassie analysis (Figure 3E-F). Within the range of 3.5 kDa to over 500 kDa, SGSs are one of the three most prevalent proteinaceous components of *An. gambiae* saliva, and the most prevalent component of *Ae. aegypti* saliva. Taken altogether, these data conclusively show that SGSs are primary components of mosquito saliva in both major mosquito lineages.

SGSs are a major immunogen in mosquito saliva

Given the prevalence of SGS4 and SGS5 in *An. gambiae* saliva, we sought to determine whether these proteins elicit an antibody response following blood feeding. Experiments where antisera from mice exposed to mosquito bites were used as primary antibodies in Western blots corroborated the discovery of SGS4 and SGS5 as major components of mosquito saliva, and also showed that they are highly immunogenic, eliciting a strong IgG response (Figure 4). Neither antisera from non-immune mice or from mice exposed to a single round of mosquito bites that occurred ≤1 week before blood collection detected any *Anopheles* salivary gland protein. However, after 3 or 6 weekly exposures to mosquito bites, SGSs were found to be one of two consistently recognized proteins in mosquito saliva, a result that was confirmed by both molecular weight and by stripping membranes and reprobing them with α-SGS_{RHS}, α-SGS4 or α-SGS5. Only one other highly immunogenic band was consistently recognized by our anti-saliva antibodies, which weighed ≈100 kDa under non-reducing conditions and ≈50 kDa under reducing conditions. One other band was observed in one instance under non-reducing conditions and weighed ≈70 kDa.

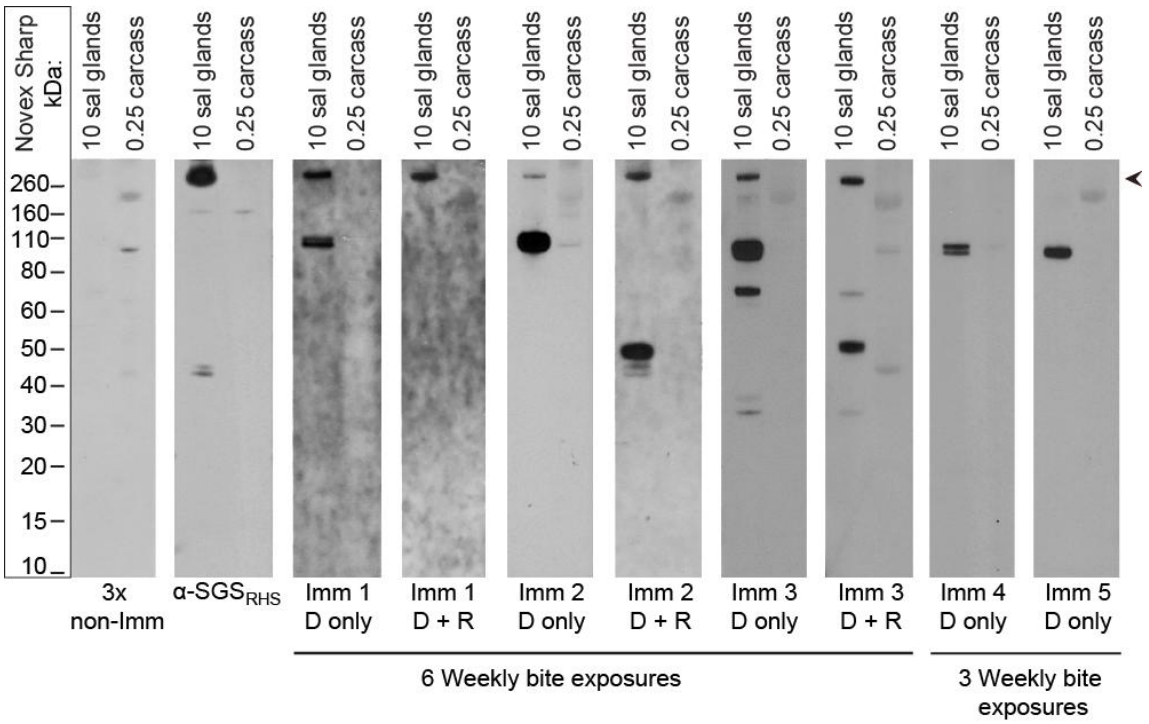

Figure 4. SGSs are one of two major immunogenic components of *An. gambiae* saliva. Western blots of salivary glands (Sal glands) and carcasses excluding salivary glands (carcass) electrophoresed in 4-12% Bis-Tris gels and probed with (from L to R): sera from non-immune mice (non-Imm; 1/80 dilution), α-SGS$_{RHS}$, mice exposed to weekly mosquito bites for 6 weeks (Imm 1-3; 1/500 dilution), and mice exposed to weekly mosquito bites for 3 weeks (Imm 4-5; 1/500 dilution). Results are shown for extracts run under denaturing (D only) and denaturing plus reducing (D + R) conditions (for sera shown only under denaturing conditions, reducing yielded identical results). Overall, the major immunogenic components of mosquito saliva are SGSs (arrowhead) and an unrelated protein that migrates at 110 kDa or 55 kDa, depending on whether it has been reduced.

Salivary gland SGS content is highest in the early evening

Because mosquito feeding behavior follows a circadian cycle, we investigated the prevalence of SGS4 and SGS5 at different times of the day. Western blots and coomassie staining of salivary glands collected every 3 h for 24 h, or 1 h into both the light and dark cycles, demonstrated that salivary gland SGS content fluctuates with the time of day, and that SGS levels are highest in the late afternoon and early evening (Figure 5A-C). The SGS circadian gradient was not always as consistent as what is seen in Figure 5C, but multiple replicates of this experiment support this trend. Moreover, from these experiments two additional trends became apparent. First, the initial onset of SGS expression occurs during the mosquito's first night as adults (Figure 5B), although protein levels remain relatively low until the second afternoon (Figure 1E). Second, circadian expression is most accentuated in younger mosquitoes and the circadian effect diminishes once peak SGS expression is reached at around 10 days of age (Figure 5A). Given that *An. gambiae* have a nighttime feeding preference, and that newly eclosed mosquitoes do not effectively blood feed, these circadian data again suggest that SGS4 and SGS5 are involved in blood feeding.

Western and bioinformatic analyses suggest SGS4 and 5 are proteolytically processed prior to secretion

Because SGSs are extremely large and are predicted to have multiple transmembrane regions, it was unexpected to find them in mosquito saliva. Hence, Western and bioinformatic analyses were performed in efforts to explain this phenomenon. The initial question pertained to the mode of secretion. Signal-P detected no classical signal peptides in *An. gambiae* SGS4 or SGS5, or in *Ae. aegypti* SGS1.

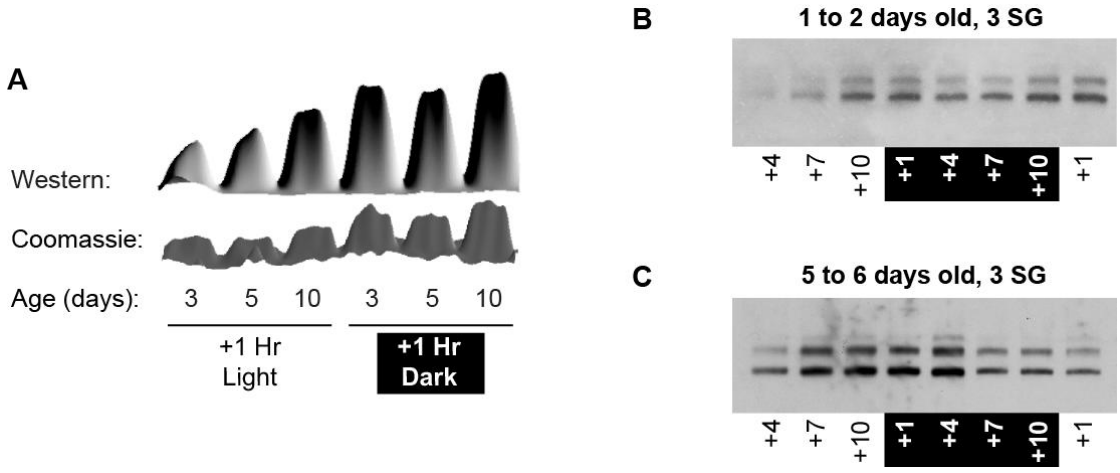

Figure. 5. SGS protein levels fluctuate within 24 hour periods and are most prevalent during the late afternoon and early evening. (A) Surface plot of relative combined band intensities of both SGS4 and SGS5 from Western (top) and coomassie (bottom) analyses of salivary glands from mosquitoes of the same cohort, at different ages, collected at +1 h into the light and dark cycles. (B-C) Western blots of salivary glands (SG) extracted from 1-2 and 5-6 day-old mosquitoes showing SGS levels over a 24-hour period.

However, Secretome P analysis using a gram-negative model predicted significant likelihoods of non-classical protein secretion for both SGS4 and SGS1 (NN-scores >0.5). When a mammalian model was used instead, SGS4 and 5, as well as SGS1, all have scores that approach the 0.5 cutoff (an insect model for non-classical secretion does not exist). These findings suggest that SGSs are secreted by non-classical means, a process that is known to involve proteolytic pathways.

The second question pertained to protein size. The Compute pI/Mw tool in ExPASy predicts that full length SGS4 and SGS5 weigh >380 kDa. However, Western blots conducted using the 3-8% Tris-acetate PAGE gels that are recommended for high molecular weight proteins, along with the HiMark™ high weight protein standard, showed that SGS4 and SGS5 weigh ≈300 kDa (Figure 6A-B) instead of the ≈220 kDa previously reported for *Ae. aegypti* SGS1 [68]. Western blots using 4-12% Bis-Tris and 4% Tris-Glycine gels and two other high weight standards confirmed the ≈300 kDa weight of SGS4 and SGS5 (Figure 6B). Analyses using gradient gels also detected a smaller doublet of immunoreactive bands that weigh approximately 47 kDa (Figs. 6A-B), and interestingly, this smaller doublet was detected when using α-SGS_{RHS}, but not when using α-SGS4 or α-SGS5 (not shown). These data suggest that SGS4 and SGS5 are each cleaved into ≈300 kDa and ≈47 kDa fragments.

The third question pertains to the cleavage process. Several sequence analysis programs predict two prophenoloxidase activating protease (PAP) type cleavage sites (consensus sequence: [ILV]X_aX_a [R][VF][GS]X_a; [39]) that are located N-terminal of the transmembrane domain of both SGS4 and SGS5 (between amino acids 2500-2650; Fig. 6C-D), and nowhere else in either protein. In both SGS4 and SGS5, one of these sites shares high similarity with the only predicted PAP site in *Aedes* SGS1 (consensus sequence from SGS1, 4 and 5: L[LT]QRVS[ER]), and is located at the same distance

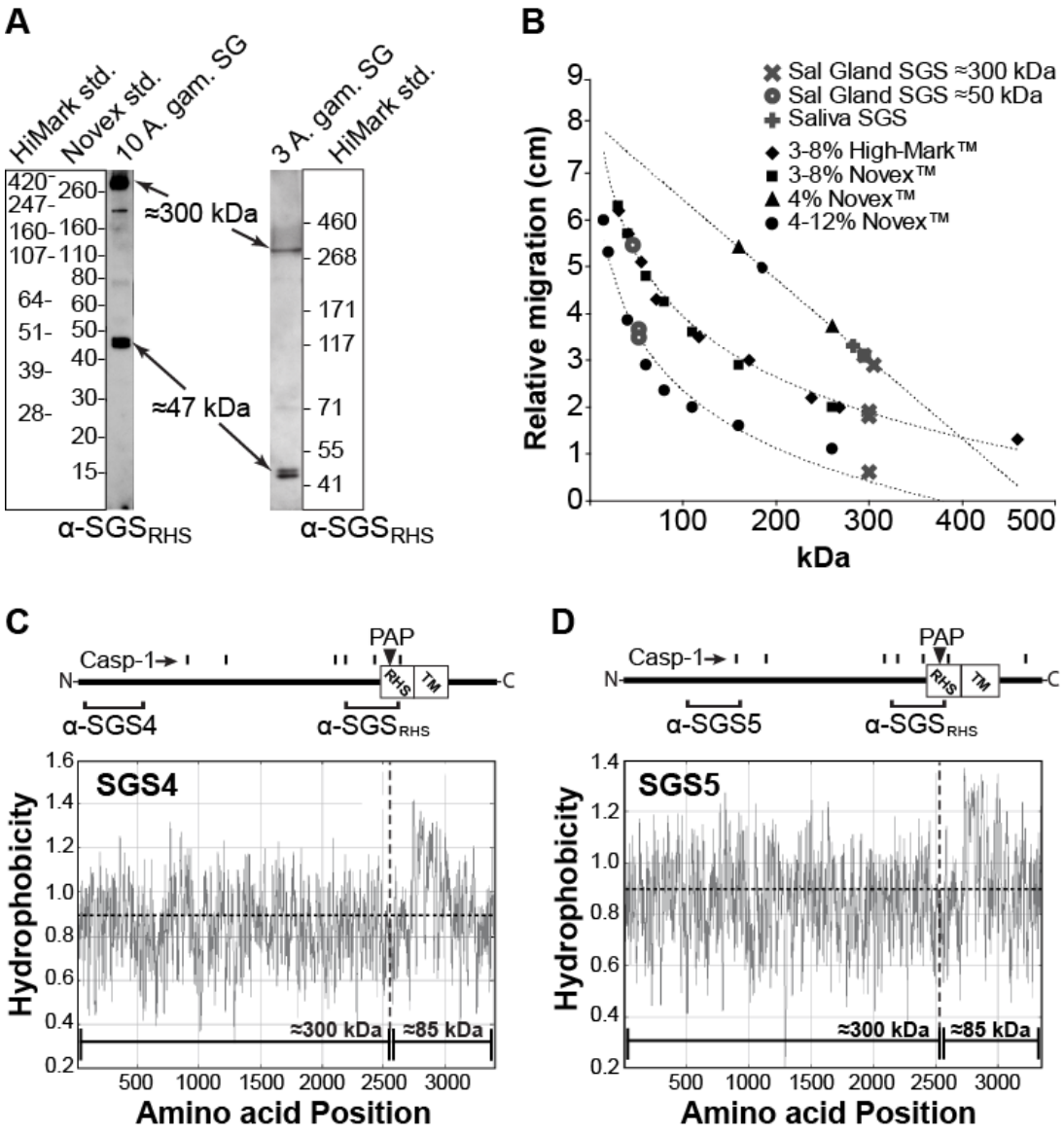
A
HiMark std.
Novex std.
10 A. gam. SG
3 A. gam. SG
HiMark std.
420-
247-
160-
107-
64-
51-
39-
28-
260-
160-
110-
80-
60-
50-
40-
30-
20-
15-
≈300 kDa
≈47 kDa
460
268
171
117
71
55
41
α-SGS$_{RHS}$
α-SGS$_{RHS}$
B
Sal Gland SGS ≈300 kDa
Sal Gland SGS ≈50 kDa
Saliva SGS
3-8% High-Mark™
3-8% Novex™
4% Novex™
4-12% Novex™
Relative migration (cm)
kDa
C
Casp-1
PAP
N
C
RHS
TM
α-SGS4
α-SGS$_{RHS}$
SGS4
Hydrophobicity
≈300 kDa
≈85 kDa
Amino acid Position
D
Casp-1
PAP
N
C
RHS
TM
α-SGS5
α-SGS$_{RHS}$
SGS5
Hydrophobicity
≈300 kDa
≈85 kDa
Amino acid Position

Figure. 6. The mass of SGS4 and 5, along with bioinformatic analyses, suggest that they are cleaved into a 300 kDa soluble N-terminal fragment and a smaller, membrane bound fragment. (A) Western blots of 10 female salivary glands run on 4-12% Bis-Tris (left) or 3-8% Tris-Acetate (right) SDS-PAGE gels and probed with α-SGS_{RHS}. A single band is seen at around 300 kDa that has been shown to correspond to a large fragment of SGS4 and 5 (one band seen here due to lack of resolution on these gels). A doublet weighing approximately 47 kDa is also observed. (B) Plot of observed protein migration distances versus two sets of standards on various gel types. Gray symbols represent SGS band migration distances while black symbols and trend-lines represent the observed migration of different standards. In all cases, SGS mass is calculated to be 300 +/- 10 kDa. (C-D) Graphical representation of SGS4 (C) and SGS5 (D) showing the locations of the putative RHS domains, transmembrane regions (TM), prophenoloxidase activating peptide cleavage sites (PAP), caspase 1-cleavage sites (Casp-1), and the regions that the anti-SGS antibodies recognize. Below these gene diagrams, hydrophobicity plots show that cleavage at the PAP sites would result in an N-terminal fragment weighing ≈300 kDa and a highly hydrophobic membrane bound fragment weighing ≈85 kDa (higher values represent higher hydrophobicity).

from the N-terminus in all three SGSs (from 2533-2549). The Compute pI/Mw tool predicts that cleavage of full-length SGS4 or SGS5 at this site should result in an N-terminal soluble fragment weighing ≈300 kDa and a membrane bound fragment weighing ≈85 kDa. The ≈300 kDa fragment is the larger mass observed during PAGE analyses (Figure 6A-B), while the smaller bands recognized by α-SGS_{RHS} migrate at ≈47kDa rather than the predicted ≈85 kDa (Figure 6A). However, this smaller fragment is also predicted to contain at least 6 transmembrane helices and to be highly hydrophobic (Figure 6C-D). High hydrophobicity is known to cause excessive SDS binding and faster migration through SDS-PAGE gels, causing a protein to appear much less massive than it actually is [169]. As expected under this scenario, the α-SGS_{RHS} antibody that recognizes sequences both N- and C-terminal of the PAP site binds both the 300 kDa and the 47 kDa fragments, but the α-SGS4 and α-SGS5 antibodies that recognize sequences located N-terminal of the PAP site recognize only the ≈300 kDa fragment. An alternative possibility for proteolytic processing involves Caspase-1-based cleavage, as this has been shown to be a regulatory mechanism of non-classical secretion [170]. PeptideCutter predicts 6 and 7 Caspase-1 type cleavage sites in SGS4 and SGS5, respectively, of which 4 are located between amino acids 2100-2670 from the N-terminus of both SGS4 and SGS5. Again, the ≈47 kDa and ≈300 kDa fragments recognized by α-SGS_{RHS} could be explained by several of the predicted Caspase-1 sites (Figure 6C-D), offering another plausible explanation for SGS cleavage and subsequent release into the saliva.

Finally, SGSs appear to undergo an additional processing step in the salivary duct of the proximal-lateral lobes. When whole salivary glands are placed in denaturing LDS buffer immediately following dissection, a ≈300 kDa SGS form is by far the most prevalent. However, when salivary glands are soaked in NP-40 prior to denaturation in

LDS buffer, the ≈300 kDa fragment is converted into a slightly less massive form (Figure 3D). This conversion, which results in an approximately 10 kDa reduction in mass, is completed within 30 min, and matches precisely the size of SGSs collected during artificial salivation experiments. Interestingly, this effect is only seen when the proximal lateral lobes are included in the non-denaturing lysate solution, showing that this processing requires a component of the proximal lateral lobes (Figure 2K). The reason for this drop in weight is unknown, but because certain amylases and proteases are only produced in the proximal-lateral lobes [171], together with the prediction that SGSs are glycosylated [68], we hypothesize that the interaction of SGSs with saliva components results in additional proteolytic cleavage or deglycosylation. Taken altogether, Western and bioinformatic analyses suggest that SGS4 and SGS5 are secreted via a non-classical pathway following proteolytic cleavage into a ≈300 kDa soluble fragment and an ≈85 kDa membrane bound fragment. The ≈300 kDa fragments are then processed into slightly less massive forms by an unknown product of the proximal lateral lobes prior to being expelled with the saliva.

Discussion:

Most research investigating the salivary glands of arthropod disease vectors has focused on uncovering the protein repertoire of salivary components in efforts to identify candidates for use in the development of epidemiological techniques [61, 67], transmission blocking vaccines [3], or novel therapeutic agents [5]. Here we characterized the spatial, temporal and functional expression of two *Anopheles* saliva proteins that are involved in blood feeding. The expression and biochemical characteristics of these proteins suggest that they play multiple physiological roles and

that they may be useful for the epidemiological surveillance of mosquito activity and in the development of disease control strategies.

The only published study to date that focuses on the biology of SGS proteins showed that a member of the *Ae. aegypti* SGS gene family, SGS1, is produced exclusively in the salivary glands, where it is embedded in the basal lamina and serves as an inadvertent receptor for *P. gallinaceum* sporozoites [68]. In the present study we found that *An. gambiae* SGS4 and SGS5 are also present on the basal side of the salivary glands, and because the major portions of these proteins are cleaved from their transmembrane domain, it is likely that they are also embedded in the basal lamina. Thus, SGS4 and SGS5 may also function as *Plasmodium* receptors in this major vector of human malaria. However, an unexpected finding was that SGS4 and SGS5 are also secreted apically into the salivary duct, where they form a major component of mosquito saliva. Because *Ae. aegypti* proteins in the SGS size range are major saliva components, it is likely that SGS1 is also secreted into the saliva.

An. gambiae SGS4 and SGS5 are produced in salivary gland regions known to produce factors involved in blood feeding [171], and production of SGS4 and SGS5 ramps up during the times of the day when these mosquitoes show a higher propensity to bite mammals [172]. Together with their substantial release with saliva during probing, these data show that they are involved in blood feeding. The precise role of *Anopheles* SGSs in this process has not been fully determined, but we show that they are among the most immunogenic proteins injected during natural blood feeding. This was not entirely unexpected, as SGSs are large proteins sharing little homology with any vertebrate protein, and thus, relatively high antibody titers would be expected from a small antigen dose. High immunogenicity opens the possibility that human anti-SGS antibodies could serve as sensitive markers for assessing exposure of humans to

mosquito bites [61, 67], and that this could be an important tool in areas of low to moderate mosquito density. Furthermore, because the large N-terminal region of the SGS proteins is highly variable, small recombinant SGS peptides could be used as species-specific and genus-specific antigens in this epidemiological strategy. Such taxon specificity has often been cited as one justification for the use of gSG6 in surveying bite exposure [61, 67], but gSG6 is only present in one mosquito genus.

When assaying the immunogenicity of mosquito saliva components, two distinct sets of proteins were identified: SGSs and a protein that weighs approximately 100 kDa under non-reducing conditions and 50 kDa when reduced. The electrophoretic pattern of the latter protein suggests that it is a disulfide-linked dimer, and interestingly, this pattern of migration is identical to that seen for SAGLIN, an *Anopheles* salivary protein that was shown to be involved in *Plasmodium* invasion of the salivary glands, along with some evidence that it is a component of mosquito saliva [173, 174]. The detection of putative SAGLIN is strong after only 3 weeks of exposure to bites, suggesting that SAGLIN may also be a sensitive target for an exposure surveillance strategy. Furthermore, given that SGS1 and SAGLIN are the only two molecularly identified candidate receptors for *Plasmodium* on the salivary gland surface, it is interesting that both are also present in the saliva. These findings suggest that their interaction with the parasite may be long-lived, and that besides serving as basal receptors they may also facilitate sporozoite traversal of acinar cells, survival in the salivary duct, and/or transmission to the vertebrate host.

It has been shown that immunomodulatory factors in arthropod saliva can enhance the transmission of protozoan parasites, and thus, a vaccine that neutralizes such factors might offer protection from pathogens [3]. For example, vaccination against a single immunomodulatory and vasodilatory protein from sandfly saliva provides

resistance to *Leishmania* infection [175]. There is now a strong body of evidence supporting an immunomodulatory effect by mosquito saliva, although the identity of these immunomodulatory proteins has not been determined [63]. One such factor is a large immunogenic protein from *An. stephensi* that possesses neutrophil chemotactic activity [151]. Another large immunomodulatory protein was discovered from *Ae. aegypti* saliva, weighs 389 kDa, and significantly lowers cytokine release and the proliferation of murine T- and B-cells [159]. Based on our proteomic analyses (Figs. 3B, 6), as well as transcriptomic analyses by others [156, 176], SGSs are the only anopheline or culicine saliva proteins whose mass approximates the value predicted for this 389 kDa protein. In support of our hypothesis that SGS4 and SGS5 are immunomodulatory, it has recently been shown that bacterial RHS/YD-repeat proteins (distant relatives of SGS) play a role during the deactivation of human macrophages by the bacterial pathogen *Burkholderia pseudomallei* [177]. If SGSs are indeed immunomodulators, they should be considered when developing transmission blocking vaccines.

Another interesting aspect of SGS proteins is that they share high sequence homology with proteins found in *Wolbachia* Proteobacteria (alignment of SGS5 and *Wolbachia* WD0513 yields 28% shared amino acid identity, 47% positives and an E-value of 0.0), and contain regional homology with the viral/bacterial RHS/YD-repeat protein family [68, 156]. It is hypothesized that horizontal gene transfer from the intracellular bacterium *Wolbachia* led to the origin of mosquito SGSs, and the relatively high expression levels of *Ae. aegypti* SGSs suggest that some of these genes have evolved to perform essential roles in mosquitoes, unlike what is often observed following transdomain horizontal transfer [158]. Our work validates this finding in anopheline mosquitoes by showing that SGS4 and SGS5 are specific to salivary tissue and are highly expressed. While the functions of non-mosquito YD-repeat proteins are not well

understood, they may be important in the interactions between microbes and their insect hosts [178, 179]. In addition, YD-repeat proteins have been implicated as participants in lectin-like heparin binding, as mediators of cellular interactions, and as cellular toxins with anti-macrophage activity [177, 178, 180, 181]. These are roles that share similarities with those proposed for mosquito SGSs, both here and by others [68]. As for why a *Wolbachia* gene would have been adopted as a major salivary gene in mosquitoes, it is tempting to speculate that the ancient horizontal transfer of an immunomodulatory factor could have been a pivotal step during the evolution of hematophagy in mosquitoes. Exaptation and recruitment of endogenous genes into novel functional roles appears to occur often during the evolution of arthropod sialomes [5, 147], but SGSs are now the first examples of a saliva protein originating through horizontal gene transfer in a hematophagous arthropod.

While we conclusively show that SGSs form a major component of the salivary glands and saliva of anopheline and culicine mosquitoes, these proteins have been largely overlooked in earlier proteomic studies (Table 1). The primary reason for this rests in the size of SGS proteins, as the electrophoretic methods most commonly used in SDS-PAGE studies (e.g., ≥10% polyacrylamide concentration) preclude proteins as large as SGSs from entering the resolving portion of the gel. In all but two studies where a band was seen to approximate SGS's size and relative intensity, the presence of the protein was not addressed. It is likely that SGS's large size either made it seem like an artifact, or that it was observed but disregarded because it was unrelated to the specific aim of the research. In one study, SGS was invoked as an explanation for a salivary band weighing 175 kDa that was consistently recognized by IgG from children exposed to high numbers of mosquito bites [150]. This same study recognized one other salivary antigen that was estimated to weigh 72 kDa under non-reducing conditions. It is likely

Table 1. Analysis of scientific papers in which mosquito saliva or whole salivary gland proteins were analyzed by SDS-PAGE, or by Western blot using antibodies from humans or rodents exposed to mosquito bites. ¶

	SGS not identified: appropriate parameters #	**SGS not identified: restrictive parameters ***	**Band approximating SGS size range, but not addressed in the article**	**SGS explicitly stated in the article**
SDS-PAGE	None	[150, 182-187]	[168, 188-191]	[192]+
Western blot (Human sera)	None	[184, 191, 193, 194]	[195]	[150]^
Western blot (Rodent sera)	None	[187, 196]	[190, 197]	None

¶ Only studies that could be clearly categorized were included in this analysis.

Parameters used should have allowed for the visualization or identification of SGSs.

* Parameters used would preclude the visualization or identification of SGSs. Restrictive parameters include the use of ≥ 10% SDS-PAGE gels (under normal running conditions, SGSs are too large to enter the resolving portion of the gel), and cropping of gel scans such that the gel portions that would show high molecular weight proteins are not shown.

+ In this article, SGS4 and SGS5 are erroneously referred to as SG4 and SG5, but the correct Genbank accession numbers are listed.

^ In this article, putative SGSs are predicted to weigh 175 kDa.

that these bands represent SGS (300 kDa) and SAGLIN (100 kDa), but that size estimates were incorrect due to the incompatibility of the gels and ladders used. Another study supports our finding that SGS is a component of mosquito saliva, although in that study the authors propose that SGS presence in the saliva is a result of contamination [192]. These results illustrate that although SGSs are prevalent immunogenic components of mosquito saliva, the methodologies commonly used when studying salivary proteins preclude their detection.

In summary, this study considerably expands our understanding of a family of mosquito proteins that have now been implicated in blood feeding, *Plasmodium* transmission, and mosquito-*Wolbachia* interactions. Given that SGSs form a major component of mosquito saliva, future studies should investigate the role these proteins play in modulating vertebrate immune responses and assess the potential use of SGSs as epidemiological markers for the surveillance of mosquito activity in disease-endemic areas.

CHAPTER VI

CONCLUSIONS

Along with preventative hygiene and prophylaxes, the reliable medical countermeasures mankind has been able to develop against infectious microbes act by: (1) specifically targeting and killing the pathogen or preventing its reproduction [198-200], (2) imparting or enabling protective immunity [201-204], or (3) interfering with critical host-pathogen interactions [205]. In the case of diseases vectored by arthropods, control of vector populations has also been effective in some instances [206]. In a way, vector control is analogous to the first medical strategy listed above. Accordingly, as is the case with disease-causing microbes and antibiotics [207], insects can rapidly develop resistance to pesticides [208]. Due to the ubiquity of mosquitoes, pesticide resistance, and finite financial resources, millions of people are still affected each year by arthropod vectored diseases, with mosquitoes reigning as the most dangerous vectors. Scientific advances have begun to make it seem probable that, in the future, interventions akin to the second and third medical strategies against infectious microbes could be applied to limit the capacity of mosquitoes to serve as disease vectors [2, 40, 58]. Specifically, pathogens could be targeted while they complete their life stages within the mosquito [2, 4], possibly by altering the mosquito's own immune system [40, 58, 209]; or their interactions with the mosquito could be manipulated in order to disrupt the disease transmission cycle [3, 59]. Along with advances in mosquito transgenesis [2, 4, 210], our understanding of how resistance to pesticides originates [208], and our understanding of insect parasites and endosymbionts [4, 211], a better understanding of

mosquito immunology and physiology offers the potential for discovery of targets for use in such strategies. To this end, we have focused on uncovering basic aspects of mosquito immunology and physiology that come into play during pathogen transmission.

While it's good to look towards the future, a better understanding of mosquito immunology and physiology could also have more immediate benefits. Classical insect control strategies continue to rely on insecticides or pathogenic microorganisms which reach the insect circulatory system through the tracheae, cuticular absorption or ingestion [212]. The mosquito circulatory system then disperses these agents throughout the body. Those who work on producing novel pesticides, repellants and attractants could be aided by a better understanding of the mechanisms of insect circulatory and waste removal systems (i.e. hemocytes and pericardial cells).

This work is also important from an evolutionary perspective. The field of evolutionary parasitology addresses the organisms that were largely unseen by Darwin, but likely subjugated his "entangled bank". There has even been speculation that, during his travels, one of these organisms might have "entangled" Darwin himself and affected his lifestyle in a way that helped bind him to less physical pursuits, like his writings (although modern analysts have started to favor a psychological disorder) [213]. Regardless, host-parasite coevolution has been postulated to be a major driving force behind the evolution of life on earth, possibly even leading to the existence of sexual reproduction [214, 215]. Although such hypotheses are supported theoretically, concrete empirical data is scarce because it is difficult to obtain and can be hard to interpret in models whose physiology are not well understood [216, 217]. A better understanding of immunological and physiological interactions at the host-parasite interface could help resolve such issues. Accordingly, this interface is the focus of a fertile and growing field of research within evolutionary parasitology, and mosquitoes are excellent models for its

study because: (1) they interact with a great diversity of microbes and the fundamentals of many of these interactions have been characterized [1, 77, 93, 94]; (2) the mosquito circulatory and immune systems have been explored using modern methods [32, 33, 41, 90, 107]; (3) the evolutionary relationships between mosquitoes and organisms like *Drosophila* and *Ixodes* provide a unique perspective on arthropod physiology and evolution of hematophagy [5]; and 4) an abundance of genomic and transcriptomic work has been completed for mosquitoes, the pathogens they vector, and their human hosts [122, 218-220].

During my time at Vanderbilt, we have helped advance knowledge of the insect circulatory and immune systems. The second, third and fourth chapters focused on these subjects, with the third chapter including hard evidence of the importance of interactions between the two systems during the fight to maintain homeostasis after infection. Our work on the dynamics of hemolymph flow strongly supported the idea that parasites utilize passive motility to migrate from the insect midgut to the salivary glands. Our work also showed that phagocytosis and sessile hemocytes are important players during infection, and likely help determine the vectorial capacity of arthropods. We also corroborated results from others showing that hemocytes increase in number following an immune stimulus, while gathering the first conclusive data that hemocytes are capable of proliferation within the hemocoel.

In the fifth chapter we showed the importance of SGS proteins during blood feeding and suggest that they might be a major immunomodulatory factor. Along with suggesting them as a possible target in future vaccine strategies, SGSs' likely role in immunomodulation is also interesting from an evolutionary perspective, because SGSs are only found in mosquitoes and *Wolbachia*. We speculate that this evolutionary event, an example of a trans-domain horizontal gene transfer [221], could represent an

evolutionary innovation that allowed mosquitoes to evolve into blood-feeders. We also found that SGSs are also highly immunogenic and could be important for future strategies in epidemiology [61]. However, while we gained no concrete data regarding the role of SGS during salivary gland invasion by *Plasmodium*, our results certainly don't preclude this possibility. In fact, our evidence regarding SGSs localization in the distal lateral lobes indirectly supports their role in salivary gland invasion, although localization within the secretory cavity suggests that they might play a different role than previously thought [68].

Regarding my own future direction, and the suggestions I can offer to other scientists who will read this, I will first address the work with insect hemocytes. From my perspective two glaring problems currently exist in hemocyte biology. First, we still need a comprehensive and precise explanation of the biology of each specific type of insect hemocyte and the roles they play. This is especially true in mosquitoes, although our work has furthered our understanding on this front (Chapters III-IV; [1, 28, 36, 37]). The types of cells present, the temporal and special localization of each type of hemocyte, and their numbers are still not agreed upon by mosquito biologists. It is also unknown if sessile hemocytes differ from circulating hemocytes in their biochemical makeup. I cannot say how to answer these questions, but I feel confident that our work sets a firm foundation to build upon in such studies. Second, we don't know where hemocytes come from in adult insects. While hemocyte production in larvae and during metamorphosis have been described, it is still unknown what is responsible for the proliferation seen in circulating hemocytes following immune stimulation [46, 48]. This is the life-stage of insect vectors that has the greatest impact on human health, and is targeted during most efforts at disease prevention [212]. So, it is important that we have a full understanding of factors such as adult immunity, which likely affect vectorial capacity. Our work with

the direct assay of hemocyte proliferation (using in vivo CM-DiI staining) and hemocyte mitosis (using tubulin staining) shows for the first time that systemic hemocyte numbers increase and that mitosis occurs in circulating hemocytes. These results suggest that autonomous proliferation might be responsible for changes in hemocyte numbers in adult insects, although much more work needs to be done to show this. One methodological suggestion I can make here would be to attempt using Thymidine incorporation or Histone-3 labeling to build upon my studies of hemocyte proliferation. It can be expected that these techniques will have some of the same problems as using any other direct mitosis assay, but there are currently no viable alternatives [127, 132]. Nonetheless, I expect that these techniques might yield some interesting comparisons to the data gathered using tubulin staining. I also think that researching the activities of hemocytes during metamorphosis could help explain the initial events of adult hemocyte production and could be achieved using many of the same techniques I have already used in adults. I have helped train junior graduate students who are already working on such projects in the Hillyer lab.

Korochkina et al. [68] left no record of the regions of *Aedes* SGS1 that were targeted by the polyclonal antibodies that blocked salivary gland invasion by *Plasmodium* [68]. Therefore, we targeted several regions of the extracellular portion of *Anopheles gambiae* SGS4 and SGS5, which bioinformatic analyses suggested could be involved in protein-protein interactions. We were unable to confirm in vivo binding of these antibodies using several techniques, and results from immunohistochemistry using different fixatives suggested that SGS might not be heavily localized on the basal side of the salivary glands and that the epitopes recognized by our antibodies are heavily buried in the proteins' hydrophobic core. Because RNAi silencing also proved to be ineffective, even using extreme experimental conditions that have worked in other studies of salivary

proteins [60, 188], it was not possible for us to gather any direct evidence regarding SGS protein interactions with *Plasmodium*. The data that we did gather about localization and processing certainly do not refute the idea that SGSs are involved during gland invasion. However, the presence of SGS4 and SGS5 primarily within the apical secretory cavities of the salivary glands suggests that *Anopheles* SGSs might play a different role during invasion than that hypothesized by Korochkina et al. [68] (i.e. they predicted a role in the initial invasion of the basal salivary gland surface). I hypothesize that SGS could act as a signal to *Plasmodium* during the invasion of the secretory cavities from within the cytoplasm of the salivary epithelial cells. This may seem implausible, but invasion of the apical cavity has been shown to involve a set of discrete processes, including a unidirectional traversal through the cytoplasm of the host cell [56]. Another possibility is that SGSs act as an important developmental cue once the sporozoites have made it into the secretory cavities. In support of this hypothesis, it is now known that unidentified cues in the secretory cavities lead to transcriptional changes that effect sporozoite survival and infectivity [57].

I will continue working on sporozoite tissue invasion during my postdoctoral studies and I also plan to revisit my work on SGS proteins at some point in the future. During my postdoctoral fellowship I will be the entomology expert on a team developing methods for completing the life cycle of *Plasmodium falciparum* in vitro. I will be heavily focused on the effect of posttranslational modifications during the invasion of the mosquito salivary glands and human liver cells. I have become particularly interested in the effect of tyrosine sulfation on cellular invasion by *Plasmodium*, and plan to continue working on this research during my postdoctoral research or during my transition into a permanent position.

References

1. Hillyer, J.F., C. Barreau, and K.D. Vernick, *Efficiency of salivary gland invasion by malaria sporozoites is controlled by rapid sporozoite destruction in the mosquito haemocoel.* Int J Parasitol, 2007. **37**(6): p. 673-81.

2. Boëte, C. and NetLibrary Inc., *Genetically modified mosquitoes for malaria control*, in *Medical intelligence unit*. 2006, Landes Bioscience: Georgetown, Tex. p. 174 p.

3. Titus, R.G., J.V. Bishop, and J.S. Mejia, *The immunomodulatory factors of arthropod saliva and the potential for these factors to serve as vaccine targets to prevent pathogen transmission.* Parasite Immunol, 2006. **28**(4): p. 131-41.

4. Wang, S., et al., *Fighting malaria with engineered symbiotic bacteria from vector mosquitoes.* Proc Natl Acad Sci U S A, 2012.

5. Mans, B.J. and I.M.B. Francischetti, *Sialomic perspectives on the evolution of blood-feeding behavior in arthropods: future therapeutics by natural design* in *Toxins and Hemostasis*, R.M. Kini, et al., Editors. 2011, Springer Science+Business Media p. 21-44.

6. Pass, G., et al., *Phylogenetic relationships of the orders in Hexapoda: contributions from the circulatory organs for a morphological data matrix.* Arthropod Systematics and Phylogeny, 2006. **64**(2): p. 165-203.

7. Strand, M.R., *Insect hemocytes and their role in immunity*, in *Insect Immunology*, N.E. Beckage, Editor. 2008, Academic Press: Waltham, Massachusetts. p. 25-47.

8. Grimaldi, D. and M. Engel, *Evolution of the Insects*. 2005, New York, NY: Cambridge University Press. 772.

9. Roberts, L.J. and J. Janovy, *Foundations of Parasitology*. 8 ed. 2008: McGraw-Hill Science. 728.

10. Bertone, M.A., G.W. Courtney, and B.M. Wiegmann, *Phylogenetics and temporal diversification of the earliest true flies (Insecta: Diptera) based on multiple nuclear genes.* Systematic Entomology, 2008. **33**(4): p. 668-687.

11. Ramachandran, S., et al., *Support from the relationship of genetic and geographic distance in human populations for a serial founder effect originating in Africa.* Proc Natl Acad Sci U S A, 2005. **102**(44): p. 15942-7.

12. Hume, J.C., E.J. Lyons, and K.P. Day, *Human migration, mosquitoes and the evolution of Plasmodium falciparum.* Trends Parasitol, 2003. **19**(3): p. 144-9.

13. Takken, W. and B.G. Knols, *Odor-mediated behavior of Afrotropical malaria mosquitoes.* Annu Rev Entomol, 1999. **44**: p. 131-57.

14. Breman, J.G., *The ears of the hippopotamus: manifestations, determinants, and estimates of the malaria burden.* Am J Trop Med Hyg, 2001. **64**(1-2 Suppl): p. 1-11.

15. Snow, R.W., et al., *The global distribution of clinical episodes of Plasmodium falciparum malaria.* Nature, 2005. **434**(7030): p. 214-7.

16. Zimmerman, G.A. and H. Castro-Faria-Neto, *Persistent cognitive impairment after cerebral malaria: models, mechanisms and adjunctive therapies.* Expert Rev Anti Infect Ther, 2010. **8**(11): p. 1209-12.

17. Gallup, J.L. and J.D. Sachs, *The economic burden of malaria.* Am J Trop Med Hyg, 2001. **64**(1-2 Suppl): p. 85-96.

18. Bockarie, M.J., et al., *Role of vector control in the global program to eliminate lymphatic filariasis.* Annu Rev Entomol, 2009. **54**: p. 469-87.

19. Greenwood, B. and T. Mutabingwa, *Malaria in 2002.* Nature, 2002. **415**(6872): p. 670-2.

20. Zwiebel, L.J. and W. Takken, *Olfactory regulation of mosquito-host interactions.* Insect Biochem Mol Biol, 2004. **34**(7): p. 645-52.

21. Aponte, J.J., et al., *Safety of the RTS,S/AS02D candidate malaria vaccine in infants living in a highly endemic area of Mozambique: a double blind randomised controlled phase I/IIb trial.* Lancet, 2007. **370**(9598): p. 1543-51.

22. Han, Y.S., et al., *Molecular interactions between Anopheles stephensi midgut cells and Plasmodium berghei: the time bomb theory of ookinete invasion of mosquitoes.* EMBO J, 2000. **19**(22): p. 6030-40.

23. Montagna, G.N., K. Matuschewski, and C.A. Buscaglia, *Plasmodium sporozoite motility: an update.* Front Biosci, 2012. **17**: p. 726-44.

24. Chapman, R.F., *The insects : structure and function*. 4th ed. 1998, Cambridge, UK ; New York, NY: Cambridge University Press. xvii, 770 p.

25. Klowden, M.J., *Physiological Systems in Insects*. 2 ed. 2007: Elsevier Academic Press. 688.

26. Hertel, W. and G. Pass, *An evolutionary treatment of the morphology and physiology of circulatory organs in insects.* Comp Biochem Physiol, Part A Mol Integr Physiol, 2002. **133**(3): p. 555-75.

27. Pass, G., *Accessory pulsatile organs: evolutionary innovations in insects.* Annu Rev Entomol, 2000. **45**: p. 495-518.

28. Hillyer, J.F. and B.M. Christensen, *Characterization of hemocytes from the yellow fever mosquito, Aedes aegypti.* Histochem Cell Biol, 2002. **117**(5): p. 431-40.

29. Jones, J.C., *The heart and associated tissues of Anopheles quadrimaculatus say (Diptera: Culicidae).* J Morphol, 1954. **94**(1): p. 71-124.

30. Yaguzhinskaya, L.V., *(New data on the physiology and anatomy of the dipteran heart- structure and function of the heart of feale Anopheles maculipennis Mgn.). In Russian.* Biull. Moskovskovo Obshchestva Ispytatelei Prirody, Otdel Biol., 1954. **59**(1): p. 41-50.

31. Jones, J.C. The circulatory system of insects. 1977, Springfild, IL: Charles C. Thomas.

32. Andereck, J.W., J.G. King, and J.F. Hillyer, *Contraction of the ventral abdomen potentiates extracardiac retrograde hemolymph propulsion in the mosquito hemocoel.* PLoS One, 2010. **5**(9): p. e12943.

33. Glenn, J.D., J.G. King, and J.F. Hillyer, *Structural mechanics of the mosquito heart and its function in bidirectional hemolymph transport.* J Exp Biol, 2010. **213**(4): p. 541-50.

34. Hartenstein, V. and L. Mandal, *The blood/vascular system in a phylogenetic perspective.* Bioessays, 2006. **28**(12): p. 1203-10.

35. Elrod-Erickson, M., S. Mishra, and D.S. Schneider, *Interactions between the cellular and humoral immune responses in Drosophila.* Curr Biol, 2000. **10**(13): p. 781-4.

36. Hillyer, J.F., S.L. Schmidt, and B.M. Christensen, *Rapid phagocytosis and melanization of bacteria and Plasmodium sporozoites by hemocytes of the mosquito Aedes aegypti.* J Parasitol, 2003. **89**(1): p. 62-9.

37. Hillyer, J.F., S.L. Schmidt, and B.M. Christensen, *Hemocyte-mediated phagocytosis and melanization in the mosquito Armigeres subalbatus following immune challenge by bacteria.* Cell Tissue Res, 2003. **313**(1): p. 117-27.

38. Beckage, N.E., *Insect immunology*. 1st ed. 2008, Amsterdam ; Boston: Academic Press. 348 p., [6] p. of plates.

39. Soderhall, K. and L. Cerenius, *Role of the prophenoloxidase-activating system in invertebrate immunity.* Curr Opin Immunol, 1998. **10**(1): p. 23-8.

40. Blandin, S.A., et al., *Complement-like protein TEP1 is a determinant of vectorial capacity in the malaria vector Anopheles gambiae.* Cell, 2004. **116**(5): p. 661-70.

41. Blandin, S.A. and E.A. Levashina, *Phagocytosis in mosquito immune responses.* Immunol Rev, 2007. **219**: p. 8-16.

42. Nakatogawa, S., et al., *A novel peptide mediates aggregation and migration of hemocytes from an insect.* Curr Biol, 2009. **19**(9): p. 779-85.

43. Miller, J.S. and D.W. Stanley, *Lipopolysaccharide evokes microaggregation reactions in hemocytes isolated from tobacco hornworms, Manduca sexta.* Comp Biochem Physiol A Mol Integr Physiol, 2004. **137**(2): p. 285-95.

44. Crossley, A.C., *The ultrastructure and function of pericardial cells and other nephrocytes in an insect: Calliphora erythrocephala.* Tissue & cell, 1972. **4**(3): p. 529-60.

45. Pal, R., *Nephrocytes in some Culicidae-Diptera.* Indian J Entomol, 1944. **6**: p. 143-148.

46. Castillo, J., M.R. Brown, and M.R. Strand, *Blood feeding and insulin-like peptide 3 stimulate proliferation of hemocytes in the mosquito aedes aegypti.* PLoS pathogens, 2011. **7**(10): p. e1002274.

47. Castillo, J.C., A.E. Robertson, and M.R. Strand, *Characterization of hemocytes from the mosquitoes Anopheles gambiae and Aedes aegypti.* Insect Biochem Mol Biol, 2006. **36**(12): p. 891-903.

48. Coggins, S.A., T.Y. Estevez-Lao, and J.F. Hillyer, *Increased survivorship following bacterial infection by the mosquito Aedes aegypti as compared to Anopheles gambiae correlates with increased transcriptional induction of antimicrobial peptides.* Dev Comp Immunol, 2012.

49. Rodrigues, J., et al., *Hemocyte differentiation mediates innate immune memory in Anopheles gambiae mosquitoes.* Science, 2010. **329**(5997): p. 1353-5.

50. Telang, A., et al., *Larval nutritional stress affects vector immune traits in adult yellow fever mosquito Aedes aegypti (Stegomyia aegypti).* Med Vet Entomol, 2011.

51. Christensen, B.M., et al., *Hemocyte population changes during the immune response of Aedes aegypti to inoculated microfilariae of Dirofilaria immitis.* J Parasitol, 1989. **75**(1): p. 119-23.

52. Armistead, J.S., et al., *A role for heparan sulfate proteoglycans in Plasmodium falciparum sporozoite invasion of anopheline mosquito salivary glands.* Biochem J, 2011. **438**(3): p. 475-83.

53. Frischknecht, F., *The skin as interface in the transmission of arthropod-borne pathogens.* Cell Microbiol, 2007. **9**(7): p. 1630-40.

54. Matuschewski, K., *Getting infectious: formation and maturation of Plasmodium sporozoites in the Anopheles vector.* Cell Microbiol, 2006. **8**(10): p. 1547-56.

55. Ghosh, A.K. and M. Jacobs-Lorena, *Plasmodium sporozoite invasion of the mosquito salivary gland.* Curr Opin Microbiol, 2009. **12**(4): p. 394-400.

56. Pimenta, P.F., M. Touray, and L. Miller, *The journey of malaria sporozoites in the mosquito salivary gland.* J Eukaryot Microbiol, 1994. **41**(6): p. 608-24.

57. Gomes-Santos, C.S., et al., *Transition of Plasmodium sporozoites into liver stage-like forms is regulated by the RNA binding protein Pumilio.* PLoS Pathog, 2011. **7**(5): p. e1002046.

58. Curtis, C.F., *Possible Use of Translocations to fix Desirable Genes in Insect Pest Populations.* Nature, 1968. **218**(5139): p. 368-369.

59. Ito, J., et al., *Transgenic anopheline mosquitoes impaired in transmission of a malaria parasite.* Nature, 2002. **417**(6887): p. 452-5.

60. Ghosh, A.K., et al., *Malaria parasite invasion of the mosquito salivary gland requires interaction between the Plasmodium TRAP and the Anopheles saglin proteins.* PLoS Pathog, 2009. **5**(1): p. e1000265.

61. Remoue, F., et al., *Evaluation of the antibody response to Anopheles salivary antigens as a potential marker of risk of malaria.* Trans R Soc Trop Med Hyg, 2006. **100**(4): p. 363-70.

62. Ribeiro, J.M.C. and B. Arcà, *Chapter 2 From Sialomes to the Sialoverse: An Insight into Salivary Potion of Blood-Feeding Insects*, in *Advances in Insect Physiology*, J.S. Stephen and C. Jeacuterocircme, Editors. 2009, Academic Press. p. 59-118.

63. Schneider, B.S. and S. Higgs, *The enhancement of arbovirus transmission and disease by mosquito saliva is associated with modulation of the host immune response.* Trans R Soc Trop Med Hyg, 2008. **102**(5): p. 400-8.

64. Thangamani, S., et al., *Host immune response to mosquito-transmitted chikungunya virus differs from that elicited by needle inoculated virus.* PLoS One, 2010. **5**(8): p. e12137.

65. Morris, R.V., et al., *Sandfly maxadilan exacerbates infection with Leishmania major and vaccinating against it protects against L. major infection.* J Immunol, 2001. **167**(9): p. 5226-30.

66. Valenzuela, J.G., et al., *Toward a defined anti-Leishmania vaccine targeting vector antigens: characterization of a protective salivary protein.* J Exp Med, 2001. **194**(3): p. 331-42.

67. Drame, P.M., et al., *Human antibody responses to the Anopheles salivary gSG6-P1 peptide: a novel tool for evaluating the efficacy of ITNs in malaria vector control.* PLoS One, 2010. **5**(12): p. e15596.

68. Korochkina, S., et al., *A mosquito-specific protein family includes candidate receptors for malaria sporozoite invasion of salivary glands.* Cell Microbiol, 2006. **8**(1): p. 163-75.

69. Klowden, A.J., *Circulatory systems*, in *Physiological systems in insects*. 2007, Academic Press: Boston. p. 357-402.

70. Nation, J.L., *Circulatory System*, in *Insect physiology and biochemistry*. 2008, CRC Press: Boca Raton. p. 339-365.

71. Chapman, R.F., *Circulatory system, blood, and immune systems*, in *The insects: structure and function*. 1998, Cambridge University Press: Cambridge, UK. p. 94-131.

72. Jones, J.C., *The circulatory system of insects*. 1977, Springfield, IL: Charles C. Thomas. 255.

73. Lee, W.K. and J.J. Socha, *Direct visualization of hemolymph flow in the heart of a grasshopper (Schistocerca americana).* BMC Physiol, 2009. **9**: p. 2.

74. Sláma, K., *Mechanical aspects of heartbeat reversal in pupae of Manduca sexta.* J Insect Physiol, 2003. **49**(7): p. 645-57.

75. Wasserthal, L.T., *Drosophila flies combine periodic heartbeat reversal with a circulation in the anterior body mediated by a newly discovered anterior pair of ostial valves and 'venous' channels.* J Exp Biol, 2007. **210**(Pt 21): p. 3707-19.

76. Tao, Y. and R.A. Schulz, *Heart development in Drosophila.* Semin Cell Dev Biol, 2007. **18**(1): p. 3-15.

77. Salazar, M.I., et al., *Dengue virus type 2: replication and tropisms in orally infected Aedes aegypti mosquitoes.* BMC Microbiol, 2007. **7**: p. 9.

78. Clements, A.N., *The circulatory system*, in *The biology of mosquitoes*. 1992, Chapman & Hall: London. p. 195-205.

79. Iaguzhinskaja, L.V., *New results on the physiology and anatomy of the dipteran heart; structure and function of the heart of Anopheles maculipennis Mgn.* Biull Mosk Obshch Ispyt Prir Otdel Biol, 1954. **59**: p. 41-50 (In Russian).

80. Wasserthal, L.T., *Functional morphology of the heart and of a new cephalic pulsatile organ in the blowfly Calliphora vicina (Diptera : Calliphoridae) and their roles in hemolymph transport and tracheal ventilation*, in *Int J Insect Morphol*. 1999. p. 111-129.

81. Tartes, U., A. Vanatoa, and A. Kuusik, *The insect abdomen--a heartbeat manager in insects?* Comp Biochem Physiol, Part A Mol Integr Physiol, 2002. **133**(3): p. 611-23.

82. Clements, A.N., *The biology of mosquitoes: Development, nutrition and reproduction*. Vol. 1. 1992: Chapman & Hall. 509.

83. Gerould, J.H., *Orders of insects with heart-beat reversal.* The Biological Bulletin, 1933. **64**(3): p. 424-431.

84. Wasserthal, L.T., *Oscillating haemolymph 'circulation' in the butterfly Papilio machaon L. revealed by contact thermography and photocell measurements*, in *J Comp Physiol*. 1980. p. 145-163.

85. Sláma, K. and L. Neven, *Active regulation of respiration and circulation in pupae of the codling moth (Cydia pomonella).* J Insect Physiol, 2001. **47**(11): p. 1321-1336.

86. Sláma, K. and R. Farkas, *Heartbeat patterns during the postembryonic development of Drosophila melanogaster.* J Insect Physiol, 2005. **51**(5): p. 489-503.

87. Dulcis, D. and R.B. Levine, *Glutamatergic innervation of the heart initiates retrograde contractions in adult Drosophila melanogaster.* J Neurosci, 2005. **25**(2): p. 271-80.

88. Angioy, A.M. and P. Pietra, *Mechanism of beat reversal in semi-intact heart preparations of the blowfly Phormia regina (Meigen).* Journal of Comparative Physiology B: Biochemical, Systemic, and Environmental Physiology, 1995. **165**: p. 165-170.

89. Lemaitre, B. and J. Hoffmann, *The host defense of Drosophila melanogaster.* Annu Rev Immunol, 2007. **25**: p. 697-743.

90. Hillyer, J.F., *Mosquito immunity.* Adv Exp Med Biol, 2010. **708**: p. 218-38.

91. Hall, J.E. and A.C. Guyton, *Guyton and Hall textbook of medical physiology*. 12th ed. 2011, Philadelphia, Pa.: Saunders/Elsevier. xix, 1091 p.

92. Pal, I. and J.D. Ramsey, *The role of the lymphatic system in vaccine trafficking and immune response.* Adv Drug Deliv Rev, 2011. **63**(10-11): p. 909-22.

93. Erickson, S.M., et al., *Mosquito infection responses to developing filarial worms.* PLoS Negl Trop Dis, 2009. **3**(10): p. e529.

94. Hillyer, J.F., S.L. Schmidt, and B.M. Christensen, *The antibacterial innate immune response by the mosquito Aedes aegypti is mediated by hemocytes and independent of Gram type and pathogenicity.* Microbes Infect, 2004. **6**(5): p. 448-59.

95. Kokoza, V., et al., *Blocking of Plasmodium transmission by cooperative action of Cecropin A and Defensin A in transgenic Aedes aegypti mosquitoes.* Proc Natl Acad Sci U S A, 2010. **107**(18): p. 8111-6.

96. Chen, Y., Z.-H. Weng, and L. Zheng, *Innate immunity against malaria parasites in Anopheles gambiae.* Insect Sci, 2008. **15**(1): p. 45-52.

97. Rosenthal, R.S. and R. Dziarski, *Isolation of peptidoglycan and soluble peptidoglycan fragments.* Methods Enzymol, 1994. **235**: p. 253-85.

98. Hunter, K.W., R.A. Gault, and M.D. Berner, *Preparation of microparticulate β-glucan from Saccharomyces cerevisiae for use in immune potentiation.* Letters in Applied Microbiology, 2002. **35**(4): p. 267-271.

99. Kaneko, T., et al., *Monomeric and polymeric gram-negative peptidoglycan but not purified LPS stimulate the Drosophila IMD pathway.* Immunity, 2004. **20**(5): p. 637-49.

100. MacKenzie, S.A., et al., *Peptidoglycan, not endotoxin, is the key mediator of cytokine gene expression induced in rainbow trout macrophages by crude LPS.* Mol Immunol, 2010. **47**(7-8): p. 1450-7.

101. Franke-Fayard, B., et al., *A Plasmodium berghei reference line that constitutively expresses GFP at a high level throughout the complete life cycle.* Mol Biochem Parasitol, 2004. **137**(1): p. 23-33.

102. Frevert, U., et al., *Intravital observation of Plasmodium berghei sporozoite infection of the liver.* PLoS Biol, 2005. **3**(6): p. e192.

103. Hillyer, J.F., et al., *Age-associated mortality in immune challenged mosquitoes (Aedes aegypti) correlates with a decrease in haemocyte numbers.* Cell Microbiol, 2005. **7**(1): p. 39-51.

104. Zinchuk, V., O. Zinchuk, and T. Okada, *Quantitative colocalization analysis of multicolor confocal immunofluorescence microscopy images: pushing pixels to explore biological phenomena.* Acta Histochem Cytochem, 2007. **40**(4): p. 101-11.

105. Guo, X., et al., *Hemocyte alterations during melanotic encapsulation of Brugia malayi in the mosquito Armigeres subalbatus.* J Parasitol, 1995. **81**(2): p. 200-7.

106. Gorman, M.J. and S.M. Paskewitz, *Persistence of infection in mosquitoes injected with bacteria.* J Invertebr Pathol, 2000. **75**(4): p. 296-7.

107. Cirimotich, C.M., et al., *Mosquito immune defenses against Plasmodium infection.* Dev Comp Immunol, 2010. **34**(4): p. 387-95.

108. Yassine, H. and M.A. Osta, *Anopheles gambiae innate immunity.* Cell Microbiol, 2010. **12**(1): p. 1-9.

109. Siva-Jothy, M.T., Y. Moret, and J. Rolff, *Insect Immunity: An Evolutionary Ecology Perspective*, in *Advances in Insect Physiology*, S.J. Simpson, Editor. 2005, Academic Press. p. 1-48.

110. Hibino, T., et al., *The immune gene repertoire encoded in the purple sea urchin genome.* Dev Biol, 2006. **300**(1): p. 349-65.

111. Olson, E.N., *Gene regulatory networks in the evolution and development of the heart.* Science, 2006. **313**(5795): p. 1922-7.

112. Weavers, H., et al., *The insect nephrocyte is a podocyte-like cell with a filtration slit diaphragm.* Nature, 2009. **457**(7227): p. 322-6.

113. Akbar, M.A., et al., *The full-of-bacteria gene is required for phagosome maturation during immune defense in Drosophila.* J Cell Biol, 2011. **192**(3): p. 383-90.

114. Haine, E.R., et al., *Antimicrobial defense and persistent infection in insects.* Science, 2008. **322**(5905): p. 1257-9.

115. Moita, L.F., et al., *In vivo identification of novel regulators and conserved pathways of phagocytosis in A. gambiae.* Immunity, 2005. **23**(1): p. 65-73.

116. Merchant, D., et al., *Eicosanoids mediate insect hemocyte migration.* J Insect Physiol, 2008. **54**(1): p. 215-21.

117. Hillyer, J.F. and T.Y. Estevez-Lao, *Nitric oxide is an essential component of the hemocyte-mediated mosquito immune response against bacteria.* Dev Comp Immunol, 2010. **34**(2): p. 141-9.

118. Blazer, V.S., J.W. Fournie, and B.A. Weeks-Perkins, *Macrophage aggregates: Biomarker for immune function in fishes?* Environmental Toxicology and Risk Assessment: Modeling and Risk Assessment (Sixth Volume), ed. F.J. Dwyer, T.R. Doane, and M.L. Hinman. Vol. 6. 1997, Philadelphia, Pennsylvania: American Society for Testing and Materials.

119. Wolke, R.E., *Piscine macrophage aggregates: A review.* Annual Review of Fish Diseases, 1992. **2**: p. 91-108.

120. Russell, D.G. and S. Gordon, *Phagocyte-pathogen interactions: macrophages and the host response to infection.*, ed. D.G. Russell and S. Gordon. 2009: ASM Press, Washington, D.C. 612.

121. Vigliano, F.A., et al., *Evidence for melano-macrophage centres of teleost as evolutionary precursors of germinal centres of higher vertebrates: an immunohistochemical study.* Fish Shellfish Immunol, 2006. **21**(4): p. 467-71.

122. Baton, L., et al., *Genome-wide transcriptomic profiling of Anopheles gambiae hemocytes reveals pathogen-specific signatures upon bacterial challenge and Plasmodium berghei infection.* BMC Genomics, 2009. **10**(1): p. 257.

123. Pinto, S.B., et al., *Discovery of Plasmodium modulators by genome-wide analysis of circulating hemocytes in Anopheles gambiae.* Proc Natl Acad Sci U S A, 2009. **106**(50): p. 21270-5.

124. Hernandez-Martinez, S., et al., *Cellular-mediated reactions to foreign organisms inoculated into the hemocoel of Anopheles albimanus (Diptera : Culicidae).* Journal of Medical Entomology, 2002. **39**(1): p. 61-69.

125. Lackie, A.M., *Haemocyte Behaviour*, in *Advances in Insect Physiology*, P.D. Evans and V.B. Wigglesworth, Editors. 1988, Academic Press. p. 85-178.

126. Melnicoff, M.J., et al., *In vivo labeling of resident peritoneal macrophages*, in *J Leukoc Biol*. 1988. p. 387-397.

127. Rieder, C.L., *Mitosis and Meiosis*, in *Methods in Cell Biology*. 1999, Academic Press San Diego. p. 489.

128. Foley, D., *Innate cellular defense by mosquito hemocytes*, in *Comparative Pathobiology*, L.A.J. Bulla and T.C. Cheng, Editors. 1978, Plenum Press: New York & London. p. 114.

129. Lanot, R., et al., *Postembryonic hematopoiesis in Drosophila.* Dev Biol, 2001. **230**(2): p. 243-57.

130. Blandin, S.A., et al., *Dissecting the genetic basis of resistance to malaria parasites in Anopheles gambiae.* Science, 2009. **326**(5949): p. 147-50.

131. Crossley, A.C., *The Cytophysiology of Insect Blood*, in *Advances in Insect Physiology*, M.J.B. J.E. Treherne and V.B. Wigglesworth, Editors. 1975, Academic Press. p. 117-221.

132. Wieder, R., *Selection of Methods for Measuring Proliferation*, in *Cell Growth, Differentiation and Senescence*, G. Studzinski, Editor. 1999, Oxford University Press: New York. p. 1-32.

133. Warrener, R., et al., *Tumor cell-selective cytotoxicity by targeting cell cycle checkpoints.* FASEB J, 2003. **17**(11): p. 1550-2.

134. Echalier, G., *4 - Karyotype and Cell Cycle*, in *Drosophila Cells in Culture*. 1997, Academic Press: New York. p. 187-226.

135. Erenpreisa, J., et al., *Endopolyploidy in irradiated p53-deficient tumour cell lines: persistence of cell division activity in giant cells expressing Aurora-B kinase.* Cell Biol Int, 2008. **32**(9): p. 1044-56.

136. McInnes, A. and D.M. Rennick, *Interleukin 4 induces cultured monocytes/macrophages to form giant multinucleated cells.* J Exp Med, 1988. **167**(2): p. 598-611.

137. Chain, B., K. Leyshon-Sorland, and M. Siva-Jothy, *Haemocyte heterogeneity in the cockroach Periplaneta americana analysed using monoclonal antibodies.* J Cell Sci, 1992. **103**(4): p. 1261-1267.

138. Oliver, J.D., et al., *Comparative analysis of hemocyte phagocytosis between six species of arthropods as measured by flow cytometry.* J Invertebr Pathol, 2011. **108**(2): p. 126-30.

139. Markus, R., et al., *Sessile hemocytes as a hematopoietic compartment in Drosophila melanogaster.* Proc Natl Acad Sci U S A, 2009. **106**(12): p. 4805-9.

140. Cinamon, G., V. Shinder, and R. Alon, *Shear forces promote lymphocyte migration across vascular endothelium bearing apical chemokines.* Nat Immunol, 2001. **2**(6): p. 515-22.

141. Decave, E., et al., *Shear flow-induced motility of Dictyostelium discoideum cells on solid substrate.* J Cell Sci, 2003. **116**(Pt 21): p. 4331-43.

142. Jung, S.H., et al., *The Drosophila lymph gland as a developmental model of hematopoiesis.* Development, 2005. **132**(11): p. 2521-33.

143. Fuentealba, L.C., et al., *Asymmetric mitosis: Unequal segregation of proteins destined for degradation.* Proc Natl Acad Sci U S A, 2008. **105**(22): p. 7732-7.

144. Matova, N. and K.V. Anderson, *Rel/NF-kappaB double mutants reveal that cellular immunity is central to Drosophila host defense.* Proc Natl Acad Sci U S A, 2006. **103**(44): p. 16424-9.

145. Park, Y., Y. Kim, and D. Stanley, *Cellular immunosenescence in adult male crickets, Gryllus assimilis.* Arch Insect Biochem Physiol, 2011. **76**(4): p. 185-94.

146. King, J.G., K.D. Vernick, and J.F. Hillyer, *Members of the salivary gland surface protein (SGS) family are major immunogenic components of mosquito saliva.* J Biol Chem, 2011. **286**(47): p. 40824-34.

147. Ribeiro, J.M.C. and B. Arcà, *Sialomes to the Sialoverse: an insight into the salivary potion of blood-feeding insects.* Adv Insect Physiol, 2009. **37**: p. 59-118.

148. Organization, W.H., *Weekly epidemiological record.* Weekly epidemiological record, 1996. **71**(3): p. 17-22.

149. Poinsignon, A., et al., *Human IgG response to a salivary peptide, gSG6-P1, as a new immuno-epidemiological tool for evaluating low-level exposure to Anopheles bites.* Malar J, 2009. **8**: p. 198.

150. Cornelie, S., et al., *An insight into immunogenic salivary proteins of Anopheles gambiae in African children.* Malar J, 2007. **6**: p. 75.

151. Owhashi, M., et al., *The role of saliva of Anopheles stephensi in inflammatory response: identification of a high molecular weight neutrophil chemotactic factor.* Parasitol Res, 2001. **87**(5): p. 376-82.

152. Kebaier, C., T. Voza, and J. Vanderberg, *Neither mosquito saliva nor immunity to saliva has a detectable effect on the infectivity of Plasmodium sporozoites injected into mice.* Infect Immun, 2010. **78**(1): p. 545-51.

153. Vaughan, J.A., et al., *Infectivity of Plasmodium berghei sporozoites delivered by intravenous inoculation versus mosquito bite: implications for sporozoite vaccine trials.* Infect Immun, 1999. **67**(8): p. 4285-9.

154. Donovan, M.J., et al., *Uninfected mosquito bites confer protection against infection with malaria parasites.* Infect Immun, 2007. **75**(5): p. 2523-30.

155. Arca, B., et al., *An insight into the sialome of the adult female mosquito Aedes albopictus.* Insect Biochem Mol Biol, 2007. **37**(2): p. 107-27.

156. Arca, B., et al., *An updated catalogue of salivary gland transcripts in the adult female mosquito, Anopheles gambiae.* J Exp Biol, 2005. **208**(Pt 20): p. 3971-86.

157. Ribeiro, J.M., et al., *An insight into the salivary transcriptome and proteome of the adult female mosquito Culex pipiens quinquefasciatus.* Insect Biochem Mol Biol, 2004. **34**(6): p. 543-63.

158. Klasson, L., et al., *Horizontal gene transfer between Wolbachia and the mosquito Aedes aegypti.* BMC Genomics, 2009. **10**: p. 33.

159. Wasserman, H.A., S. Singh, and D.E. Champagne, *Saliva of the Yellow Fever mosquito, Aedes aegypti, modulates murine lymphocyte function.* Parasite Immunol, 2004. **26**(6-7): p. 295-306.

160. Boorman, J., *Induction of salivation in biting midges and mosquitoes, and demonstration of virus in the saliva of infected insects.* Med Vet Entomol, 1987. **1**(2): p. 211-4.

161. Bowen, M.F., *Sensory aspects of host location in mosquitoes.* Ciba Found Symp, 1996. **200**: p. 197-211.

162. Billingsley, P.F., et al., *Detection of mature malaria infections in live mosquitoes.* Trans R Soc Trop Med Hyg, 1991. **85**(4): p. 450-3.

163. Livak, K.J. and T.D. Schmittgen, *Analysis of relative gene expression data using real-time quantitative PCR and the 2(-Delta Delta C(T)) Method.* Methods, 2001. **25**(4): p. 402-8.

164. Harlow, E. and L. David, *Antibodies: a laboratory manual*. 1 ed. 1988, New York: Cold Spring Harbor Lab Press. 726.

165. Castellanos-Serra, L. and E. Hardy, *Negative detection of biomolecules separated in polyacrylamide electrophoresis gels.* Nat Protoc, 2006. **1**(3): p. 1544-51.

166. Sasse, J. and S.R. Gallagher, *Staining proteins in gels.* Curr Protoc Mol Biol, 2009. **Chapter 10**: p. Unit 10.6.

167. Rao, M.J.K. and P. Argos, *A conformational preference parameter to predict helices in integral membrane proteins.* Biochim Biophys Acta, 1986. **869**(2): p. 197-214.

168. Francischetti, I.M., et al., *Toward a catalog for the transcripts and proteins (sialome) from the salivary gland of the malaria vector Anopheles gambiae.* J Exp Biol, 2002. **205**(Pt 16): p. 2429-51.

169. Rath, A., et al., *Detergent binding explains anomalous SDS-PAGE migration of membrane proteins.* Proc Natl Acad Sci U S A, 2009. **106**(6): p. 1760-5.

170. Keller, M., et al., *Active caspase-1 is a regulator of unconventional protein secretion.* Cell, 2008. **132**(5): p. 818-31.

171. Juhn, J., et al., *Spatial mapping of gene expression in the salivary glands of the dengue vector mosquito, Aedes aegypti.* Parasit Vectors, 2011. **4**: p. 1.

172. Saunders, D.S., *Insect clocks*. 3rd ed, ed. C.G.H. Steel, X. Vafopoulou, and R.D. Lewis. 2002, Amsterdam: Elsevier Science. xv, 560 p.

173. Ghosh, A.K., et al., *Malaria parasite invasion of the mosquito salivary gland requires interaction between the Plasmodium TRAP and the Anopheles saglin proteins.* PLoS pathogens, 2009. **5**(1): p. e1000265.

174. Okulate, M.A., et al., *Identification and molecular characterization of a novel protein Saglin as a target of monoclonal antibodies affecting salivary gland infectivity of Plasmodium sporozoites.* Insect Mol Biol, 2007. **16**(6): p. 711-22.

175. Reddy, V.B., Y. Li, and E.A. Lerner, *Maxadilan, the PAC1 receptor, and leishmaniasis.* J Mol Neurosci, 2008. **36**(1-3): p. 241-4.

176. Calvo, E., et al., *The salivary gland transcriptome of the eastern tree hole mosquito, Ochlerotatus triseriatus.* J Med Entomol, 2010. **47**(3): p. 376-86.

177. Dowling, A.J., et al., *Genome-wide analysis reveals loci encoding anti-macrophage factors in the human pathogen Burkholderia pseudomallei K96243.* PLoS One, 2010. **5**(12): p. e15693.

178. Degnan, P.H. and N.A. Moran, *Diverse phage-encoded toxins in a protective insect endosymbiont.* Appl Environ Microbiol, 2008. **74**(21): p. 6782-91.

179. Iturbe-Ormaetxe, I., et al., *Distribution, expression, and motif variability of ankyrin domain genes in Wolbachia pipientis.* J Bacteriol, 2005. **187**(15): p. 5136-45.

180. Minet, A.D., et al., *Teneurin-1, a vertebrate homologue of the Drosophila pair-rule gene ten-m, is a neuronal protein with a novel type of heparin-binding domain.* J Cell Sci, 1999. **112**: p. 2019-32.

181. Youderian, P. and P.L. Hartzell, *Triple mutants uncover three new genes required for social motility in Myxococcus xanthus.* Genetics, 2007. **177**(1): p. 557-66.

182. Brennan, J.D., et al., *Anopheles gambiae salivary gland proteins as putative targets for blocking transmission of malaria parasites.* Proc Natl Acad Sci U S A, 2000. **97**(25): p. 13859-64.

183. Jariyapan, N., et al., *Analysis of female salivary gland proteins of the Anopheles barbirostris complex (Diptera: Culicidae) in Thailand.* Parasitol Res, 2010. **107**(3): p. 509-16.

184. Malafronte, R., S., et al., *The major salivary gland antigens of Culex quinquefasciatus are D7-related proteins.* Insect Biochem Mol Biol, 2003. **33**(1): p. 63-71.

185. Moreira, C.K., et al., *Analysis of salivary gland proteins of the mosquito Anopheles darlingi (Diptera: Culicidae).* J Med Entomol, 2001. **38**(5): p. 763-7.

186. Siriyasatien, P., et al., *Analysis of salivary gland proteins of the mosquito Armigeres subalbatus.* Southeast Asian J Trop Med Public Health, 2005. **36**(1): p. 64-7.

187. Jeon, S.H., J.W. Park, and B.H. Lee, *Characterization of human IgE and mouse IgG1 responses to allergens in three mosquito species by immunoblotting and ELISA.* Int Arch Allergy Immunol, 2001. **126**(3): p. 206-12.

188. Boisson, B., et al., *Gene silencing in mosquito salivary glands by RNAi.* FEBS Lett, 2006. **580**(8): p. 1988-92.

189. James, A.A., et al., *Isolation and characterization of the gene expressing the major salivary gland protein of the female mosquito, Aedes aegypti.* Mol Biochem Parasitol, 1991. **44**(2): p. 245-53.

190. Racioppi, J.V. and A. Spielman, *Secretory proteins from the salivary glands of adult Aedes aegypti mosquitoes.* Insect Biochemistry, 1987. **17**(3): p. 503-511.

191. Waitayakul, A., et al., *Natural human humoral response to salivary gland proteins of Anopheles mosquitoes in Thailand.* Acta Trop, 2006. **98**(1): p. 66-73.

192. Orlandi-Pradines, E., et al., *Antibody response against saliva antigens of Anopheles gambiae and Aedes aegypti in travellers in tropical Africa.* Microbes Infect, 2007. **9**(12-13): p. 1454-62.

193. Peng, Z., H. Li, and F.E. Simons, *Immunoblot analysis of salivary allergens in 10 mosquito species with worldwide distribution and the human IgE responses to these allergens.* J Allergy Clin Immunol, 1998. **101**(4 Pt 1): p. 498-505.

194. Penneys, N.S., et al., *Mosquito salivary gland antigens identified by circulating human antibodies.* Arch Dermatol, 1989. **125**(2): p. 219-22.

195. Brummer-Korvenkontio, H., et al., *Detection of mosquito saliva-specific IgE and IgG4 antibodies by immunoblotting.* J Allergy Clin Immunol, 1994. **93**(3): p. 551-5.

196. Chen, Y.L., F.E. Simons, and Z. Peng, *A mouse model of mosquito allergy for study of antigen-specific IgE and IgG subclass responses, lymphocyte*

proliferation, and IL-4 and IFN-gamma production. Int Arch Allergy Immunol, 1998. **116**(4): p. 269-77.

197. Barreau, C., et al., *Identification of surface molecules on salivary glands of the mosquito, Aedes aegypti, by a panel of monoclonal antibodies.* Insect Biochem Mol Biol, 1999. **29**(6): p. 515-26.

198. Ehrlich, P., et al., *The Experimental chemotherapy of spirilloses*. 1911: Rebman. 181.

199. Fleming, A., *On the specific antibacterial properties of penicillin and potassium tellurite. Incorporating a method of demonstrating some bacterial antagonisms.* The Journal of Pathology and Bacteriology, 1932. **35**(6): p. 831-842.

200. Fischl, M.A., et al., *The efficacy of azidothymidine (AZT) in the treatment of patients with AIDS and AIDS-related complex. A double-blind, placebo-controlled trial.* N Engl J Med, 1987. **317**(4): p. 185-91.

201. Pasteur, L., *Le traitement de la rage*. 1886, C. Marpon et Flammarion: Paris

202. Jenner, E., *An Inquiry Into the Causes and Effects of the Variolæ Vaccinæ, Or Cow-Pox.* 1798.

203. Salk, J.E., *Considerations in the preparation and use of poliomyelitis virus vaccine.* J Am Med Assoc, 1955. **158**(14): p. 1239-48.

204. Committee on New Directions in the Study of Antimicrobial Therapeutics, *Promising Approaches to the Development of Immunomodulation for the Treatment of Infectious Diseases*, in *Treating Infectious Diseases in a Microbial World: Report of Two Workshops on Novel Antimicrobial Therapeutics*. 2006, National Academies Press: Washington D.C.

205. Baba, M., et al., *A small-molecule, nonpeptide CCR5 antagonist with highly potent and selective anti-HIV-1 activity.* Proc Natl Acad Sci U S A, 1999. **96**(10): p. 5698-703.

206. *MALARIA control and eradication in Taiwan: progress report, May 1952 50 June 1957.* Bull World Health Organ, 1958. **19**(4): p. 595-620.

207. Neu, H.C., *The Crisis in Antibiotic Resistance.* Science, 1992. **257**(5073): p. 1064-1073.

208. Read, A.F., P.A. Lynch, and M.B. Thomas, *How to make evolution-proof insecticides for malaria control.* PLoS Biol, 2009. **7**(4): p. e1000058.

209. Alphey, L., *Natural and engineered mosquito immunity.* J Biol, 2009. **8**(4): p. 40.

210. Labbe, G.M., D.D. Nimmo, and L. Alphey, *piggybac- and PhiC31-mediated genetic transformation of the Asian tiger mosquito, Aedes albopictus (Skuse).* PLoS Negl Trop Dis, 2010. **4**(8): p. e788.

211. Harrington, M., *Bacterial infection may limit spread of dengue fever.* Lab Anim (NY), 2009. **38**(2): p. 40.

212. Pedigo, L.P., *Entomology and pest management*. 1989, New York: Macmillan; Collier Macmillan. xxii, 646 p.

213. Keynes, R.D., *Charles Darwin's Beagle diary*. 1988, Cambridge: Cambridge University Press.

214. Dawkins, R. and J.R. Krebs, *Arms Races between and within Species.* Proceedings of the Royal Society of London Series B-Biological Sciences, 1979. **205**(1161): p. 489-511.

215. Ridley, M., *The Red Queen: Sex and the Evolution of Human Nature* 1993, Penguin. p. 288.

216. Jokela, J., M.F. Dybdahl, and C.M. Lively, *The maintenance of sex, clonal dynamics, and host-parasite coevolution in a mixed population of sexual and asexual snails.* Am Nat, 2009. **174 Suppl 1**: p. S43-53.

217. Wolfe, K.H. and P.M. Sharp, *Mammalian Gene Evolution - Nucleotide-Sequence Divergence between Mouse and Rat.* Journal of Molecular Evolution, 1993. **37**(4): p. 441-456.

218. Gardner, M.J., et al., *Genome sequence of the human malaria parasite Plasmodium falciparum.* Nature, 2002. **419**(6906): p. 498-511.

219. Holt, R.A., et al., *The genome sequence of the malaria mosquito Anopheles gambiae.* Science, 2002. **298**(5591): p. 129-49.

220. Venter, J.C., et al., *The sequence of the human genome.* Science, 2001. **291**(5507): p. 1304-51.

221. Bordenstein, S.R., *Evolutionary genomics: transdomain gene transfers.* Curr Biol, 2007. **17**(21): p. R935-6.